University of Central Florida

Orlando FL

The College of Optics and Photonics

Senior Design

8/27/2021

Remotely Controlled Diffused Surface Laser Beam Imaging System

9/9/2021 - 4/22/2021

Members

Name	Major	Graduation date
Madelaine Smith	Optics and Photonics	5/7/2022
Devin Benjamin	Optics and Photonics	5/7/2022
Daniel Oquendo	Computer Engineering	5/7/2022
Miguel Ortiz	Electrical Engineering	5/7/2022

Technical Advisor

Dr. Martin Richardson

Haley Kerrigan

Table of Contents

Figures Index

1. Executive Summary

Outdoor high energy laser propagation experiments are impacted the inefficient preparation process. Many personnel are required to set up sensitive equipment far from the laser output and that is not intended for outdoor use. The aim of this project is to aid in reducing the amount of personnel required to prepare long range testing and provide weatherproof equipment to do so. The final design aims to create a device that is remotely controlled to find, track and characterize a laser beam off a diffused target board. The user would be able to stay at the laser output and view a live image of the beam. Characteristics like the intensity profile, intensity tracking, and beam tracking will be provided as well.

Investigation into several key components will be conducted. A lens zoom system must be designed to be able to view the 10x10 ft target and then zoom in on the beam, at least 4x magnification. A filtration system needs to be able to filter out ambient sun light. The power source must be designed to be chargeable and if possible, solar powered. The movement of the zoom lenses and the movement of the entire device will be investigated. The data transmission and user interface options will be investigated as well.

Several constraints impede the design, such as economic, environmental, manufacturability and sustainability.

2. Project Description

This section will describe in brief the purpose of the project through discussion of the background, objectives, goals, and approach.

2.1 Project Background

Our team is working with a graduate research group, the Laser Plasma Laboratory at CREOL UCF, to solve a problem that occurs during outdoor high power energy experiments. Currently there are few devices on the market which are built specifically for outdoor high energy laser propagation testing. Without access to such devices, setting up outdoor laser experiments can be both extremely time consuming and inefficient. Current equipment must be aligned by hand and monitored from both the laser output as well as the target. This distance varies but for the purposes of this design the distance is a kilometer. With an automated system that can locate the laser beam and record its characteristics, the amount of personnel on the ground can be reduced. Due to experimenting outdoors, sunlight can make it quite difficult for camera systems to read the laser beam on the surface of the target board. However, a specially designed filter system can control the amount of ambient light entering the system. The equipment being used traditionally is not designed to deal with the outdoor elements. When weather changes sporadically all equipment must be quickly salvaged and covered as to not get damaged. Most optical equipment on the market right now uses a direct power source to power the instruments, which is inefficient for outdoor use. Large batteries or a backup generator are needed to power the equipment. The solution to this is to incorporate a power source which is both chargeable and solar powered. With such a large distance a remotely controlled device will not only cut out the need for additional personnel, saving time and potential costs, but will be able to withstand any weather without the need to be physically covered or removed from its optimal testing location.

2.2 Objective

Design and build a remotely controlled, solar powered and waterproof system that can image and track a laser beam from collected light off of a diffused surface.Goals of building the device are to design and build a zoom system that will be remotely controlled to locate the laser beam on an outdoor diffused surface. Design a filter to control the amount of ambient light introduced to the device. The laser signal captured by the camera system will be sent to a corresponding receiver device and the vital information about beam location and

various characteristics will be displayed on the receiver. Design a battery source which can deliver the appropriate power to each individual system within the device and integrate solar panels for solar charging of the battery. This device will be controlled remotely from the laser's output location (roughly a kilometer away).

2.3 Project Goals

The core goals are to have a battery-operated device that will be able to transmit imaging data 3 meters at one wavelength. Our device will be remotely controlled, at 3 meters, to find and track a beam and its characteristics on a diffused target board.

The advanced goals are to have solar charged battery-operated device that will be able to transmit imaging data 3 meters at multiple wavelengths. Our device will be remotely controlled, further than 3 meters, to find and track a beam and its characteristics on a diffused target board.

The stretch goals are to have a solar powered device that will be able to transmit imaging date more than 3 meters at multiple wavelengths. Our device will automatically find and track a beam and its characteristics on a diffused target board.

2.4 Methodological Approach

Several approaches will be used to optimize the projects outcome. Optical simulation tools such as Zemax will be used to design the zoom system for the camera. CAD software will be used to simulate and design the movement system which will control the tilt and spin of the device. Thorough testing will allow a progressive scale of laser power and wavelengths. Theoretical exploration will help make informed decisions about sensing filters used to filter out ambient lighting. The most efficient way to transfer data is also being discussed and thought out. Ideally our system would transmit data over a medium which does not have to be hardwired. The system will be powered by solar energy. It will have (estimate size) solar panels which will
be connected to a rechargeable battery, providing power to the system. The system will use direct power coming from the solar panels. In the case of low sunlight, i.e. rain or cloudy, the battery will provide its charge to the system. In the case of full sunlight, the system will use the excess power to charge the battery. Between the panels and the battery, a charge controller will regulate the power given to the battery, and supervise the battery charge, avoiding excess charge or discharge, in order to avoid damage. A microcontroller will hold the connections to the components which will allow the camera to move accurately

and detect the beam. The components connected to the microcontroller also include an estimate of two motors adding a precise movement to the system gears. There are two displacement options which are in an angular rotation from left to right, and up and down. The other displacement option is a linear motion vertically and horizontally. Signals to the motors will be controlled through a motor driver that will receive a signal in real time directing the camera platform to follow the beam on the target. Also connected to the controller is the camera, requiring a lower amount of power than the motors. In order to handle the different types of components with varying types of currents and voltages, DC to DC converters will be designed as well as implemented, in order to scale up or down the voltage coming from the solar panels. Since the proposed project will be a weatherproof system, a case will be built in order to keep the components safe. This will increase the heat coming from the components, meaning that a couple of fans will also be powered through solar energy. Heating sensors will be connected inside the housing, which will throw a signal to the controller activating the cooling fans, that way no power is consumed till it’s absolutely needed.

3. Project Requirements

This section will cover the restrictions on this project that exist from specifications set by the team internally and by external factors.

3.1 Overall Requirement Specifications

Light Filtration	
Lens Zoom System	
Magnification	At least 4x
Length	Less than 12 in
Camera adjustment system	
Horizontal tilt	90 degrees
Vertical tilt	90 degrees
Remote control system	
Wireless connection	At least 3 m
System delay	Less than 100 ms
Combined Filter/Lens/Camera systems	
Weight	Less than 25 lbs
Size	Less than 4 cubic feet
Power discharge time	At least 30 min between charges
Housing	Water/weatherproof

Table 1: Design requirements

3.2 Constraints

Several constraints impede the design, the main concerns being, economic, environmental, manufacturability and sustainability. The economic constrain is that due to worldwide shortages certain devices and materials are either unavailable or outside of design budget. The environmental constrain involves the weather for outdoor testing. The design of this device needs to be weatherproof, and temperature controlled. Health and Safety constraints are a main factor when testing this device. The testing laser diode is a class 3B laser, and the proper safety eyewear is needed when in its proximity. Additionally, any indoor facility needs to be approved for such devices. However, the devices for any demonstration are safe for everyone
in proximity. Materials used must be commercially available, easily accessible, and do not require customization. This device needs to be sustainable in that the

designed battery is chargeable, can be used for at least 30 minutes, and charged with a solar power.

3.3 Standards

This section covers any social, political, environmental, and economic standards that have been found that this project will be under the purview of and must be followed.

3.3.1 Radio Frequency Spectrum Standards

The Federal Communications Commission (FCC) sets the allocations of the radio frequency spectrum as used in the jurisdiction of the United States. The allocations are set for various uses ranging from radio/television broadcasts, radionavigation, satellite communications, and for scientific research using radio waves in things like radio telescopes (i.e. not telling a camera control mechanism what to do). As demonstrated on the United States Frequency Allocation Chart released by the United States Department of Commerce National Telecommunications and Information Administration, amateur/public use is allowed in various bands across the spectrum, the ones below being the most relevant: 2.39-2.4835 GHz (referred to as the 2.45 GHz band) and 5.65-5.925 GHz (referred to as the 5.8 GHz band).

3.4 House of Quality

			Engineering Requirements									
			Cost	Weight	Delay	Signal [illegible]	Magnificatio	Power [illegible]	Filtration	Sensor	Size	Camera Adjustment
			-	-	-	+	+	+	+	+	-	+
Marketing Requirements	Compact	+	↓	↑↑			↓	↓↓			↑↑	↓
	Ease of Set up	+	↓	↓	↓	↑	↑	↑			↓	↑
	Weatherproof	+	↓	↓↓		↓					↓	↓
	Ease of Use	+	↓	↓	↓	↑	↑				↓	↑
	Engineering Requirement Targets		<$2500	< 25 lbs	<100 ms	> 3ms	TBD	> 30 Min	TBD	TBD	< 3ft^3	≥ 90° V & H

Table 2: House of Quality

Legend:

- \+ Positive Polarity
- – Negative Polarity
- ↑ Positive Correlation
- ↓ Negative Correlation
- ↑↑ Strong Positive Correlation
- ↓↓ Strong Negative Correlation

4. Research and Investigation

The following is the technical research the means by which this project may come together and develop into a functioning system. This covers our investigations of the optical, electrical, and computational components of the project and our decisions made based on those investigations.

4.1 Surfaces

When a laser beam is incident upon a smooth surface the propagation characteristics are easily quantified. The material used will dictate the amount of absorption, transmission, and specular reflection that takes place on the incident signal. The material will also have differed effects on the beam depending on the wavelength transmitted. Some surfaces are sensitive to wavelengths and may alter the polarization, amplitude, or even wavelength of the incident signal. Typically, with a smooth surface the incident light will strike the surface at some angle and the reflected light will travel at the same angle transversely to the incident beam. This type of reflection is specular reflection. Specular reflection most commonly occurs when light is incident upon smooth surfaces. Specular reflection typically will give the surface a glossy appearance. Most specular reflection occurs when light is incident upon glass or a glossy coated smooth material. Coatings can be used on the smooth surface as well to design the propagation response. Certain coating will have a higher reflectance percentage of the light thus can be designed to reflect whatever percentage of the beam desired. Certain coatings can reflect close to 100% of the original beam if required, since there will always be a small loss due to the medium the signal is travelling through.

In contrast a diffused surface is not as predictable to calculate the propagation behavior of the laser beam after striking the materials surface. Diffused surfaces consist of a structure which is not of equal crystalline construct throughout like a smooth surface. This inconsistency in lattice structure causes a unique propagation response from the laser beam depending on the material. The wavelength of the incident beam can be altered depending on the spacing of the diffused surface and how close the distance between the imperfect lattices atomic structure. When the laser beam is incident upon the diffused surface the wave fronts will experience absorption, transmission, diffused reflection, and specular reflection. Both reflections will be in many directions. When a laser signal propagates and is incident upon a diffused surface the light beam experiences transmission, diffused reflection, specular reflection, and absorption. The degree to which each response of the beam occurs and what percentage of

light signal experiences the effects depends on the properties of the diffused surface. Diffused surfaces typically have a matte appearance which is due to the non-homogenous construct of the material. For this experiment the light which will be collected by the device will be reflected light from the diffused surface. Diffused reflection occurs due to the randomness of the materials lattice structure on the surface as well as in the lattice structure. The surface is considered non-uniform and will reflect the different rays of the light source uniquely. Each ray travelling within the wave packet of the laser beam will strike the surface at differing orientations of the surface. The surface is ridged and will have random peaks and troughs of differing angular orientation. Each individual photon will strike the diffused surface at differing location and angles and will reflect accordingly. The randomness of this surfaces construct makes predicting the behavior of the light signal challenging. Some of the incident light will also transmit through the body of the diffused surface. The construct of the material will dictate the refractive index and how the light will travel inside of the material. Due to the lattice also being of random alignment the light will internally reflect randomly and the photons that are not absorbed will transmit back out of the surface as scattered light. The scattered light reflection is what will be observed by the camera of the device. Due to the randomness and differing directions of which the light will scatter, a percentage of the intensity of the original signal will be lost when collecting data. Along with the surface being non-uniform and causing random reflected beams some of the light which reaches the surface will transmit through into the structure and have internal refection which will cause body reflection and randomly scatter light.

The diffused surface for this experiment will be coated so that it has Lambertian characteristics. Lambertian refers to Lambert's cosine law which states "*the measure of radiant energy from a surface that exhibits Lambertian reflection is directly proportional to the cosine of the angle formed by the measurement point and the surface normal".* This law is depicted in the following equation:

For example, considering a light source as a point source, this point source will have a luminous intensity in all directions. This can be states as the luminous flux divided by four pi. At a calculated distance from the point source a screen is placed. The illuminance at a point directly in front of the source at an angle of zero degrees will be the maximum intensity and can be calculated by dividing the luminance intensity of the point source by the distance away from the screen squared. Now for a point on the screen at an angle theta the illuminance at his point will be the luminous intensity multiplied by cosine of theta than divided by the distance of the points source from the screen squared. This point at an angle can also be written as the maximum intensity multiplied by the cosine of the angle theta, which is Lamberts cosine law which is depicted in the equation below.

$$I = I_0 Cos(\theta)$$

The Lambertian surface when viewed form any angle will appear equally as bright from all directions. This phenomenon is directly correlated to the Lambertian BRDF. The measure of diffused reflection is notated as the albedo or symbolized as ρ. The albedo is measured from a range of zero to one. Zero being a completely black surface and one being a completely white surface. The completely lower the albedo (closer to black) the more absorption will take place versus reflectance and vice versa for the white surface which will experience a much higher reflectance as albedo increases. The Lambertian BRDF is the albedo divided by pi. This is proportional to brightness of a surface when incident light is reflected from the surface. The geometry of the surface is a factor which will change how to calculate the diffused reflection variable. Albedo is considered the hemispherical-directional reflectance. This is the measurement of how much light is reflected from any direction for the incident light around the surface normal of the object. Albedo is calculated using the following integration where f_r is the BRDF at the position x for any incident radiance travelling along w_i and w_o integrated along the full hemisphere:

$$\rho = \int_{\Omega} f_r(x, \omega_i, \omega_o)(\omega_i . n) d\omega_i$$

Through experimentation it will be observed at what particular angles the device is placed in front of the diffused surface which will aid in collecting the most reflected light rays to have the most accurate intensity profile data. The lab experimentation with the 532 nm laser light source will be used to gauge how the light beam reflects at differing positions of incidence on the diffused surface. The diffused surface will be marked at differing locations and distances along the surface. These marked surfaces will than be shone up with the laser at an incidence angle of zero degrees. Data will be collected at each of the different locations to compare the amount of light intensity collected by the devices at each of the points on the surface. Next the previous procedure will be repeated by at differing angles of incident light. The laser source will be placed upon a rotation stage which will aid in accurate angular measurements. The laser will again be shone upon the marked regions at differing angles and the intensity of the light will be recorded. The piece of material used in experimentation will have to be the same as the one used in the demonstration since it is a diffused surface, and a different piece would not have the same build and results. Once the data is recorded with multiple angles at differing locations along the diffused surface, the angle of the actual device will be altered. This data will help aid in understanding how the differing angles of both the incident light and orientation

of the device affect the ability for the lens system to collect the most reflected light rays as possible. The optimal position will be found through this experimentation.

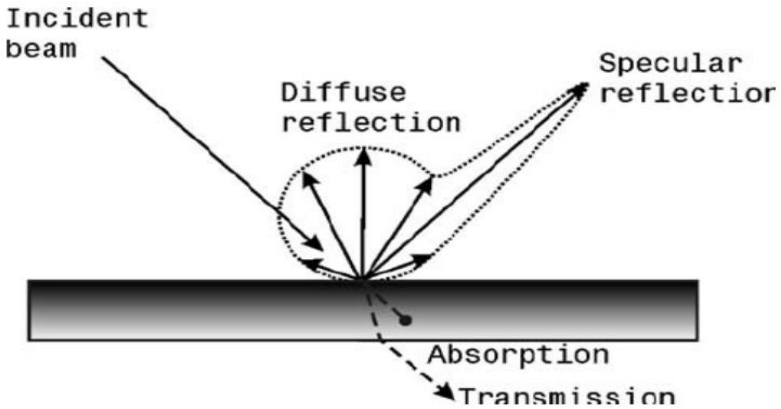

Figure 1: Light Interaction When Striking a Diffused Surface
Photo taken from (The influence of incident angle, object colour and distance on CNC laser scanning)

4.2 Camera Working Properties

ADC stands for analog to digital converter and represents the ability to convert the captured image into a digital file. ADC is given in units of bits, which corresponds to the amount of color values each pixel has access to. A higher ADC allows for the camera to capture more values and create an image with smoother gradients and better shadows. The minimum ADC determines the dynamic range which is the range of darkest value to brightest value. 8 bit has 256 possible values per pixel while 12 bit has 4,096. Because we are going to be developing an intensity profile based on the image captured, a higher ADC is a high priority. The slight variations of pixel value will give a more accurate profile of the beam (Plumridge, 2020).

Dynamic range is the ratio of the largest signal and the smallest possible signal that a sensor can generate. A large dynamic range increases the detail and contrast in a captured image. Brighter pixels capture photons faster than darker pixel so oversaturation can lead to blooming and image distortion. High contrast images typically have the most issues with dynamic range because high intensity light can blow out highlights and reduce the overall detail in the image (Plumridge, 2019).

Back focus is the distance from the sensor to the front of the camera. Shorter back focuses give you more flexibility with what you can include in your system. Its also useful if you’re looking to use smaller filters with larger sensors

as the close distance can reduce vignetting.” However, several issues can arise from short back focus systems. Condensation can become an issue with cooled sensors being close to optical windows. Reflections from the optical window can produce artefacts in the image (Plumridge, 2018).

Frame rate this is the speed in which images are shown in a video. 24 fps is a similar frame rate that our eyes see. 30 fps is usually the frame rate used for television, while 60 fps is used in slow motion video or sports recordings, because high motion recording typically require higher frame rates (Brunner, 2017).

The higher the frame rate the more detail will be collected in the context of this project. However, it is not determined how much the beam moves on the target at this time. If the beam traves around the frame a lot, we may need to consider a higher frame rate to keep up with the detail needed to be collected. 60 fps or more will probably be unnecessary for data collection (Brunner, 2017).

Full well is the amount of charge that can be stored within an individual pixel without the pixel becoming saturated. There is a linear relationship between the light intensity and the signal degradation as the pixel approaches the saturation limit. A higher full well is needed for the application of this project because intensity profiles are likely to have highly saturated pixels. If pixels become over saturated, then the intensity profile will be inaccurate (Instuments).

Blooming is an image artifact that results from over saturated pixels. When a pixel reaches saturation, they are unable to contain any additional charge, so the charge begins to spread into adjacent pixels. This will cause rings or a saturated blob around the high intensity pixel along with a long vertical streak down the image. The streak is due to the direction the signal travels in the sensor during the CCD readout (Instuments).

Mega pixels refer to the resolution the image, and one mega pixel is one million pixels. A higher megapixel spec allows for zooming or cropping of a photo without an optical zoom system. This does not seem to be a defining specification for our purposes.

Peak quantum efficiency, sometimes called spectral sensitivity, describes the ability for the sensor to absorb photons at a particular frequency. The peak quantum efficiency would be the maximum efficiency the sensor can guarantee, often found between 500 and 600 nm, corresponding to green (495-570 nm) to orange (590-620 nm) colors.

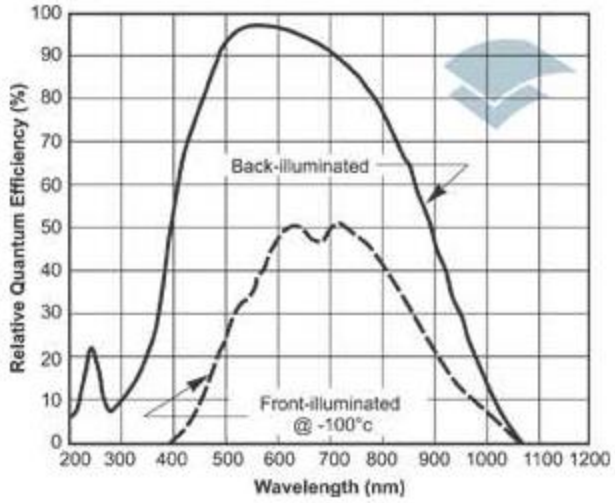

Figure 2: Quantum efficiency in cameras. The peak quantum efficiency lays between 500 and 600 nm. Taken from (Andor, 2018)

Read noise is main source of noise in a short exposer image. The specification is given in a median value in units of e-. the lowest read noise is the most desirable because this permits high dynamic range and detection of low-level signals. Read noise is affected by the user settings and applications the camera is used for. Typically, settings that increase the frame rate will increase the read noise

4.2.1 CCD vs CMOS Sensors

CCD (charge coupled device) and CMOS (complementary metal-oxide semiconductor) are camera sensors whose main functions is to convert photons into electrons. CCDs physically transport the charge across the sensor to a corner of the pixel matrix when in read out while CMOS sensors transport the charge using wire. The CCD is not as flexible in design because each pixel cannot be read individually (Karim Nice, 2020). Both sensors have their place within camera design, but each have advantages and need to be looked at in order to choose which is best for a given application.

The CCD sensor is arranged at a pixel array comprised of photodiodes specifically designed to process and create distortion-less images, in the way they transport electrons. The sensor can create low noise images with high quality light sensitivity. Historically the CCD sensor has a longer production run, and the technology is more mature, giving users more pixels and higher quality images. CCD sensors, though, consume more power, nearly 100 times that of the CMOS sensor and can often be more expensive (Karim Nice, 2020).

CMOS sensor have a pixel array that is comprised of transistors situated directly next to one another. Because of this arrangement, light sensitivity can be an issue and the images are susceptible to blooming and other saturation problems. The read noise is typically not as low as that of the CCD sensor. CMOS sensor consume little power, has a long battery life, and are easily manufactured, making them an inexpensive alternative to CCDs.

While the image quality is better in a CCD sensor, the battery life and power consumption is appealing for this project. Additionally, the price of the CMOS sensor cameras is in budget while the CCD cameras are far more expensive. Though knowing the difference and the pros and cons related to both help make educated decisions based on the capabilities.

4.3 Zoom System

This section covers investigation into the properties of the zoom system to be used in the project and the considerations that are to be made in this area.

4.3.1 Zoom Lens System Properties

Zoom lens systems are a collection of lens groups, where each group has their own function within the system. The entire system creates an image with a magnification that is equal to the product of the magnifications of the individual groups. One or more group moves along the optical axis, changing the magnification of the individual group and therefore the entire system.

$$magnification = m'_1 m'_2 m'_3 \dots m'_n$$

When designing the zoom lens system, the first group's magnification is always considered zero, so the focal length is used instead. The image plane remains the same in a zoom system, but as the groups move, the focal length of the system varies continuously. The effective focal length of the system is then the product of the first group's focal length and the remaining group's magnification, at any position in the zoom.

$$effective\ focal\ length = f'_1 m'_2 m'_3 \dots m'_n$$

The zoom ratio, γ, also known as the zoom range, is the ratio of the max focal length to the min focal length attained by the zoom of the system. Small zoom range corresponds to γ range between 1-2, medium zoom is γ between 3-12, and large zoom is where γ>12. The larger the zoom ratio, the more complex the lens system must be for significant performance.

The groups of the lens system are named for their function. There are two consistent groups spanning a wide range of design types. These groups are the variator and the compensator. The variator typically moves linearly, while the compensator generally moves nonlinearly. The nonlinear path that the compensator move in is called the cam curve. The variator controls the zoom magnification of the system, while the compensator keeps the image plane stationary. Careful attention must be given to the internal magnification of the design, otherwise situations can easily arise where multiple groups devolve into variators which increase the possibility of discontinuity. Other lens groups include fixed, moving, focusing, and field correcting groups, all of which provide unique function within the system.

Optically compensated zoom was one of the first developed zoom system types. In this configuration, both the compensator and the variator moved in the same way, preventing clear images at all positions through the zoom range. Also, there are fewer elements which cannot sufficiently minimize aberrations. Though seldom used today, optically compensated zoom is an important historical concept that led to mechanically compensated zoom, commonly used today. Mechanically compensated zoom allows the compensator and variator to move autonomously with different and optimized motion paths.

Assuming a thin lens design, the conjugate changes when any of the lens groups move.

$$object\ to\ image\ distance = f'(2 - \frac{1}{m'} - m')$$

A main concern when designing a lens system is the aberrations of the image caused by the series of lenses. Distortions in the image emerge from rays not converging to one focal point due to the limitations of the lenses and the system. Accuracy in image after passing through the zoom system is crucial for correct intensity profiles and collected data.

4.3.2 Afocal vs. Focal Systems

Afocal systems involve two or more lenses where the input light and the front focal point are located at infinity. This type of configuration is common in beam expanders, telescopes, and binoculars. In a two-lens configuration, where zoom is not factored and the magnification is unchanging, the rear focal point of the first lens and the front focal point of the second lens coincide. The incoming rays are parallel to the optical axis in the object space, and the output rays in the image space are parallel to the axis but conjugate to the incoming rays. The transverse and longitudinal magnification do not change in this type of set up. Afocal zoom systems do not focus the light, rather, simply changes the size of the incoming beam.

Focal systems are optical systems where all incoming rays are focused to a particular focal point. Even rays originating at infinity are focused to the focal point in this type of system. Focal systems have a consistent magnification, though are able to resolve high quality images.

Afocal systems are consistently used in zoom systems, though require a focusing lens behind the system to create a clear image.

4.3.3 Two–Group Zoom

The most basic, conceptually, configuration and the best starting point when designing a zoom lens system is the Two-group zoom. A two-group lens system refers to a zoom design only containing two groups. These two groups are the compensator and the variator. By changing the spacing between the two components, t, the optical power, Φ, of a system in air is given as:

$$\Phi = \Phi_A + \Phi_B + t\Phi_A\Phi_B$$

There are four possible configurations of lens groups, where N is negative optical power and P is positive optical power. These configurations are PP, NN, PN, and NP. The NN configuration cannot work, as it is unable to focus collimated light. The three remaining configurations, the PP, PN and NP arrangements, are conducive to the zoom lens system design. In these arrangements the first group is considered the compensator and the second group, the variator.

Though PP configurations can provide zoom, they are undesirable due to the systems length. The zoom ratio is small, while the barrel length is large, making it impractical for most applications.

The PN configuration, usually called a telephoto lens, is compact with a minimal barrel length. However, PN type constructions have a limited field of view and limited zoom ratio, and it does not correct for aberrations sufficiently. Small zoom range is ideal for this configuration. This type of design is often employed in photography applications.

When designing zoom systems, wide angle positions (semi- angle coverage >20°) need large front group diameter. The NP arrangement forces the entrance pupil to be located nearest the front group, overcoming this difficulty. The NP configuration allows for a large field of view, large zoom ratio, and favorable aberration compensation. Still, the NP design is not compact as the back focal length is far larger than that of the PN arrangement. In addition, the second positive group typically result in diameters that are at least as thick as the first negative group, which is not ideal. Rather, it is better to consider PNxx arrangements, with lens groups that decrease in diameter, as it is more advantageous in mass and movement. Common in compact PNxx type systems,

added aperture stops near the front group allow wide angle issues to be overcome, however, it requires that the stop also move during zoom.

Two-group zoom designs are limited in design freedoms because the choice of optical power for both the compensator and variator are constrained. For the two-group system with an object at an infinity, the light must be collimated, and the system must provide focused light. Adding additional lens group(s) so that there are lens groups on both sides of the image kernel, the light is no longer required to be collimated, and the variator and compensator can then receive and deliver convergent or divergent light.

While two-group zoom is not as robust or complex as larger group systems, sharp images can be attained, and first order aberration requirements can be achieved. Higher order aberrations are a concern however in this type of lens arrangement.

4.3.4 Three–Group Zoom

Three-group zoom lens systems offer more design freedom and flexibility than its two-group counterpart because of the added complexity in lens groups. The three-group system allows for larger zoom ratio than two-group zoom. Typically, arrangements are that of NPN and PNP Donders telescopes. A Donders telescope is an afocal three-group system where there is one fixed prime lens in addition to the variator and compensator groups. The prime lens holds the location of the image plane stable and is usually located in the rear of the system.

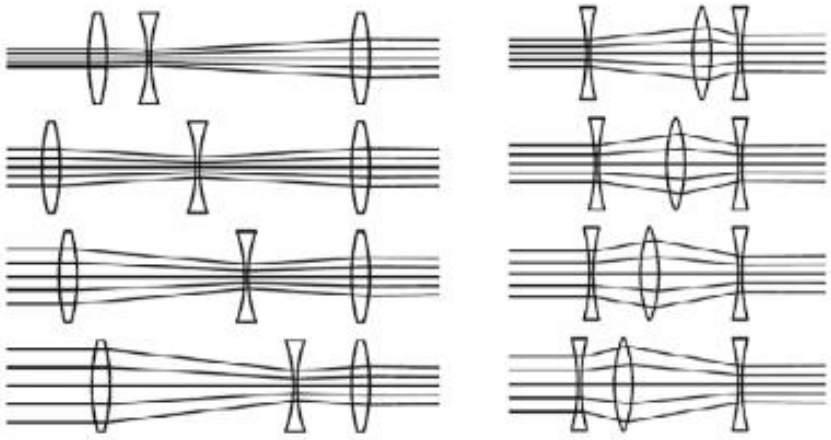

Figure 3: lens systems where incoming light is from the left, and outgoing light to the right. The camera in this type of system would lay behind the third lens to the right of these set ups. PNP lens configuration, left and NPN lens configuration, right Donders type telescope. Both these lens configurations are afocal. Taken from (Sasian 2019)

Fourth order aberrations can be corrected in this configuration, as three-group zoom systems has more complex lens groups and group design, than the two-group arrangement. Spherical aberration, astigmatism and coma can be corrected at the limits of the zoom by adding complexity to the lens groups. Aberrations can be overcome simply by splitting the singlets into multiple optical elements, commonly doublets or triplet, but some designs utilize more. More control of the aberrations comes at the expense of the systems simplicity.

Several considerations effect designs of three-group zoom systems. As complexity increases in each group, they then become thicker. In this case, overlapping lenses must be avoided. Additionally, the position of the compensator and its cam curve require careful attention, as the zooming mechanism cannot overcome steep changes quickly.

4.3.5 Four–Group Zoom

Four-group zoom lens systems increase the design flexibility because of the increase in complexity of the groups in addition to adding a focusing group. The focusing group is the first lens group in this type of configuration. This group maintains the conjugate distance to the following kernel groups.

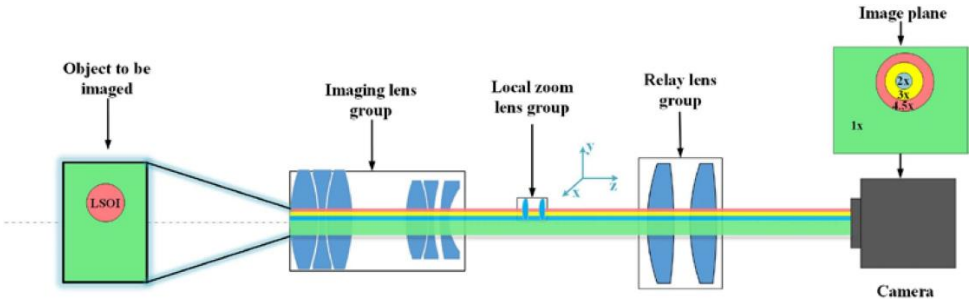

Figure 4: Four-group zoom lens configuration with camera and image plane design

The four-group zoom system increases the zoom ranges as well as improves the resulting image quality. Four-group systems are the best when the design is used to meet specific focusing requirements.

An interesting effect that can arise from the addition of the focusing group is called breathing. It occurs because this group inherently changes the field of view of the following lenses. This can create unnatural movements of bodies within the object plane and can be unacceptable in applications of high movement or detail-oriented imaging.

4.4 Light Collecting Plano Convex Lens

A large concern of the design is the ability to collect as much of the diffused light of the laser reflected from the diffused surface into the optical system. The initial approach was to have the front lens of the zoom system to act as the collecting lens but due to budgetary restrictions the optics for the zoom system will be too small to act as a collecting lens. A collecting lens is typical a large diameter plano convex lens which will be able to collect a large array of the light rays and focus them to its focal length. There are some restrictions and trade offs which must be considered when selecting the proper lens for the design. Since all real lenses have some thickness and are not the ideal thin lens the focal point is calculated using the following equation where R is the radius of curvature and n is the index of refraction. The material for the lenses being looked at is N-BK7 which has a refractive index of 1.5195 at a wavelength of 532 nm.

$$f = \frac{R}{n-1}$$

The F-Number, lens diameter, and numerical aperture of the lens are the main properties which are taken into account when choosing the best light collecting lens. The diameter of the lens and its corresponding focal length are the first variables which are examined with a collecting lens. A larger diameter lens will be able to collect more light versus a smaller diameter lens. The relationship between focal length (f) of the lens and its diameter (D) are what dictate the F-Number of the lens. This relationship between diameter and focal length is shown below.

$$F\# = \frac{f}{D}$$

An increase in diameter of the lens will in turn lower the F-number. Essentially this means that the lens will be able to collect more radiant flux (ϕ_c), but there is a tradeoff. The amount of radiant flux collected by the lens is the inverse of the F-number squared as seen below.

$$\phi_c = \frac{1}{(F\#)^2}$$

Although more radiant flux is collected when the F-number low the radiant flux information collected may introduce undesired affects into the system including aberrations. The aberrations introduced will negatively impact the

quality and coherence of the light rays entering the system. Any undesired effects of the light rays entering the system from the collecting lens will only be compounded on as it travels through the zoom system to the CMOS sensor. It is crucial to have the proper collecting lens that will be able to collect enough radiant flux from the diffused reflected light while in turn not adding negative qualities to the wave fronts of the light travelling through the lens. In reality the convex lens will have some thickness to it which will refract the light, the thinnest possible thickness is being sought for the lens. The lenses that are being looked at are from Thorlabs and are uncoated N-BK& Plano convex lens. Uncoated lenses do have the potential to cause reflection interference which can affect the propagation of the light through the system. A coated lens would be more suitable but are out of budget for the design. The undesired effects of the uncoated lens will be analyzed through zemax first to determine the appropriate Plano convex lens to purchase. This is still in the works and will be decided before the submission of the final paper.

4.5 Laser Source

For testing the functionality of this optical design, a laser light source is required. The two wavelengths which were being considered were 632 nm and 532 nm. A high energy handheld red laser pointer with a wavelength of 532 nm and a high energy handheld green laser pointer of 632 nm. The red lasers is classified as a class 3a laser and the green laser is classified as a class 3a or 4 laser dependent upon the wattage. A class 4 laser is considered hazardous and will require safety goggles and equipment to avoid eye damage or other harm to the body whereas a class 3a laser will still need eye protection but burning is not of concern. The green laser was ultimately chosen for a multitude of reasons. The CMOS camera being used for the design is much more sensitive to green light than that of red light which is the main reason for choosing the green laser. Since the device is collecting light from a diffused surface the intensity will already be much lower, so using a wavelength which is more sensitive for the camera is the ideal choice. When it comes to costs and searching around on the internet the red lasers are cheaper than the green lasers. The pricing differential is not too significant whether buying the red laser pointer or green laser pointer of the same wattage. Where the price does significantly increase is when the wattage is increased and also the quality of the antireflective coating and crystal within the laser cavity. Regardless of which light source is chosen the costs will stay within budget. The green laser is a shorter wavelength, ultimately meaning higher energy per photon versus the red laser which will make the green laser more efficient for the longevity of use during experimentation. Also, the fact that the green laser pointer is handheld and portable makes testing the device in different environments much more accessible. So that the stretch goal of outdoor use can also be experimented. How the green laser lases is also significant. An

infrared beam of 808 nm passes into a neodymium-doped crystal. This neodymium-doped crystal will be excited by the infrared beam and expel the extra energy as the 532 nm green light. Along with the green light is a longer infrared light of 1064 nm. The laser pointer is designed with reflective filter coatings to block out the 1064 nm wavelengths and only allow the 532 nm wavelength to lase out of the laser pointer device. It is important that the quality of the laser and its components be experimental grade and not just for everyday pointing use. The types of filters and antireflective coatings to block out the infrared light must be high grade to avoid high levels of infrared light from being transmitted while experimenting. The additional infrared light signal can be considered noise and although filters will be placed inside of the device, the less undesired noise the more accurate the experiment.

4.5.1 Laser Comparison

Listed below are a few green laser pointers that were examined for purchase.

Brand	Wavelength	Power	Class	Price
Laserpointerpro	532 nm	50 mW	IIIb	19.99 $
Laserpointerpro	532 nm	1000 mW	IV	79.99 $
BigLasers	532 nm	500 mW	IV	379.95 $
Laserpointerpro	532 nm	5 mW	IIIa	19.99 $
GX1	532 nm	100 mW	IV	100.00 $

Table 3: Laser pointer comparison chart

The laser pointer that has been chosen for the project is the Laserpointerpro 5 mW 532 nm green laser. This laser pointer should have enough power for lab applications and for experimentation. The perk of this laser compared to the others is it is a class IIIa so it will be safe to use in public and in the lab setting. Another reason this is the right choice to start with is because it is unlikely to burn the diffused board used for experimentation. If through experimentation it is found that the 5 mW laser is not sufficient and is attenuated too much through the optical system than the next choice would be the 50 mW laser. The 50 mW laser is a class IIIb which is still safer than the class IV and is comparable in price to the 5 mW laser. The class IIIb will not penetrate as deep as a class IV and should not burn the diffused surface. These two laser pointers should have enough power required for the experimentation while also being composed of reliable and durable components that will not allow an extreme amount of infra-red-light leakage. The Laserpointerpro brand also has an impressive battery lifetime which should be sufficient to use throughout the entire course without having to purchase a new battery. There is an option to purchase

additional safety equipment and lenses with each laser, which is being chosen as a safety precaution as being funded personally and not out of the budget of the project.

The aforementioned approach has changed because of a more in depth look at the quality of the products. When looking at the sites for laserponterpro the reviews all were negative and dictated that the quality of the product is not to the standard necessary to perform experimentation. Instead, a 50 mW laser from a trusted site has been chosen for experimentation. The 5mW laser as previously chosen as the starting point will not transmit enough power. The power needs to be higher (10x) higher to transmit enough intensity to the camera for a reading. A 532 nm green laser dot module 50 mW diode has been chosen for experimentation instead. This laser will need to have a battery designed for it. The working voltage of this diode is three volts, and the duty cycle is 45 seconds ON, 15 seconds OFF. The laser costs 19.99 on Amazon. This laser will be used for initial testing and if a different laser is necessary, it will be purchased.

4.6 Optical Filters

An optical filter is typically made up of film materials which may be stacked with a specific thickness which have unique properties allowing a selected band of frequencies of a travelling optical signal to pass through. The outer band or bands of frequencies outside of the desired band are a blocked by absorption, interference, or reflected. Whether certain frequencies of the propagating wavefronts are absorbed, reflected, or interfered with depends on the type of optical filter and the materials it is made from. Optical filters also are used to split up an optical frequency into its many differing wavelength components for thorough analyzation of a single wavelength of an optical signal. Optical filters which are angle sensitive act similarly to a prism or grating. These types of filters can be used in applications which require spectroscopic analysis or the splitting of frequencies throughout an optical system. An optical signal propagating through an optical cavity, sent over some pre-determined distance without being directly coupled will experience some type of noise or interference throughout the length of travel. This extra noise and interference can completely destructively interfere with the signal or alter it to the point that the receiver on the other end cannot decipher the original signal sent. A way to repair the altered signal back to its original form is to place optical filters within the path of the optical signal as it travels through the optical system. What type of optical filter used depends on the application and the type of light source being emitted at the input of the optical system. Optical filters are used in a variety of applications including but not limited to machine vision, spectroscopy, microscopy, chemical analysis, and imaging. The optical filters working properties that are most important in deciding the appropriate filter for a design project include the optical filter’s central wavelength, bandwidth, full width half maximum, blocking range (optical density),

slope, cut on wavelength, cut off wavelength, edge steepness, and ripple. Optical filters also have certain physical properties as well which determines the propagation of the light signal travelling through. These physical properties are related to both the thickness of the filter and the materials which are used to create the optical filter. There are many types of filters available on the market including long pass filters, short pass filters, bandpass filters, notch filters, neutral density filters, and interference (dichroic) filters. Each type of filter functions with unique properties to block undesired frequencies along specified bands of the electromagnetic spectrum. Before choosing a particular type of optical filter for a design the working properties and physical properties of the optical filter must be understood. With this knowledge one can confidently decide the proper type of optical filter that will best suit the design or experiment being conducted. There are many ways to approach using optical filters in an experiment. Optical filters can also be stacked in a parallel construct to selectively choose a particular bandwidth region of wavelengths to pass through the optical system. Both a short pass and long pass filters stacked will create a unique bandpass filter which will be designed to have a particular bandwidth region of selected frequencies which can propagate through. Filters can be placed anywhere along an optical system. Optical filters may be placed at the input of an optical system for filtering out certain frequencies of light from an input source with either a narrow bandwidth (laser light) or broader bandwidth (lamp source or L.E.D). Optical filters may be placed within the system in front of certain optical equipment to filter out generated frequencies that are created through excitation within the system (this is where the optical filters for this design are placed). Optical filters may also be placed near the end of the optical system. This is generally to filter out any unwanted frequencies at the output, so the signal at the receiver has can reconstruct the original signal sent or decipher the newly created filtered signal

4.6.1 Optical Filter Working Properties

Optical filters have many unique properties which make them crucial to be used within many design experiments. The cut on wavelength of an optical filter determines where the wavelength transmission will begin to increase significantly from an area of attenuated frequency transmission to a frequency area of very high transmission. At this threshold the transmission will increase to about 50% transmission. Typically, $\lambda_{Cut\text{-}On}$ is used to denote the cut on wavelength. The cut on wavelength is also referred to as the 5% absolute transmission line of the optical filter transmission spectral band. The cut on wavelength is the edge parameter of a long pass optical filter. The cut off wavelength of an optical filter essentially is the opposite spectrum from the cut on. The cut off wavelength determines where the wavelength transmission will begin to decrease significantly. At the cut off threshold the transmission will begin to decrease by about 50%. $\lambda_{Cut\text{-}Off}$ is used to denote the cut off wavelength. The cut off

wavelength similar to the cut on wavelength is also referred to as the 5% absolute transmission line of the optical filter transmission spectral band. The cut off wavelength is the edge parameter of a short pass optical filter. The cut on and cut off wavelengths of a bandpass optical filter will determine the central wavelength. The central wavelength is the center passband or notch of the optical filter. A notch is the band reject region of an optical filter. It is the opposite of the passband, where only the notch region will be rejected or absorbed. The central wavelength is used to describe both a passband filter or a notch filter. The central wavelength can be determined by using the following equation:

$$\frac{2(\lambda\text{Cut}-\text{On})(\lambda\text{Cut}-\text{Off})}{\lambda\text{Cut}-\text{Off}+\lambda\text{Cut}-\text{Off}} = \text{Central Wavelength } (\lambda_{CW})$$

The bandwidth of the bandpass filter is the allotted band of wavelengths which are able to travel through the optical filters. The bandwidth of bandpass filter will be between the two edges of the cut on and cut off wavelengths. This region of the spectrum is determined by the absolute points on the spectrum that the optical signal will be able to achieve > 50% transmission. The width of the bandpass filter divided by the central wavelength and multiplied by 100 will give the band width as a percentage. The width is crucial for design and determines how many what band of wavelengths will travel through. A broader bandwidth will allow more frequencies to travel into the system whereas a narrower bandwidth will only allow a very precise range of wavelengths into the system. A laser has a much narrower band width than that of an L.E.D or lamp source. The full width half maximum is the region half power is transmitted through the system. This parameter is used to describe band pass filter and relates to the two edges of the pass band. The blocking range of an optical filter is the spectral area of frequencies which are attenuated out by the filter. The blocking range is also directly related to the optical density of the optical filter. For a bandpass optical filter, the blocking range region would be the spectral area outside of the pass band, whereas for a notch optical filter this region would be the spectral area inside of the band. The blocking range of the optical filter is denoted as the optical density and can be calculated using the following equation:

$$Optical\ Density\ (OD) = -log_{10}(Transmission)$$

Optical density is traditionally notated as a number falling from one to eight. One being the least optically dense and eight being the most optically dense. The higher the optical density the less light that will be able to travel

through the optical filter in the block band regions. For example, an optical density of one will allow ten percent of the light to travel through the optical filter. Whereas an optical density of two will allow one percent of the light through an optical filter. This scale is logarithmic with each increase in optical density value, will have one tenth the amount of light able to travel through. When stacking optical filters with their own optical densities it is easy to assume that the overall density would just be the addition of the two optical densities. Optical density is not linear in that way and will only slightly increase the optical density. For example, creating a bandpass filter with a short pass filter and long pass filter of optical density 2. The overall optical density will only be slightly over 2. Selectively placing the optical filters a calculated distance from each other can increase the optical density and is required for interference filters. The optical density parameter is crucial to design and can affect how much of the signal is attenuated. If the original signal is quite low in intensity, a high optical density may cause little to none of the signal to be able to be propagate to the receiver. Optical filters can either absorb undesired spectral frequencies, reflect undesired spectral frequencies, or use interference through multiple layers within a single optical filter of desired thickness. Slope is a variable related to the specifications of an edge filter (long pass and short pass optical filters). The slope is indicative of when the transition takes place from peak blocking of frequencies to peak transmission of frequencies as the signal travels through the optical filter. The edge steepness of an optical filter is the calculated distance between the region where the optical density is greater than six (essentially the non-transmittable region blocked by the short pass, long pass, or band pass filter) and the point at which 50% transmission occurs on the spectrum. Edge steepness is pertinent to edge filters such as short pass, long pass, and band pass optical filters. The edge steepness is related to how quickly a transition between the transmission region of the filter occurs and its complimentary optical density region. Edge steepness can be calculated using the following equation:

$$100 * \frac{|\lambda(50\%transmission) - \lambda(Optical\ Density)|}{\lambda(50\%transmission)}$$

Ripple relates to the fluctuations within the frequency band of the optical filter. This band can either be a pass band of stop band. Ripple directly effects the performance of an optical filter system. Ripple is measured in dB and is ideal to be as low as possible for the best performance.

4.6.2 Optical Filters Physical Properties

Optical filters physical properties are both the thickness of the optical filter itself and the material used to make the filter. The thickness of the optical filter is directly related to the transmission percentage of the optical signal which travels through. A filter can be one of either extreme, too thick or not thick enough for the experiment. The thickness parameter is important to take into consideration when dealing with an optical system with many optical devices where the light signal will be travelling through. The materials refractive index along with the thickness will control the behavior of the optical signal propagating through. The more optical devices introduced into the optical system such as lenses, gratings, beam splitters, etc. the more the optical signals intensity will be attenuated. It is important to know what power of the light signal is required at the output when deciding which types of optical devices to use within the system. If there are so many optics that the final light signal at the output is too weak to get any pertinent reading, then the experiment will not result in accurate experimental data to be analyzed. The filter can also be too thin with a low optical density and not block out the undesired frequencies sufficiently. When this occurs there will be bleed of frequencies at the output signal which in turn can cause the inability to decipher an original optical signal from both noise and undesired frequency interference. Thickness of the filter is also considered when stacking optical filters. Stacking optical filters will allow for more control over which spectral frequencies are allotted to travel through the system. Stacking of the optical filters will result in a thicker optical filter and a higher optical density. Each optical filter have their own transmission percentage. When these optical filters are stacked the transmission percentage will also stack and inevitably determine the total transmission of the pass band for the optical filter system. The optical filter system as a whole unit, when there are no non-linear optics involved is a linear system, resulting in a linear transformation and transmission percentage calculation. For the following example two optical filters will be denoted as optical filter one H_1 and optical filter two H_2. Since the system is linear it does not matter which order the optical filters are stacked in because the end result of transmission will be the same. This also applies to differing types of filters which do not have non-linear behaviors.

$$H_1 * H_2 = H_2 * H_1.$$

It is necessary to take this into account when stacking optical filters for if the transmission of one is much lower than that of the other it will lower the

transmission of the optical signal significantly. The following equation can be used to calculate the total optical transmission through the system:

$$H_{1(transmission)} * H_{2(transmission)} = H_{Total(transmission).}$$

For example, if optical filter one (H_1) has a transmission rate of 65% and optical filter two (H_2) has a transmission rate of 85%. The total transmission rate of the two stacked optical filters in this optical system would be equal to 55.25%. That is almost half of the original signal being transmitted through. This again is why it is necessary to be aware of the transmission rates of all optical devices within the system. Whether the filters are starting at the input, in between, or at the output of the optical system, the amount of optical signal travelling through is attenuated 50% before travelling through any other optical devices within the optical path length. The material used in creating the filter will dictate the propagation characteristics of the optical signal as it travels through the filter. Filters can also change the polarization of the wavefronts travelling through it. Optical filters thickness selectively controls the transmission of the optical signal through the optical system, and the material controls the refractive nature of the optical signal. Most filters are typically composed of either a glass or a polymer. The material used is important and will directly affect the design aspect of creating an optical filter. Optical filters are passive devices and will not consume any power from the battery source of the design.

4.6.3 Types of Filters

There are many different types of optical filters on the market today which can be designed to match any necessary requirements for experimentation. These types of optical filters include long pass filters, short pass filters, bandpass filters, notch filters, neutral density filters, absorptive filters, interference (dichroic) filters, and refractive optical filters. Each type of filter may be used for differing applications or within the same system with multiple differing optical filters. Different types of optical filters may also be stacked to design a particular desired output spectrum. Each type of optical filter has different working properties and are composed of different materials. The material used will dictate how the propagating light will be refracted as it travels through the optical filter. Long pass filters are edge filters which

Reflection of spectral frequencies typically takes place when a signal will be directed on another path within the optical system. This typically happens when an optical beam is split within the optical system by the optical filter itself. The wavelengths can be split and sent into differing directions for experimentation that is needed to separate wavelengths. When the signal is split there are angles of incidence that must be considered which adds another

component to the equation of characterizing the behavior of the optical system. Absorption is typically used when reflectance is not necessary for the optical system (most commonly used for applications). Absorptive filters typically are colored filters which absorb particularly spectra by design ranging from far U-V to far infrared. The thicker the absorptive filter the more effective it becomes by being able to absorb more of the undesired wavelengths within the optical signal.

Absorptive filters traditionally are composed of glass which is tinted using both organic and inorganic dyes which aid in capturing the undesired optical signal frequencies and allow the desired optical signal frequencies to transmit. The absorption of the undesired wavelengths is converted into heat within the optical filter. These types of optical filters do not depend on angle of incidence. Absorptive filters are ideal to use for experimentation when a particular band of frequencies that is sought or when a reflective filter will introduce unwanted noise into the system. Absorptive filters are typically less expensive to fabricate. While being more cost efficient, they are limited to particular spectrums which can cause designing to be difficult if the desired filtered region is not compatible with absorptive spectrum that is available.

Interference (dichroic) filters are optical filters which are designed to have several layers within the filter of a particular thickness. These layers are traditionally thin films which are stacked on top of each other and are angle sensitive. Every layered component of an interference pattern must be precise to get the desired spectrum on the output of the optical filter. The thickness of each sub layer must be the exact dimension required for the desired spectrum to be produced. As the optical signal travels through the filter the edge of each sublayer will reflect some of the incoming light just perfectly to constructively interfere and filter out the undesired wavelengths. This process continues to happen through each sublayer until the final output is the desired optimal optical spectrum. Any slight mis calculation of thickness will undoubtedly cause the optical signal on the output to be slightly off the required spectrums central wavelength. These types of filters are more expensive and are typically used in specialized experimentation.

Neutral density filters are optical filters which suppress all wavelengths of light evenly by a certain optical density degree. These types of filters are used when the intensity of the light signal needs to be decreased by a certain percentage. Neutral density filters are also used to block out ambient light from a detector during experimentation.

Long pass optical filters are edge filters which by design will attenuate shorter wavelengths while allowing longer wavelengths to transmit through. Longer wavelengths lie on the lower energy region of the electromagnetic spectrum. These optical filters have a cut on wavelength and a rejection wavelength range. Long pass optical filters are typically not sensitive to angle of incidence which makes them ideal in experimentation that is not sensitive to the angle of which the light signal propagates through the optical system. Long pass

optical filters are ideal for applications when higher energy shorter wavelengths must be attenuated out of the optical system.

Short pass optical filters are also edge filters that attenuate longer wavelengths. Short pass optical filters allow transmission of wavelengths which are shorter or toward the higher energy region of the electromagnetic spectrum. Short pass optical filters have a cut off wavelength and a rejection wavelength. Similar to the long pass filters, short pass optical filters are also not sensitive to the angle of incidence making them ideal for experimentation that is not sensitive to the angle of which the light signal propagates through the optical system. Short pass optical filters are ideal for applications when lower energy longer wavelengths must be attenuated out of the optical system.

Bandpass optical filters are a combination of both an optical short pass filter and optical long pass filter stacked together. These optical filters have a bandwidth of wavelengths which are able to be transmitted through. Outside of the edges of the band pass region the optical density begins to increase and the outer spectrum will be rejected. Bandpass optical filters have a center wavelength where transmission is the highest. Depending on how the bandpass filter is designed the transmission percentage will begin to lower on both edges until it reaches the cut on and cut off regions of the pass band. Bandpass optical filters also have a full width have maximum cut on and cut off wavelengths. Bandpass optical filters are not sensitive to the angle of incidence of the incoming light signal. Bandpass optical filters are ideal for applications that need a specific bandwidth of transmission such as fluorescence applications, spectral radiometry, machine vision and laser line separation. The bandpass filter is what will be designed for this project and ideally will have a narrow bandwidth of a few nm width and filter out all other frequencies with an optical density of at least 2.

4.7 Light Source

The light source used in experimentation will be a full visual spectrum light source. These types of light sources emit light similar to the spectrum of the sun and will aid in testing outdoor application of the device within a laboratory setting. The full spectrum lights are rated based off of their color rendering index. Color rendering index of a light source refers to how closely the emitted light spectrum is to sun light or commonly referred to “natural light”. Quality full spectrum light bulbs typically have a color rendering index ranging from 90% to 96%. Full spectrum lights use filters of wavelengths that range including the full spectrum from ultraviolet to infrared, mimicking natural light. There are also similar spectrum lights which only produce the visual spectrum for testing devices where the eye may be used. Another important factor is the number of lumens that the

light bulb emits. The higher the lumens the higher the quality of the light bulb and its emission spectrum. As a reference the sun gives off roughly 16.24 quintillion lumens that reach Earth. To scale that in a lab setting is nearly impossible, but a full spectrum light with at least 800 lumens will be the starting point for experimental testing. With this type of light bulb artificial natural light will be introduced to the system within a lab setting and then it can be compared to outdoor settings at a later time. This approach will guide how to the properly differentiate the frequencies that are entering the device from the wave fronts reflecting off of the diffused surface versus the full spectrum emission from the light bulb. The optical filter system will filter out the majority of wavelengths outside the cut on and cut off regions of the narrow bandpass of 532 nm. For the stretch goal the device will be outdoors and exposed to the blackbody radiation of the sun which emits all frequencies from ultraviolet to the far infrared. Due to the Earth's natural barriers, portions the majority of ultraviolet frequencies do not reach the earth. The frequencies that mostly penetrate the earth are the visible spectrum to far infrared. Both the 632 nm wavelength and 800 nm wavelength of the sun's spectral irradiance will propagate and mix with the diffused laser light into the system. The aperture size at the input will be tested to find the optimal window of allowed light irradiance into the device for best results. There are many full spectrum light sources on the market for laboratory simulation of outdoor testing. The full spectrum light bulb will be attached to a portable lamp that can be used in differing settings. Analysis of the experiment will also take place using the incandescent lab lights to see how differing light sources affect the light collection by the device and the corresponding data collected by the camera. When the lab space is not in use by other students the full spectrum light will be used and the lab incandescent light will be turned off. After looking around online at the many options for a full spectrum light source, the best option found with a sufficient number of lumens is sold on amazon. The light bulb is an eleven-watt bulb which produces 800 lumens of light. It is a NorbSMILE full spectrum light bulb and costs 19.99$. This bulb will be used initially for testing and if a brighter light is required than it will be purchased.

4.8 Battery

Different specs of a battery are measured and compared along this paper, where it will show the steps taken to choose a battery efficient, and powerful enough to energize our system and all its components. Next, we will show the engineering investigation done, which guided us towards understanding the important values to calculate and compare for a smooth product search.

Along with calculating the overall consumption of power by our system, our group made an effort to understand what type of battery chemistry would match well with the area where the system will be utilized. Understanding how to calculate a battery's capacity, in order to forecast a battery life cycle, as well as the amount of time a device can be run without any interruptions. Some extra key factors which affect a battery and its efficiency are important to list and to also mention how these factors can be related to our system.

4.8.1 Battery Chemical Composition

Choosing a battery is a heavy task, because it’s giving life to our entire system which is looking for reliability and accuracy. Batteries are manufactured in many ways, two of the most common batteries in the market right now are Lead-Acid batteries and Lithium-ion batteries, the names being the chemical approach for each. A Lead-Acid battery brings a couple more variables to the design. The way this specific style of battery is implemented, it could bring some more physical adjustments to the system. It’s always important that there are specifications that cannot be surpassed. Knowing this, there still a great amount of Lead-Acid batteries in the market which could still be implemented into our system. On the other hand, Lithium-ion batteries are increasingly popular in the electronics circle. By using lithium salt to increase the efficiency of energy. This efficiency and other useful characteristics of this battery makes implementation with this battery favorable during the research process. Another important point (besides the values in the datasheet), Lithium-ion batteries are in the high price range. Careful research is going to be conducted in order to calculate a stable system with power supply that will not hinder the system. As a tip seen by professors and professionals, always overshoot the values.

4.8.2 Battery Capacitance

As we select batteries for our system, the battery's capacity is a key measurement for the system to have adequate power. Knowing the capacity for a battery for a fixed amount of time is key, to understand when the battery needs to recharge. The equation below allows us to calculate for the capacity when the current drawn and the time running are known.

$$C = x*T$$

Where C is for capacity, x is for current drawn and T is the time running. There are strategies that will allow us to perhaps get a longer life cycle than what the batteries promote. One of the strategies is to run the battery normally till its capacity hits 80%. The equation below extends the equation above for finding the battery capacity needed for some specific variables, and calculates the capacity needed for a battery to run efficiently till 80%.

$$C' = C/0.8$$

Where C' is the new capacity needed for the batter to run till it hits 80%.

4.8.3 Key Factors of a Battery

As mentioned in the previous section, there are a variety of factors that could affect the efficiency and the life cycle of the battery. First factor is the temperature surrounding the battery when in use. As the temperature increases there's a possibility for the batter to lose long term capacity. Keeping an eye on the temperature of the battery by adding a few temperature sensors will help us control the temperature and get a longer life cycle. Another promising feature of a Lithium-ion battery is that they require low maintenance and are not as delicate to temperature as Lead-Acid batteries.

A second factor is the rate at which a battery is discharged or charged. For high charge or discharge values, the battery life cycle and capacity rates will be affected. This happens because as you increase the discharge/charge rate it increases the temperature inside the battery damaging it inside. A third factor is the limit of the voltage as you charge it, typically a battery should not be charged to its 100% capacity, since it will decrease its charge cycles. One recommendation that was found during our engineering investigation was that it might be ideal to charge the battery to 85% of its capabilities.

4.9 Motor

One of the key features of our system is the freedom of movement of our camera. This is able to happen because of the motors. We've been investigating different types of motors, the top two in our list are a stepper motor and a servo motor. Two movements are going to be provided by whichever motor is chosen, both are going to be rotational movements. One motor will provide the force for the camera to rotate 180 degrees from left to right, the other motor will provide

the camera to rotate 180 degrees up and down. Each motor will have a shaft diameter of around 5 mm, where a timing belt pulley will be attached. A timing belt will be connected to the pulley attached to the motor, and a bigger pulley (around 80 tooth). This will provide a slower speed for each rotation and will also help control this rotation with more precision, since our camera will move small angles when searching for the laser. For our system we need our motor to move clockwise and counterclockwise, that way we can find the right position for the laser refraction. Depending on the chosen motor (stepper or servo), a different design will be used in order to make the back-and-forth movement possible, since each of these motors use extra components which allow the motors to function correctly. One key topic when investigating a motor is its power, we are shooting for an average of 36 Watts per motor, which will result in a total of 72 Watts for our system's motors. Along with power, holding torque is important, our system requires between 51 oz. in - 63 oz. in. These torque values will allow the system to maneuver smoothly without any stalls, when holding the camera. The camera will be size, power, accuracy, torque, and cost are some of the few key components when choosing a motor that will be right for our system.

4.9.1 Motor Sizing

In order to find the right size for each motor that will allow the system to move in each desired direction without any error, three main areas out of the system must be calculated. These are the load torque, load inertia and speed. Our system contains two different types of motions, along with different weights. For example, our overall system is going to be weighing an estimated 4.5 kg, which will be handled by the two large motors (M1 & M2). Our system will be designed to be a rectangular body of lengths of around 50 cm, with a width of around 17 cm. In order to create movement to the body of the system when it is stationary, it's important to be able to calculate the load inertia in order to take into account the amount of resistance against movement. investigating the amount of torque needed from the motor, we calculate the two components that will be present in the time of use. Frictional load will be observed at the point of contact and rotation, which is located at one end of the system. Both M1 and M2 will be placed along some gears which increase the torque. Friction can be measured at the axis, where all the weight of the system sits, adding some pressure to the contact point creating fractional load. As for anybody of mass, gravity plays a big role in systems where a load is lifted up, while also maintaining its position. As mentioned before, M1 and M2 are the larger motors out of the four, because it's holding the overall system. Not only the overall weight of the system will affect the gravitational load, but the distance where the axis of rotation is located, and the force given by the motors.

The following sections will go over each component that composite the system. As mentioned through this paper, the overall system will have the capabilities of rotating around two different axes. It will also contain a sub system, which will move two bodies of mass linearly, and independently. Our group is using a range between 11 Ncm to 45 Ncm torque size motors, each individual motor will be sized ideally to hold, start motion from a stationary position, and stop from a motion to a stationary position, at a fairly low speed. Using knowledge from previous sections, we calculate the moment of inertia of each load, along with each external force that will act on each individual motor. The motor must be selected specifically to sustain all these forces with a large enough torque, including a safety factor. Setting the right speed for each individual motor is a value which can reduce the required torque for our motors to reach, also reducing the cost for components. The following sections will calculate each motor's speeds, compare it with torque, and display numerically and visually the effects that both values have on each other.

4.9.2 Motor Speed

Speed is the third key element for the sizing of each motor. For our system, the speed at which the 'arm' rotates vertically or horizontally is not critical. For the 'arm' of the system, a reasonable angular speed is required for the load to move more smoothly. Our group understands that the rectangular casing protecting our entire system will not need movies at high speeds. Having this in mind, calculations for an estimated velocity will be conducted by using the previously mentioned equation which calculator the speed of an object;

Speed = Distance / (time - acceleration time)

Where, the distance the object covers is divided by the time it takes the object to get from point A to point B, subtracting this time by the time it takes for the load to reach a constant acceleration, or the acceleration time. Using the formula above, and by selecting the rectangular casing to rotate a distance of 2π radians. Also reaching this distance in a time of 60 seconds and an acceleration time of 2 seconds, to reach a constant speed. This results in an angular velocity 0.1083 rad/s for the rectangular casing. This means that ideally our system will move 0.1083 radians every second.

Now inside the filtering subsystem, we calculate the linear velocity that our motors M3 and M4 will need, in order to reach a specific constant velocity for the filters. Solving for the speed using the previous formula, with a target distance of 0.3048 m, to be covered by the load in 40 seconds, with an acceleration time of 2

seconds. This results in a speed of 0.008 m/s, having the load moving 0.008 m every second. Our system is does not have an urgency for high speeds rotation or translation, a reliable low velocity for each of these bodies of mass is acceptable, since the application where the system will be used, does not require quick acting movements Figure 5.1.6 illustrates the speed versus time motion profile, where the velocity and the speed to reach that velocity will be labeled.

4.9.3 Servo Motors

Servo motors are very popular for their precision and reliability, that is the reason our team had to look into this option, in order to open our options and compare prices with other motors. Servo motors are implemented as a closed loop connection, making them very efficient and reactive to feedback from the load being controlled. Servos can be divided into two different types, one being standard servos whose angle or rotation ranges from 0 degrees to 90 degrees. This type of servo can be useful for our system and can be implemented to create motion for the filter system. As it will be discussed in further sections, the filters will cover a very small distance compared to the other two motors which will give motion to the entire system itself. The second type of servo is continuous, this type will rotate their shaft in the range of 0 degrees to 360 degrees. As it can be assumed, having the versatility of rotating 360 degrees will give our system the freedom of rotating with no limit. Following our system idea, for the filter system, a continuous servo would not be as essential, as it is from the motors that add horizontal and vertical motion. One of the downsides of the Servo motors is the weight of the servo, meaning that in the case our system needs more torque, the weight of servo will increase more than the steppers. Also, servo motors can claim the price later relatively rapidly since the component itself is more complex than a stepper.

4.9.4 Nema 17 Stepper Motor

There are two options when it comes to a stepper motor, unipolar or bipolar. Both are promising for our system, since our system does not hold much weight. At this point, there is more interest in bipolar having a higher torque than unipolar. There is much interest in a stepper motor that averages a current of 3 amps, along with voltage of 12 Volts. This will result in a reasonable wattage, which can be powered with a 12 volt battery. We're also interested in the step angle of the motor, for our system we're looking for a 1.8 degrees step angle. This is important to know, since a stepper motor has to be implemented with a motor driver. By knowing that 1.8 degrees is equivalent to 200 pulses per revolution, we can program our driver to send signals to our motor appropriately.

Nema 17 is an example of a stepper motor that provides a compact design, averaging 42 mm all around (frame size and body length).

4.10 Gears

In order to aid the motor with the task to hold and move the weight which this system is composed of, technology investigation towards gears was conducted. There are many types of gears combinations which the group filtered through, in order to find the most efficient gear-motor combination. Understanding the values that physically affect a gear, will be key for when it's time to utilize two gears, where they will transfer energy to one another. Each time power is transferred from one gear to another, one of three stages is happening; it increases speed, increases force, or changes direction. An important fact about gears is transferring power from a bigger to a small gear will increase speed, as well as decrease force. Vice versa, if power is transferred from a small to a bigger gear speed decrease, but force increases. As mentioned earlier, there are adjustable values or variables which affect the physical specifications for a gear. We will be describing the purpose of these specifications and how they affect the performance of gear combination. This information helps our group to set an understanding and combine it with our project requirements to set a doable goal.

4.10.1 Torque

Our project will be utilizing three different motors, which will be holding and moving different amounts of payloads. As we begin our investigation, we can approximate using three different types of motor sizes, because as we will show along this presentation, our system will hold and move different types of weights, which is a main priority for a motor decision. Torque is the force which will allow the motor in a joint of the system, to be able to hold the link which includes the payload. Torque can be calculated by using the following equation;

$$t = r * F \qquad \text{(Eq.4.10.1)}$$

Where, r is the radial distance from the axis of rotation and the force vector, and F is the force applied at that distance. This shows torque being a crucial value to have in consideration when picking a motor. Our system needs to hold a certain amount of weight when receiving the laser beam, and also be able to hold the position for around 20 minutes without any errors. With that being said, our system also needs to be able to move and carry the payload weight without any "stalls", which is when a motor misses a step when in rotation carrying payload. Having this in mind, careful calculations of the torque have to

be taken, as the system can fail to hold the right weight and damage the equipment. The gravitational force, and the angular acceleration are two important values for our needed torque value of our system's motors. By understanding what each of these values affected, we will be able to make an informed decision about what motors to buy for the prototype stages, and final design.

4.10.2 Gravitational Force

Force as shown in equation 4.10.1, can be described also as;

$$F = m * g \qquad \text{(Eq.4.10.2)}$$

Where, m is the mass of the payload and g is the gravitational acceleration. When talking about our system, the force is coming from the casing that is sounding the camera, filter subsystem (including a motor), and any connections needed. Meaning, we need to size the motor to contradict this gravitational with some room for errors. The sketch below shows a simple example of a force on a rectangular body with its axis of symmetry in the middle of the body. This simple sketch is very useful, because this movement is one of the three that our system will showcase. In order to hold the rectangular body (our camera connected to our filter subsystem) in an angle, the motor's torque will need to work against the gravitational force.

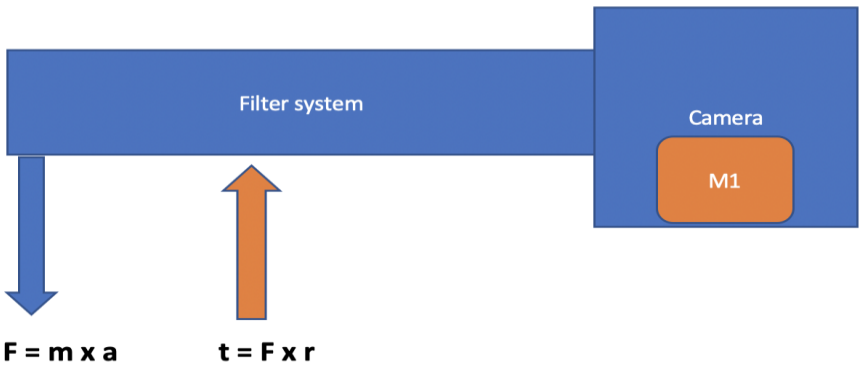

Figure 5: Force on a rectangular body with symmetry in middle of body

4.10.3 Angular Acceleration

Along with gravitational force, angular acceleration is one of the components that will show the required torque for our system's motors. Angular acceleration gives the system the ability to add movement to a link, and payload. Torque can be calculated from the following equation.

$$t = I \times \alpha \qquad \text{(Eq. 4.10.3)}$$

Where, I is the rotational inertia and α is the angular acceleration. Rotational inertia is the force that works against the body slowing the increase of velocity. In our system it is important to have angular acceleration in mind, since this acceleration is correlated directly to the motor's resistance to a change of velocity. The group will find the right torque that will overcome the rotational inertia that our system's filter components will create. A side view of our system demonstrating the torque working against the rotational inertia is shown in figure 6. M2(motor creating the horizontal motion), produces an angular acceleration (seen in blue), which will work against the force (seen in red) preventing the body of the system to start accelerating. Having this knowledge, along with the understanding that our system will not need to be implemented with high speed is key to creating a lightweight system, for our motor, battery, and efficiency.

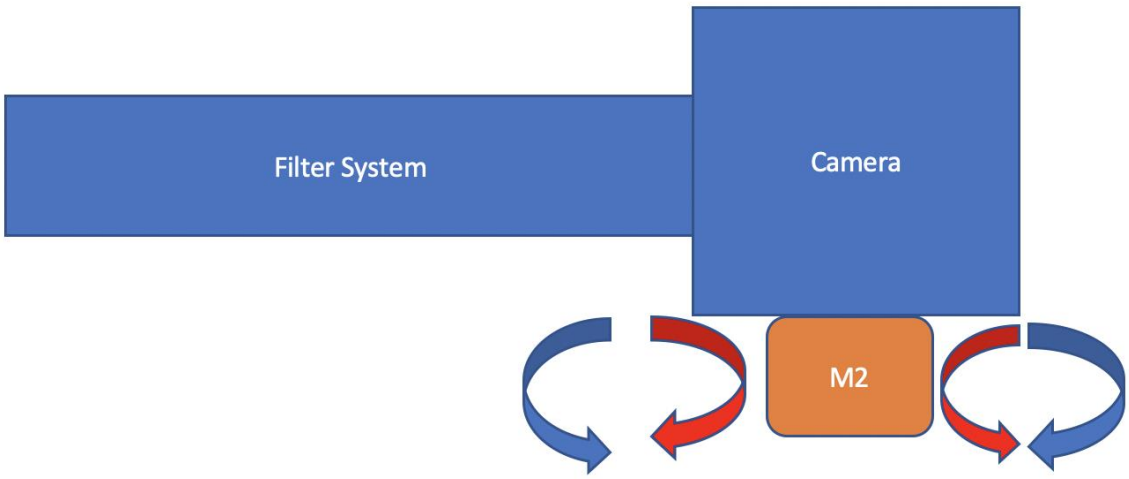

Figure 6: Torque vs rotational inertia

4.10.4 Moments of Inertia

First, our group focused on vertical motion, our system will be around 50 cm long and 16 cm of width. By estimating the body of the system to be around 4.5 kg, the moment of inertia will be calculated by the following inertia formula for an off-center axis, as mentioned in the previous sections:

$$J = (1/12) \times m \times (w^2 + B^2 + 12L^2),$$

where m is the mass of the body, w is the width of the body, B is the length of the body and L is the distance between the axis of rotation and center of mass of the body. After calculations, the system's moment of inertia results at 0.03317 kg-m^2. This inertia was concerning at first, since it can be difficult to find a motor with a rotor inertia large enough to handle the load. As we build a prototype, it is important to design and experiment with a few body frames with different specifications. Figure 5.1.2 shows the outer case of the body with each dimension. Our group understands that in order to find the right size of a motor, adjustments to the dimensions of the body might need to be done. As seen in the formula above, the width, length or even the distance between the center of the body and the axis of rotation, can make a significant result on the moment of inertia.

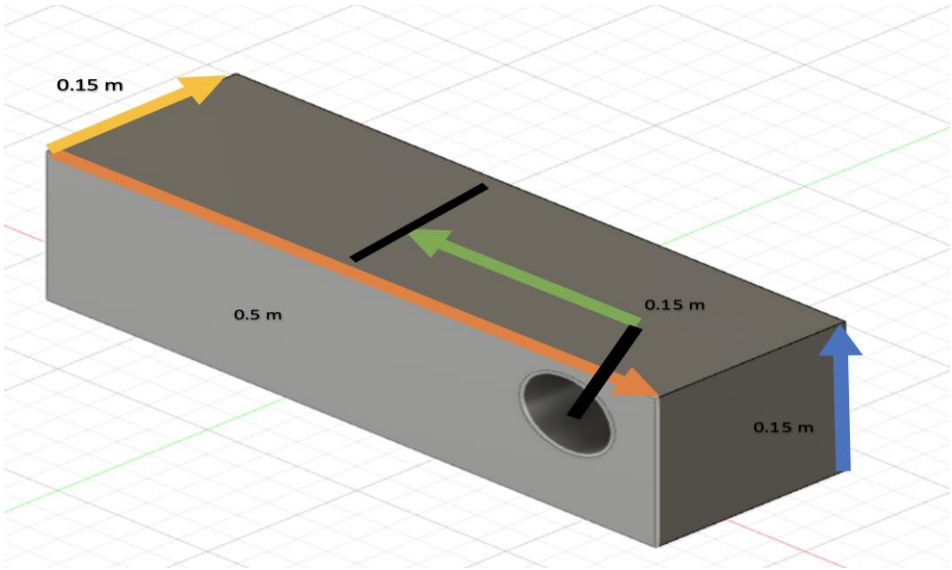

Figure 7: System's arm, with an of center axis

In a similar situation, motor two (M2) will be located on the same side as M1, which will be on the right side of the system's body. Figure 5.1.3 illustrates both a side and front view of the system, in the left side, the side view shows where the motor is planned to be located and on the right image, the rotation given to the system's body is illustrated from a front view. As seen in these images, M2 will

be connected to the rotary surface, where the motor will rotate the driver gear, which rotates the driven gear in order to obtain more torque. Comparing M2 to M1, which is in charge of the vertical motion, M1 does not have a large amount of gravitational force, since M1 will be the motor that will have enough holding torque to hold the load without any assistance from other motors. The key functionality of M2 is to add vertical motion to the system's body when needed to locate the refracted laser beam. In order to get this done, change acceleration must be done by M2, where the system body's moment of inertia will create a resistance to this attempt to motion. Having in mind that M2 is also creating movement for the entire system's body, the moment of inertia against M2 will be equal to the moment of inertia against M1, which is 0.03327 kg-m^2. As mentioned earlier, this moment of inertia is quite high, so our group will use the strategy of using gear reduction in order to increase the torque given by the motors alone. Further down this report, we will explain our approach to this issue.

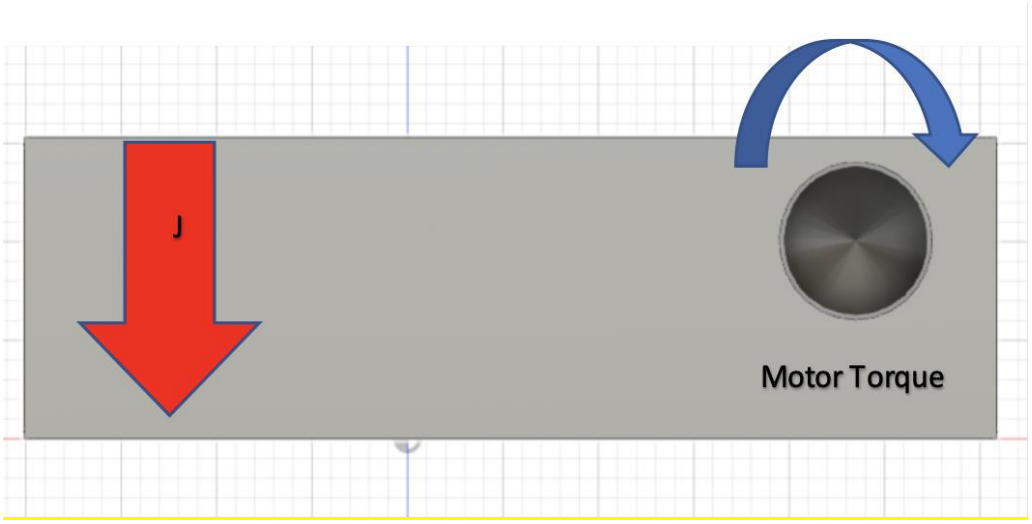

Figure 8: Side view of system's arm. Moment of inertia against the motor's torque

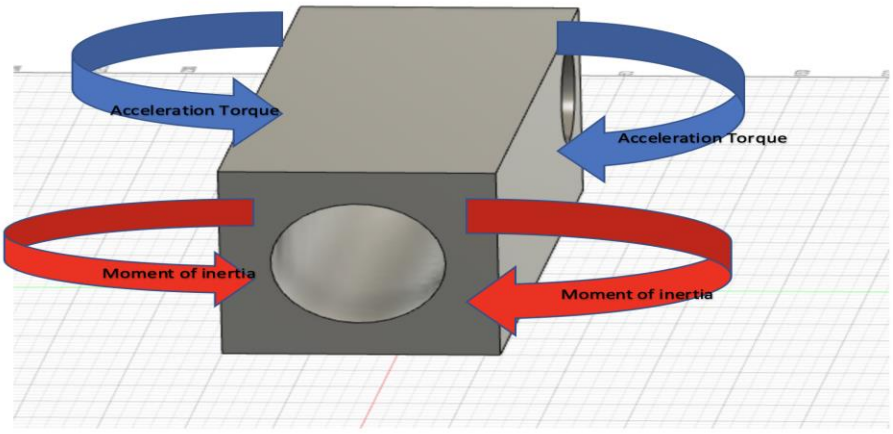

Figure 9: Front side of system, with moment of inertia and acceleration torque

Now, we take a look into our system which is a composite of two independent linear motions. Our system consists of a rectangular body, where at one end will encase all the electrical components, along with the camera. As the rectangular body of our system extends, along the ‘arm’ will encase a filter system which is composed of four laser filters. Each filter’s job is different and was explained in earlier sections. As explained earlier, we know that two of these filters will be in motion independently and will also carry a load linearly back and forth inside the ‘arm’ of our system. Fortunately, the filters being used for our filtering system will be light, at around 5 grams each filter. Utilizing the formula for the moment of inertia of a linear moving body, as explained in earlier sections, we calculate inertia as.

$$J = m \times (A/2pi)^2 ,$$

Where m is the mass of the load, and A is the unit of movement. Having in mind that the overall mass includes the filter and the platform which the filter is sitting on. Plugin in the overall mass to the previous equation, the moment of inertia results in 0.0007958 kg-m^2. With this result, we understand that the resistance created from the filter’s motion will not be as significant as the resistance seen by M1 and M2. For this subsystem, Moment of Inertia will be manageable, and it will allow us to select smaller motors, which will add less weight to the system’s overall weight. It’s important to our group to find the lightest components when it comes to the ‘arm’ of the system. This is because we want to find the best ways to add the least moment of inertia that affects both M1 and M2.

We have calculated the moment of inertia of each moving body in our system. The overall weight of the system, where it’s mechanics would imitate an ‘arm’, with the motors attached to one side of the rectangular casing which surrounds the electronics, will be held by the motors. The moment of inertia of our system will allow the group to choose the right motors to give the body of the system enough acceleration and deceleration to move and to stop, when moving around positions looking for the laser beam. From the calculations obtain in this section, both motors M1 and M2 have to be able sustain a minimum moment of inertia of 0.03317 kg-m^2, and M3 and M4 will have to be able to sustain a minimum moment of inertia of 0.0007958 kg-m^2 when motion is required. It’s important to remember that moment of inertia is only a factor when the ‘arm’ of our system is in motion, where load torque, which will be discussed next, maintains the system stationary. Table 4 illustrates the effects of the moment of inertia, from the dimensions of the rectangular casing, as well as the distance between the center of mass and the center of rotation. The table helps shine a light on having in mind the dimensions of the system could help lower the cost of the system overall, without lowering efficiency.

Mass (kg)	Width (m)	Length (m)	Offset for axis(m)	Moment of inertia (kg -m^2)
2.27	0.152	0.254	0.1016	0.04
4.54	0.127	0.254	0.1016	0.06
4.54	0.152	0.254	0.0508	0.04

Table 4: Moment of inertia resulted from different dimensions

4.11 Light Sensor

Multiple ideas have been examined about how to approach the light sensor for the design. The intensity of the light being introduced into the system will be recorded using the CMOS camera. As the light travels through the optical system there will be a conflict with ambient light due to the suns blackbody radiation spanning from the ultraviolet into the infrared (blackbody radiation). For accurate measurement of the only the lasers intensity, the sun's intensity must be subtracted from the total intensity profile captured by the device. The initial idea for this approach was to have a spectrometer within the system along with a spectral camera. The diffused light from the laser along with the ambient light from the outdoors/lab full spectrum lighting will both enter the optical system. As the light travels through the designed lens zoom system it will eventually be focused onto the optical filters. As the light signal travels through the optical filters the majority of the undesired ambient light will be absorbed by the optical filters. What will transmit through is a narrow bandwidth of light including the desired laser wavelength. Within that narrow bandwidth will also include the intensity of the undesired ambient light which will give an inaccurate reading to the true intensity of the laser.

The initial approach was to have a beam splitter in the path of the optical lenses. The beam splitter specifications required would only split about 10% of the light perpendicular to the light signal path and allow the other 90% to travel into the optical filters into the camera. That small percentage of light would be focused onto a spectrometer or similar spectral reading instrument to give a basis of the intensity spectrum of light entering the optical system prior to being filtered. The other portion of the optical signal would travel through the optical filters and a spectral camera would measure and display the actual intensity reaching the camera. By having the base measurement from the spectrometer and the reading from the spectral camera, the two sets of data can be analyzed and subtracted to result in the true intensity. This idea does not work because both the split signal and the filtered signal would still be a superimposed signal of

the sun light at 532 nm and the laser light at 532 nm. The signal that reaches the camera although filtering out the undesired frequencies on the outside edges of the band pass filter, would still be a similar superimposed signal of the two mixed light signals. The signal reaching the camera would be much more attenuated than that of the one reaching the spectrometer so subtracting the signals will not work. Also, spectrometers tend to be quite expensive in the range of thousands of dollars so this would but the design way over budget.

The second approach was to use a hyperspectral sensor or a multichannel spectral sensor. There are many different types of these light sensors on the market which can be easily designed. The multichannel sensor would have been a two-channel sensor one being sensitive to the 532 nm green laser light and the other being sensitive to the 800 nm laser light for the stretch goal. The sensor will need to be both sensitive to the visual spectrum as well as the infrared spectrum. The hyperspectral sensor After further research, this approach is not going to result in the desired response for the system.

Instead of the aforementioned approaches, an ambient light sensor. Ambient light sensors are broken down into three different categories. These sensors are photodiodes, photoconductive cells, or phototransistors (photodetector and amplifier). The ambient light sensor collects the lux intensity of the light which is shone upon it and then will transmit a voltage of proportional intensity to the ambient light. This sensor will be able to detect the differences between laser light, sunlight, and the full spectrum light bulb introduced into the design of the system. Important characteristics of the ambient light sensor are the operating temperature, the required voltage, The ambient light sensor will be used to control the amount of light entering the camera as well as detect the luminous intensity of the light signal travelling through the device. The device will have a housing and will be absent of light other than what is allowed in by the aperture. A full visual spectrum light will be used as the ambient light source which will mimic the visual spectrum of a day outdoors while in a laboratory setting. The ambient light sensor will adjust the camera to the incoming light. The camera will be able to be adjusted to a brightness of optimal reading of the incoming signal. There are many different types of light sensor will be able to measure the appropriate intensity of the incoming light signal and relay that data to be compared with the recorded spectral reading from the camera. The sensor being sought for experimentation is sensitive to the red, blue, green visible spectrum. The sensor will attenuate infrared light which will help keep the band integral of data to only the visible spectrum. The stretch goal is to be able to block out the undesired wavelengths of light through the optical system and then sense, how much of the wavelength is actually being measured from the 800 nm laser versus the full spectrum visible light source. The full spectrum light source will introduce 532 nm wavelength into the system superimposed with that of the diffused wavefronts from the laser pointer source. The color sensor will be able to detect the differences in the laser wavefronts from the full spectrum ambient

lights source. This will aid in being able to deduct the additional 532 nm light introduced by the full spectrum ambient light source and get an accurate reading on the intensity of the diffused wavefronts of the laser signal reaching the camera. This approach is to be tested to find the appropriate way to differentiate the additional 532 nm wavelength entering the device from the laser. Initially a baseline will be recorded by testing the device in the dark with only the laser light on. This information will be used as the baseline before the full spectrum ambient light source is turned on. Another reading with the ambient light source only on will be recorded to analyze how much of the 532 nm light is coming into the device from the device. The ambient light source can be both an active or passive device depending on the specific type. A photoconductive cell does not require a direct power source. The photoconductive properties will change when directly exposed to electromagnetic radiation. Photoconductive cells are considered passive devices. Similar to the photoconductive cell is the light dependent resistor which is a piece of semiconductor material that's resistance will change when light is exposed upon the surface. The resistor will create electron hole pairs as more light is shone upon it and the resistance will decrease as the illumination increases. These types of sensors tend to have a longer response time, so they are not ideal for this specific project. A photodiode light sensor is a P-N junction which has a much better response and sensitivity to lower energy light near the red and infrared regions. When electromagnetic radiation falls upon the surface of a photodiode electron hole pairs are created and a current is given off. This current is proportional to the light intensity on the photodiode. These sensors are typically a much faster response time than the photoconductive cell. This type of sensor may be good for the stretch goal but not for the main objective of the design. The phototransistor on the other hand is similar to the photodiode but is amplified and much more sensitive. and will require power from the battery source. Ideally the size of the device will weigh heavily on both the optical design as well as the size of the power source. A sensor with the lowest power consumption is ideal in this design. The sensor must have a strong spectral response on the order of the photopic response of the light coming in. The sensor will neglect additional infrared wavelengths and aid in proper lighting for the camera. The ideal choice for spectral and intensity measurements of the ambient light for this device will be a photodiode. There are vast variety of different types of photodiodes on the market which can be designed and specialized with specifications. The photodiode necessary for this experimentation will need to be very sensitive to 532 nm wavelengths and ideally will require a low voltage for operation. There are many photodiodes on the market currently which meet these specifications.

4.11.1 PIN Photodiode

To properly detect how much ambient light from the full spectrum light source and blackbody radiation of the sun a PIN photodiode is the best choice. PIN photodiodes operate with a reverse bias voltage applied which is also known as the photoconductive mode. The photoconductive mode increases the depletion regions depth as well as the strength of the electric field. A larger depletion region means that the sensor will be much more sensitive. Also along with a larger depletion region the junction capacitance is also significantly decreased. A lower junction capacitance in turn allows for the PIN photodiode to have a larger cut off frequency. A large cut off frequency in turn means a larger bandwidth region of detection. The advantage of the PIN photodiode compared to other types of photodetectors is its higher speed, a more linear measurement of current, a lower capacitance, and higher quantum efficiency. A disadvantage of a photodiode versus other types of sensors is that it lacks an amplifier. The main constraint on accurate measurement that is introduced to the photodiode is a larger dark current which must be taken into consideration when analyzing the data obtained. The dark current refers to the flow of current through the photodiode even when there is no illuminance on the surface. The dark current can lead to inaccurate measurements if not taken into account. The dark current can be measured prior to experimentation to have a baseline and be subtracted from the overall intensity measurement to get an accurate reading. The PIN photodiode is the right choice for this design because of its high sensitivity in the visible to near infrared regions. This type of photodiode is suitable for both the showcase 532 nm sensitive device and stretch goal of the near infrared 800 nm experimentation. The cutoff region of the broadband is dependent upon the thickness of the intrinsic region of the PIN photodiode. The rise time of electron-hole pairs to get from the intrinsic region to the doped region limits the bandwidth of the device. Some important characteristics and equations for selecting the proper PIN photodiode are listed below.

Responsivity (R_D): Current produced (I_P) / Input optical power (P_{in})

$$\frac{I_p}{P_{in}} = R_D$$

Quantum Efficiency (η) : α are the losses and L is the length of the intrinsic region.

$$\eta = 1 - e^{-\alpha L}$$

Rise Time (T_r): τ_{tr} is the electron transit time and τ_{RC} is the time constant of the circuit.

$$T_r = ln\,9\,(\tau_{tr} + \tau_{RC}),$$

Bandwidth (Δf):

$$\Delta f = \frac{1}{2\pi(\tau_{tr} + \tau_{RC}}$$

Dark current also introduces noise to the system known as shot noise or dark noise. It is ideal to have a high sound to noise ratio (SNR). The lower the SNR the more corrupted the signal will be at the receiver sometimes to the point its not even decipherable. The noise of the photodiode and the SNR are calculated using the equations below.

RMS value of Shot noise (I_{sn}): I_d is dark current and I_p is average current.

$$I_{sn} = \sqrt{2q\left(I_P + I_D\right)\ f}$$

RMS value of Thermal noise (I_{jn}): R_L is load resistance

$$I_{jn} = \sqrt{\frac{4k_B T\ f}{R_{SH}}}$$

Sound Noise Ratio (SNR):

$$SNR = \frac{I_p^2}{(I_{sn}^2 + I_{jn}^2)}$$

4.12 Wireless Communication

For the purposes of this project wireless communications will be utilized, as these means provide adequate convenience regarding set up and making this solution more practical. For the distances the components for this project are to be designed to operate in wired means of communications between components would be unwieldly for set up unless the setup is to be more permanent which is

not desired from this design. A wired setup would also have additional issues depending on implementation, as this project is oriented towards outdoor use and as such the cables used would need to meet certain requirements for such conditions. As such utilizing wireless communications would be the preferred option.

4.12.1 Private Wi-Fi Network

A common technology for wireless communications in most consumer electronics and in come commercial applications is the use of Wi-Fi. Wi-Fi has plenty of draws, including a base range of 300 meters in outdoor environments with the ability to utilize devices such as repeaters to extend the range further. This would also be a good solution regarding video transmission as this would allow the images from the camera to be transmitted to the user without sacrificing image resolution. The drawbacks however are the limitations that would be faced in either setting up the LAN every time or in implementing a permanent solution. The limitations for both implementations being the issue of how long it would take to set up the network and configure the devices into the network and troubleshooting any issues with the network as they may arise. This would also be one of the more expensive solutions with the added cost of a router and whatever means for achieving the desired range, as well as the additional cost due to the recent increase in demand in such devices as a result of the COVID-19 pandemic.

4.12.2 Bluetooth

Bluetooth is the standard regarding short-range wireless communications, generally having an optimal operating range within 10 meters. Bluetooth is used in various applications in devices used in healthcare, security, and consumer electronics amongst other areas. Bluetooth operates along the 2.4 GHz band of frequencies (2.402 - 2.480 GHz). Although Bluetooth was standardized by the IEEE under IEEE 802.15.1 back in 2002, that standard has since become defunct, and the standard is now governed by the Bluetooth Special Interest Group (henceforth referred to as SIG) which notably handles the developed specifications of Bluetooth and manages the qualification program. In order to maintain signal quality between devices Bluetooth utilizes Frequency-Hopping spread spectrum (FHSS) which “hops” between the frequencies in the 2.4 GHz band. FHSS has the added benefit of security from eavesdropping as a result of the rapid shifting of frequencies.

While Bluetooth would be adequate for transmitting the control signals from the control device to the camera control setup at the range used in the demonstration at the conclusion of Senior Design 2 (3 meters), but for the more

extensive range of 1 kilometer that this project is to be designed for Bluetooth is simply not suitable. Bluetooth utilization would also hamper the use of video in this project, as the technology doesn't have the required bandwidth in order to adequately transmit the video data, at least not as anything other than a few images per second.

4.12.3 Radio Frequency (RF)

RF is a commonly used solution for communication between devices over various distance ranges due in part to its versatility in design and simple implementation. RF can achieve distances much longer than the other means evaluated, with lower frequencies having the longer ranges. The constraints that exist Regarding the hardware necessary for implementation for the controls, modules can be used for transmitting and receiving signals between the devices. These modules can be obtained for prices that are much more friendly for the allocated budget for the transmission portion of this project, especially when compared to the necessary expenses to implement solutions such as the private Wi-Fi network.

4.12.4 Video Transmission Considerations

For video transmission Bluetooth is not an optimal option Bluetooth does not have enough of the necessary bandwidth for adequate video transmission and is only optimal for short range communications within 10 meters. As the device is intended to work at an extended distance from the device and the target the device is to be aimed at in the stretch goals of this project, a means of long-distance video transmission should be considered for this project. Unfortunately, most commercial solutions for wireless video transmission are either cost prohibitive for this project, notably those utilizing wireless HDMI video transmitters, or are impractical for the intended use of this project, such as Wi-Fi video transmitters that would require the two devices to be on the same short-range Wi-Fi network. Luckily there is a solution to implement wireless video transmission, which is to utilize the same analog First-Person Video (FPV) transmission tools used in devices such as those used in remote controlled planes and quadcopter drones. These FPV video transmitters generally utilize the 5.8 GHz frequency band that is legal for amateur use which has a wider bandwidth and many channels for use that are not as commonly occupied like the 2.4 GHz band is. In the United States the allowed frequencies are between 5.685 GHz and 5.905 GHz. There are various considerations to make regarding analog video transmitters including the power requirements for transmitting the signal, the frequency band of the transmitter, and the maximum range of the transmitter.

4.13 Microcontroller

For this project we will need a microcontroller to operate the motors in the camera adjustment system. The considerations that will need to be made regarding which controller is used will come down to the following factors:

- low power draw,
- development support,
- cost,
- availability,
- output.

The need for low power draw from the MCU comes from the assumption that the system will need to be operating on battery power given its application. Given the camera doesn't need to be continuously adjusted the entire time it is in operation for experiments, the MCU does not need to be sapping power while the motors are on standby. Some form of low power or standby modes for the MCU would be highly desired for this application. For development support the means by which the microcontroller is programmed to and the existing knowledge of those who will be developing the software needed to operate the microcontroller are important considerations to consider. A microcontroller that has plenty of accessible documentation and can be programmed using a language that is known or at least very simple to adapt to for the developer is along the lines of what is desired in the microcontroller that is to be used. The cost of the microcontroller and the availability of the board are also important considerations, especially as this project is being done during a time of major shortages for electronic components where it is unlikely vendors will know when they will have a given component back in stock after it is out, and the prices of components may increase given those shortages.

4.13.1 Arduino Nano Every

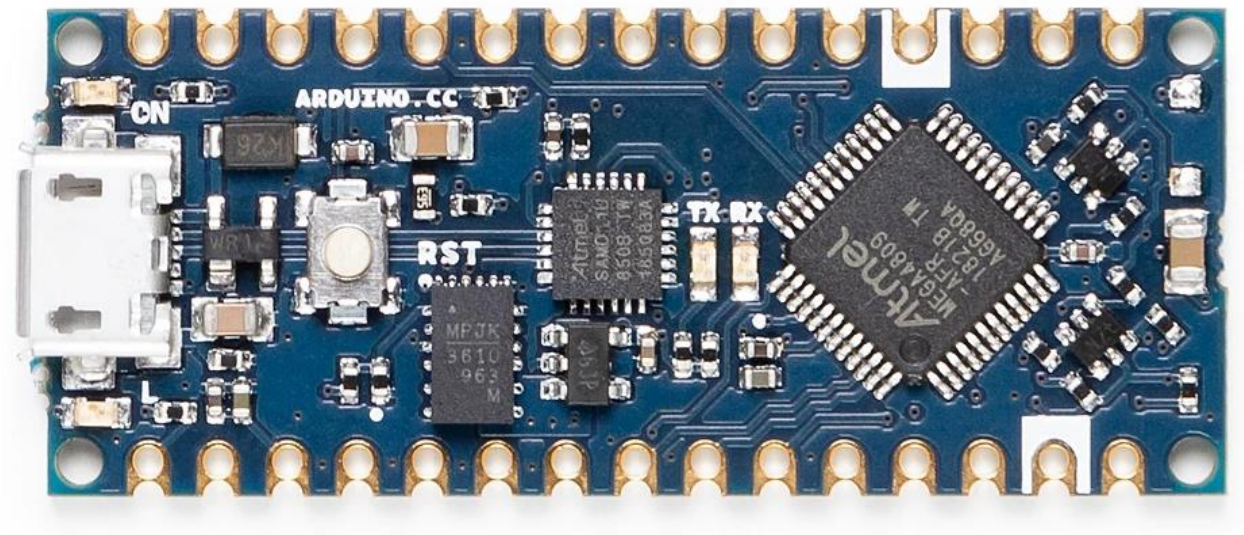

Figure 10: Arduino Nano Every Board (Arduino AG, 2021)

The Arduino Nano Every is an incredibly small single board microcontroller that is popular in DIY electronics and educational projects that require the use of small and easy to use controllers. A major factor in the board's popularity comes from the extensive support for the board, with plenty of extensive libraries that are user-friendly, with this board being one of the more novice friendly options available, and the fact that due to Arduino's Creative Commons licensing for hardware the boards can be made by various suppliers using the same specifications as the official Arduino boards. Regarding specifications the board utilizes the ATMega4809, an 8-bit RISC microcontroller running on a 20MHz clock and utilizes 41 GPIO pins. In active mode the board has an absolute maximum power consumption of 425 µA/MHz at peak operating temperature and highest clock speed, with the maximum power consumption at the board's low power mode being 15 µA/MHz. Regarding temperature tolerances the board can operate in temperatures between -40°C and 125°C, making this one of the more flexible and resilient boards available in that aspect. The operating voltage is between 1.8V and 5.5V, again making this one of the more flexible boards for voltage tolerance. For memory the board has 6KB of SRAM available and has 48KB of onboard flash memory. The board does allow for UART, I2C, and SPI.

The Arduino Nano Every utilizes the Arduino Integrated Development Environment, or Arduino Software (IDE) is an IDE written in Java and utilizes the C/C++ language alongside simplified functions in the IDE. Arduino boards are known for not requiring high level knowledge of programming languages, adding to the accessibility of the boards.

Overall, this board is a strong choice for this portion of the project, as the low power draw combined with the strong development support around this board very much indicate why this board is a popular choice overall in various projects. The low cost of the board as well as its current availability are additional pluses for the board. There are some features that will need to be added to the board to implement necessary functions of the board, specifically a wireless communication module.

4.13.2 MSP430FR6989

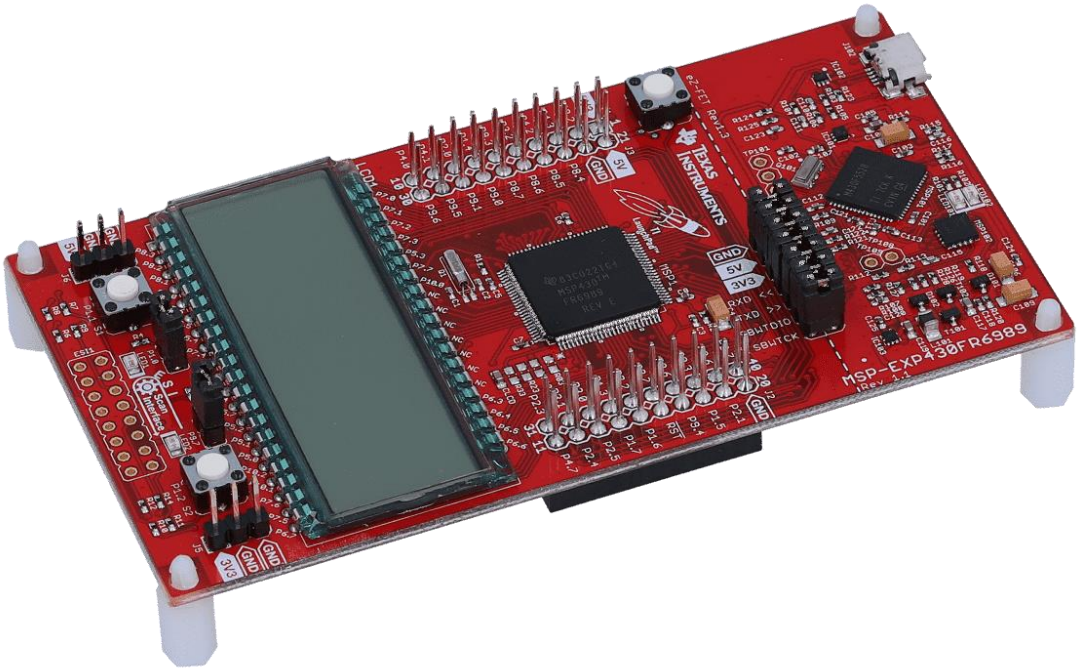

Figure 11: MSP430FR6989 Development Board (Texas Instruments Inc., 2020)

The MSP430FR6989 from Texas Instruments (TI) is also a viable option given its reliability and power. The board is easy to implement, with the thorough documentation provided by TI along with experience with development using this board for Embedded Systems labs at the university. Regarding the specifications of this microcontroller, the roughly $5.00 controller has a 16-bit RISC architecture running on a 16MHz clock. The controller also has 83 GPIO pins, the most amongst the boards being considered. Regarding memory the controller has 128KB of FRAM and another 128KB of flash. In active mode the controller has a maximum power consumption of 100µA/MHz at worst operating conditions, and in low power the maximum consumption is approximately 17µA/MHz at worst operating conditions. Speaking of worst conditions, the controller has temperature tolerance of between -40°C and 80°C, meaning the board has the worst peak operative temperature of the considered boards. Operating voltage is between 1.8V and 3.6V.

For this project, the MSP430FR6989 microcontroller works well regarding low power consumption, lots of GPIO pins, communication interfaces and onboard memory.

4.13.3 Raspberry Pi Pico

Figure 12: Raspberry Pi Pico Board (Raspberry Pi Trading LTD, 2021)

The Raspberry Pi Pico is the inaugural microcontroller from the developers of the Raspberry Pi line of single board computers. The microcontroller utilizes the RP2040 SoC, which runs on a 32-bit RISC architecture ARM processor with a 133MHz clock and 264KB memory (but no onboard flash memory). Compared to other ARM processors the power efficiency of the chip is strong but compared to the other options explored this is still quite power hungry. This board also contains around 30 GPIO pins, also lacking when compared to the other reviewed boards. The board is also not as great regarding temperature tolerance compared to the Arduino, but on the high-end of the scale still does slightly better than the MSP430. For operating voltage, the board, the range is from 1.8 – 3.3V, which would require more consideration regarding how the board is powered.

MCU As such this board tends to be used in Internet-of-Things (IoT) applications where the high clock and memory are in higher demand than lower power consumption. For this application the board is likely to be overpowered and may

not be resilient enough for the given the conditions that the board would experience.

4.13.4 Microcontroller Comparison

MCU	**ATMega4809**	**MSP430FR6989**	**RP2040**
Cost	$1.58	$5.00	$1.00
Architecture	8-bit RISC	16-bit RISC	32-bit RISC (ARM)
Max. Power Consumption (Active)	425µA/MHz	100µA/MHz	718µA/MHz
Max. Power Consumption (Low-Power)	15µA/MHz	17.1875µA/MHz	-
I/O pins	41	83	30
Clock	20MHz	16 MHz	133MHz
RAM	6KB (SRAM)	128KB (FRAM)	264KB (SRAM)
Operating voltage	1.8 - 5.5V	1.8 - 3.6V	1.8 - 3.3V
UART	1	2	2
I2C	1	4	2
SPI	1	2	2
Flash	48KB	128KB	none, supports up to 16KB external
Temperature Tolerance	-40 to 125°C	-40 to 80°C	-20 to 85°C

Table 5: Comparisons between the considered microcontrollers

4.13.5 Microcontroller Selection

The Arduino Nano Every using ATMega4809 is the board and MCU selected for use in this project. This board/MCU combo is a strong choice for this portion of the project, as the low power draw of the controller combined with the strong development support around this board very much indicate why this is a popular choice overall in various projects. The low cost of the board as well as its current

availability are additional pluses for the board. This board also has plenty of documentation with projects that are in some ways related to this project in regard to RF control which can be referenced and depending on the project can adapted for the purposes of this project, making the development process quicker and easier.

5. Similar Products or Projects

This section covers similar projects (academic or enthusiast) and commercial products that exist in the same area as this project, mostly in the area of camera mounts and camera tracking systems.

5.1 Existing Products of Projects

While there is not much in the way of camera mounts used exclusively to track laser beam profiles, there are plenty of examples of robotic and automatic camera mounts that can be used to either track a subject or complete a specified series of motions for filming. These mounts are used in a variety of different fields of photography, from capturing the movement of celestial bodies to tracking the movements of someone walking around a lecture hall. These devices utilize the input of whatever camera is connected to them and depending on the mount's capability can either automatically track a subject, follow a set of preconfigured movements, or be actively adjusted by a user remotely. One of the projects shows a great design of a pan tilt mount which points us into the right directions on how to create a movement for our system. The next project provides the techniques and implementation options to add a third motion to the previous project mentioned. In this project the sliding rail is bought in one piece, which alleviates time to focus on the motor implementation and electric connection. As mentioned before, the second example project utilizes a sliding rail already built, but in order to control the budget of our system, investigation was done in order to see the possibility of building a sliding rail. Matt, who has it's own youtube channel "DIY" perks has a great video about building a sliding rail, which gives a great option for our group, since the materials used are not complicated to obtain or can be relatively affordable

5.2 Robotic/Automatic Camera Mounts

Some of the closest products to the basic function of this project are camera mounts that are developed to utilize remote operation of a camera, shifting movements to track the motions of certain subjects or to combine images into a form of panorama. There are plenty of commercial solutions available for various types of cameras and applications, whether they are for DSLR cameras used for professional photography, film cameras steadily moving through a scene, or for amateur photographers using small digital cameras. The more high-end professional solutions tend to be somewhat cost prohibitive, leading to some

DIY solutions, such as the *Pan-Tilt-Mount* project on GitHub from isaac879 (2020). These solutions may or may not implement automatic tracking of a subject, which when implemented can be used for tracking the subject in the camera's range of view (with some limitations). Like what would be expected in the stretch goals for this project, some specialized camera mounts are developed for tracking celestial bodies (stars, planets, etc.), whether it be for purposes of tracking the position of a body in the sky over night, making sure no ICBMs are approaching during the Cold War, or just for some nighttime timelapse photography.

5.3 Commercial Video Drones

Video drones can be seen as a rather elaborate form of camera mount, with the technologies developed for it being very beneficial for our purposes. As video drones operate remotely from the operator usually at a distance from the operator, the technologies that allow the operator to control the drone's movements and to view what the camera of the drone is capturing are rather useful to our applications of operating a device at a distance while also requiring a video input from the device. These drones also operate on a minimal amount of power in order to operate, providing another point of similarity. Understanding how these drones work and are able to do so at the lower costs they are now available for is beneficial for determining how to implement our solutions.

6. Design

This section covers what design considerations are made and what we propose for this project based on the prior research and technical investigations.

6.1 Design Overview

The design of the remotely controlled diffused surface laser beam imaging system aims to find, track, and characterize important data of the beam. A live image of the beam will be captured by the camera within its field of view, as depicted in figure(). The live image will be transmitted to the user who is remotely controlling the zoom and movement of the device. The movements are comprised of an up-down rotating motion, and a left-right rotating motion. These movement help the user manually locate the beam on the target board from the remote location, likely at the laser output. The zooming ‘in-out’ motion will also be controlled manually by the user. The field of view will become narrower as the zoom increases.

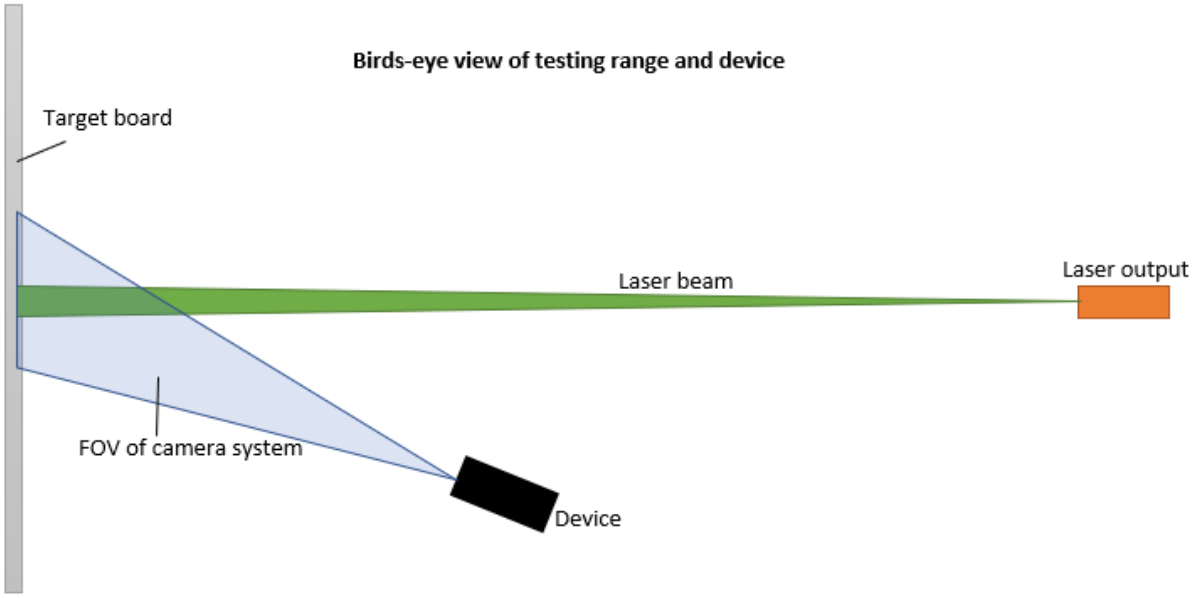

Figure 13: Birds-eye view of device being tested

The design of the remotely controlled diffused surface laser beam imaging system is comprised of several key subsystems. An overview of the final design of these systems are recorded below. The main systems are the zoom-camera system, filtration system, motor movement, data transmission, and power source.

The zoom- camera system is comprised of three lenses. Two bi-convex lenses and a bi-concave lens. The zoom lens system will contain two moving lenses and one stationary lens. Two small motors move the lenses to 5 preprogramed distances from the camera, ensuring an in-focus image at 5 zooms. Allowing the lens movements to be continuous introduces complexity to the code, due to the nonlinear path that the third lens, the compensator lens, needs to travel. Additionally, it would require a high precision in the motors' movement which is not guaranteed.

The optical filters are designed to filter out ambient light introduced to the system and have cut on and cut off wavelengths when superimposed to strictly allow the 532 nm wavelengths to propagate through the system to the camera.

The PIN photodiode is going to be an external element which will measure the ambient light of the environment and map out an accurate intensity profile of the ambient light. This data will be used to determine how much radiant flux is introduced from the ambient light versus the diffused reflected laser light.

6.2 Surface

The current outdoor experimentation being done with the 800 nm laser uses a Lambertian surface. The Lambertian surface used in the current outdoor experimentation is a ceramic cloth. A piece of this exact type of ceramic cloth will be used for lab experimentation of the device. In conjunction with the ceramic cloth and for a more in-depth analysis of the working properties of the experiment a separate Lambertian surface will be designed. The Lambertian surface designed for lab experimentation will consist of an aluminum surface which is covered in a matte paint. The aluminum surface will have some thickness to it. The matte paint will be sourced from a local paint store. The specifics of the type of paint and the exact aluminum are still being discussed. The type of paint and aluminum must be selected carefully because of how the light will diffuse with the materials.

6.3 Zoom System (Zemax Simulation)

The overall simulation and design process were a work in progress over the entire semester and consist of three rounds of computer modeling and improving designs. This process is recorded here, ending with the finalized design that was the basis of purchased equipment and official demonstration. Zemax is an optical design studio software used for the lens design simulations.

6.3.1 Zemax simulations (1)

Round one preliminary Zemax simulation is recorded here. The current simulation and calculations are not complete and are a work in progress. The main issue that needs to be overcome before the end of this semester and the purchasing of lenses is the spherical aberrations.

To start, a three-group zoom design was chosen for its advantages in aberration correction and design flexibility discussed in research and investigation. A four-lens design increased the control over aberrations, while maintaining relatively low complexity. The PNP design was chosen because a fixed positive prime lens can focus incoming light to one point better than a negative prime lens.

The Zemax simulations uses Thorlab lenses, to ensure that they are accurate to what the real experimental results would look like. Additionally, it was important to ensure that designed lenses would be easily obtained without being too expensive. The total cost of the lenses used in the simulation did not cost more than $200, as was the goal in the initial budget. The first group, the compensator, is a ½ in. plano-convex lens with a radius of curvature of 51.5mm. The second, variator group is comprised of two plano-concave lenses, the first of which is a 1/2 in. lens with a radius of curvature of -51.5mm and the second that is a 1 in lens with 38.6mm radius of curvature. The final prime lens is a ½ in. biconvex lens with radius of curvatures 30.4 and -30.4 mm. The lens data and distances between each lens at each of the three positions in the simulation are shown figure (4).

	Surface Type	Comment	Radius	Thickness	Material	Coating	Clear Semi-Dia	Chip Zone	Mech Semi-Dia	Conic	TCE x 1E-6
0	OBJECT Standard		Infinity	Infinity			0.000	0.000	0.000	0.0...	0.000
1	STOP Standard		Infinity	20.480			10.000 U	0.000	10.000	0.0...	0.000
2	(aper) Standard		51.500	2.200	N-BK7		12.700 U	0.000	12.700	0.0...	-
3	(aper) Standard		Infinity	20.000 V			12.700 U	0.000	12.700	0.0...	0.000
4	(aper) Standard		-51.5...	4.000	N-BK7		12.700 U	0.000	12.700	0.0...	-
5	(aper) Standard		Infinity	0.500 V			12.700 U	0.000	12.700	0.0...	0.000
6	(aper) Standard		Infinity	3.500	N-BK7		17.124 U	0.000	17.124	0.0...	-
7	(aper) Standard		38.600	54.000 V			17.068 U	0.000	17.124	0.0...	0.000
8	(aper) Standard		30.400	6.000	N-BK7		12.700 U	0.000	12.700	0.0...	-
9	(aper) Standard		-30.4...	31.990			12.700 U	0.000	12.700	0.0...	0.000
10	IMAGE Standard		Infinity	-			33.725 U	0.000	33.725	0.0...	0.000

	Surface Type	Comment	Radius	Thickness	Material	Coating	Clear Semi-Dia	Chip Zone	Mech Semi-Dia	Conic	TCE x 1E-6
0	OBJECT Standard		Infinity	Infinity			0.000	0.000	0.000	0.0...	0.000
1	STOP Standard		Infinity	20.480			10.000 U	0.000	10.000	0.0...	0.000
2	(aper) Standard		51.500	2.200	N-BK7		12.700 U	0.000	12.700	0.0...	-
3	(aper) Standard		Infinity	40.000 V			12.700 U	0.000	12.700	0.0...	0.000
4	(aper) Standard		-51.5...	4.000	N-BK7		12.700 U	0.000	12.700	0.0...	-
5	(aper) Standard		Infinity	0.500 V			12.700 U	0.000	12.700	0.0...	0.000
6	(aper) Standard		Infinity	3.500	N-BK7		17.124 U	0.000	17.124	0.0...	-
7	(aper) Standard		38.600	30.000 V			17.068 U	0.000	17.124	0.0...	0.000
8	(aper) Standard		30.400	6.000	N-BK7		12.700 U	0.000	12.700	0.0...	-
9	(aper) Standard		-30.4...	31.999			12.700 U	0.000	12.700	0.0...	0.000
10	IMAGE Standard		Infinity	-			33.725 U	0.000	33.725	0.0...	0.000

	Surface Type	Comment	Radius	Thickness	Material	Coating	Clear Semi-Dia	Chip Zone	Mech Semi-Dia	Conic	TCE x 1E-
0	OBJECT Standard		Infinity	Infinity			0.000	0.000	0.000	0.0...	0.000
1	STOP Standard		Infinity	20.480			10.000 U	0.000	10.000	0.0...	0.000
2	(aper) Standard		51.500	2.200	N-BK7		12.700 U	0.000	12.700	0.0...	-
3	(aper) Standard		Infinity	42.500 V			12.700 U	0.000	12.700	0.0...	0.000
4	(aper) Standard		-51.5...	4.000	N-BK7		12.700 U	0.000	12.700	0.0...	-
5	(aper) Standard		Infinity	0.500 V			12.700 U	0.000	12.700	0.0...	0.000
6	(aper) Standard		Infinity	3.500	N-BK7		17.124 U	0.000	17.124	0.0...	-
7	(aper) Standard		38.600	10.000 V			17.068 U	0.000	17.124	0.0...	0.000
8	(aper) Standard		30.400	6.000	N-BK7		12.700 U	0.000	12.700	0.0...	-
9	(aper) Standard		-30.4...	31.990			12.700 U	0.000	12.700	0.0...	0.000
10	IMAGE Standard		Infinity	-			33.725 U	0.000	33.725	0.0...	0.000

Figure 14: Table of lens data, simulation 1: Position 1, at the front of the zoom path (top). Position 2, at the center of the zoom path (center). Position 3, that the back of the zoom path (bottom)
As the simulation shows in figure (5), the variator moves from the front of the system to the back as it zooms. The entire length of the system is maximum at 14.2 cm, which is within the design parameters for this project. The camera will sit beyond the image plane.

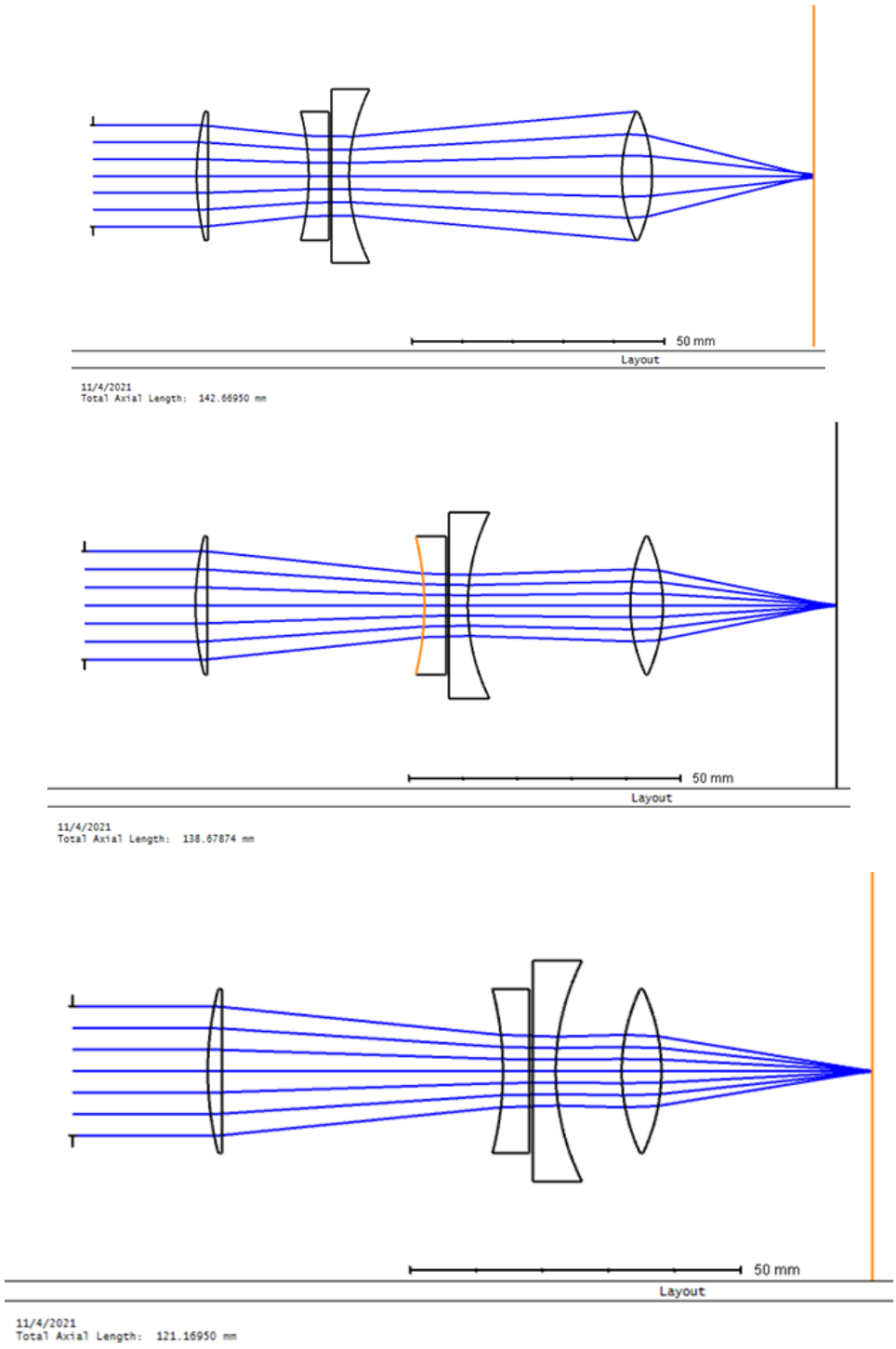

Figure 11: Simulation of focal zoom system: Position 1, at the front of the zoom path (top). Position 2, at the center of the zoom path (center). Position 3, that the back of the zoom path (bottom). The incoming light is from the left, and outgoing light to the right, where it will hit the image plane. The camera will sit at or beyond the image plane.

Although the simulation appears to focus on one spot in the image plane, spot size analysis shown in figure (6) shows a large RMS radius. The RMS radius is a sufficient measure of resolution and is used to tell if the beam is focused to one spot on the image plane. The smaller the RMS spot size, the more focused the image is. The RMS radius for the first position is 108.43, while the second position is 699.261, and the final

position is 59.827. The large RMS radius for the first and second position needs to be resolved before the design can be confirmed.

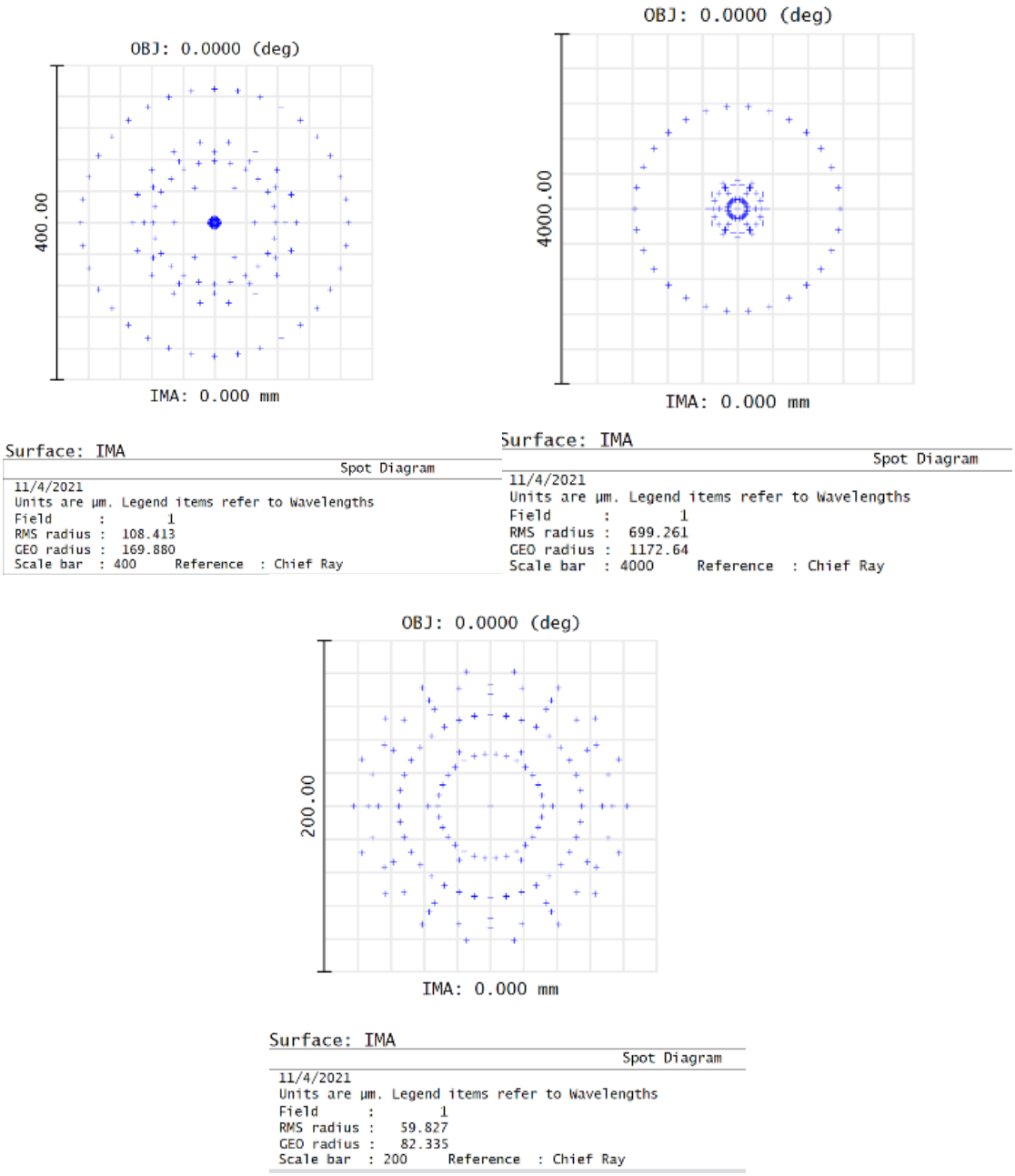

Figure 12: Spot size analysis, simulation 1: Position 1, at the front of the zoom path (top left). Position 2, at the center of the zoom path (top right). Position 3, that the back of the zoom path (bottom).

Future Zemax simulations will adjust the lenses and distances used. The design is based off a cook triplet, a common starting point for zooming designs. This may need to be looked into further and adjusted for a more accurate focus. The main issue is the spherical aberration that is occurring due to the light rays

not all converging to one point. This will effect the intensity profile made at the output of our project design because the image data will not be completely accurate. More research needs to be conducted on some of the functions within the zemax software, so that astigmatism can be checked and corrected as well. Coma should not be an issue in this design because we will be reading a narrow line of frequencies, however it can be checked in future simulations.

6.3.2 Zemax simulations (2)

Once again, the Zemax simulations uses Thorlab lenses, that are commercially available for ease of use and acquisition. Additionally, the total cost of the lenses used in the simulation did not cost more than $100, which is within initial budgetary goals. The first group, the compensator, is a 1 in. biconvex lens with a radius of curvature of 76.6 mm and focal length of 75 mm. The second, variator group is a 1 in. biconcave lens with a radius of curvature of -39.6 mm and focal length of -25 mm. The final prime lens is a 1 in. biconvex lens with radius of curvatures 179.8 mm and focal length of 175 mm. The lens data and distances between each lens at each of the three positions in the simulation are shown figure (7). The entire length of the system is 14.0 cm throughout the entire simulation, which is within the design parameters for this project.
The main difference in this simulation vs the simulation ran initially is that the variator group is no longer split into two lenses. Though, the variator doublet design may be revisited, a single lens reduced cost and complexity while giving sufficient results. Additionally, the zoom system is afocal rather than focal. A focusing lens may need to be added, though the camera might be built in such a way that a focusing lens is already in front the sensor. This will need to be determined before assembling our device. However, the afocal zoom is a separate entity from this lens and the focusing lens is not considered a lens group in the zoom system.

	Surface Type	Comment	Radius	Thickness	Material	Coating	Clear Semi-Dia	Chip Zone	Mech Semi-Dia	Conic	TCE x 1
0	OBJECT Standard		Infinity	Infinity			0.000	0.000	0.000	0.0...	0.000
1	STOP Standard		Infinity	5.000			10.000 U	0.000	10.000	0.0...	0.000
2	(aper) Standard		76.600	4.100	N-BK7		12.700 U	0.000	12.700	0.0...	-
3	(aper) Standard		-76.6...	3.000 V			12.700 U	0.000	12.700	0.0...	0.000
4	(aper) Standard		-39.6...	3.000	N-BK7		12.700 U	0.000	12.700	0.0...	-
5	(aper) Standard		39.600	92.000			12.700 U	0.000	12.700	0.0...	0.000
6	(aper) Standard		179.8...	2.900	N-BK7		12.700 U	0.000	12.700	0.0...	-
7	(aper) Standard		-179....	30.000 V			12.700 U	0.000	12.700	0.0...	0.000
8	IMAGE Standard		Infinity	-			21.028	0.000	21.028	0.0...	0.000

	Surface Type	Comment	Radius	Thickness	Material	Coating	Clear Semi-Dia	Chip Zone	Mech Semi-Dia	Conic	TCE x 1E-
0	OBJECT Standard		Infinity	Infinity			0.000	0.000	0.000	0.0...	0.000
1	STOP Standard		Infinity	50.000			10.000 U	0.000	10.000	0.0...	0.000
2	(aper) Standard		76.600	4.100	N-BK7		12.700 U	0.000	12.700	0.0...	-
3	(aper) Standard		-76.6...	22.000 V			12.700 U	0.000	12.700	0.0...	0.000
4	(aper) Standard		-39.6...	3.000	N-BK7		12.700 U	0.000	12.700	0.0...	-
5	(aper) Standard		39.600	28.000			12.700 U	0.000	12.700	0.0...	0.000
6	(aper) Standard		179.8...	2.900	N-BK7		12.700 U	0.000	12.700	0.0...	-
7	(aper) Standard		-179....	30.000 V			12.700 U	0.000	12.700	0.0...	0.000
8	IMAGE Standard		Infinity	-			8.075	0.000	8.075	0.0...	0.000

	Surface Type	Comment	Radius	Thickness	Material	Coating	Clear Semi-Dia	Chip Zone	Mech Semi-Dia	Conic	TCE x 1E-
0	OBJECT Standard		Infinity	Infinity			0.000	0.000	0.000	0.0...	0.000
1	STOP Standard		Infinity	72.000			10.000 U	0.000	10.000	0.0...	0.000
2	(aper) Standard		76.600	4.100	N-BK7		12.700 U	0.000	12.700	0.0...	-
3	(aper) Standard		-76.6...	24.000 V			12.700 U	0.000	12.700	0.0...	0.000
4	(aper) Standard		-39.6...	3.000	N-BK7		12.700 U	0.000	12.700	0.0...	-
5	(aper) Standard		39.600	4.000			12.700 U	0.000	12.700	0.0...	0.000
6	(aper) Standard		179.8...	2.900	N-BK7		12.700 U	0.000	12.700	0.0...	-
7	(aper) Standard		-179....	30.000 V			12.700 U	0.000	12.700	0.0...	0.000
8	IMAGE Standard		Infinity	-			6.664	0.000	6.664	0.0...	0.000

Figure 17: Table of lens data, simulation 2: Position 1, at the front of the zoom path (top). Position 2, in the middle of the zoom path, (center). Position 3, at the back of the zoom path (bottom)
As the simulation shows in figure (8), the variator moves from the front of the system to the back as it zooms. The camera will sit at or beyond the image plane, highlighted in orange. Both the incoming and outgoing light rays are focused at infinity, however are closer together as the variator lens moves closer to the image plane and the zoom increases. The compensator lens moves to compensate the rays and keep the image plane stationary. The final lens group, the prime lens, does not move and fixes the image on the image plane.

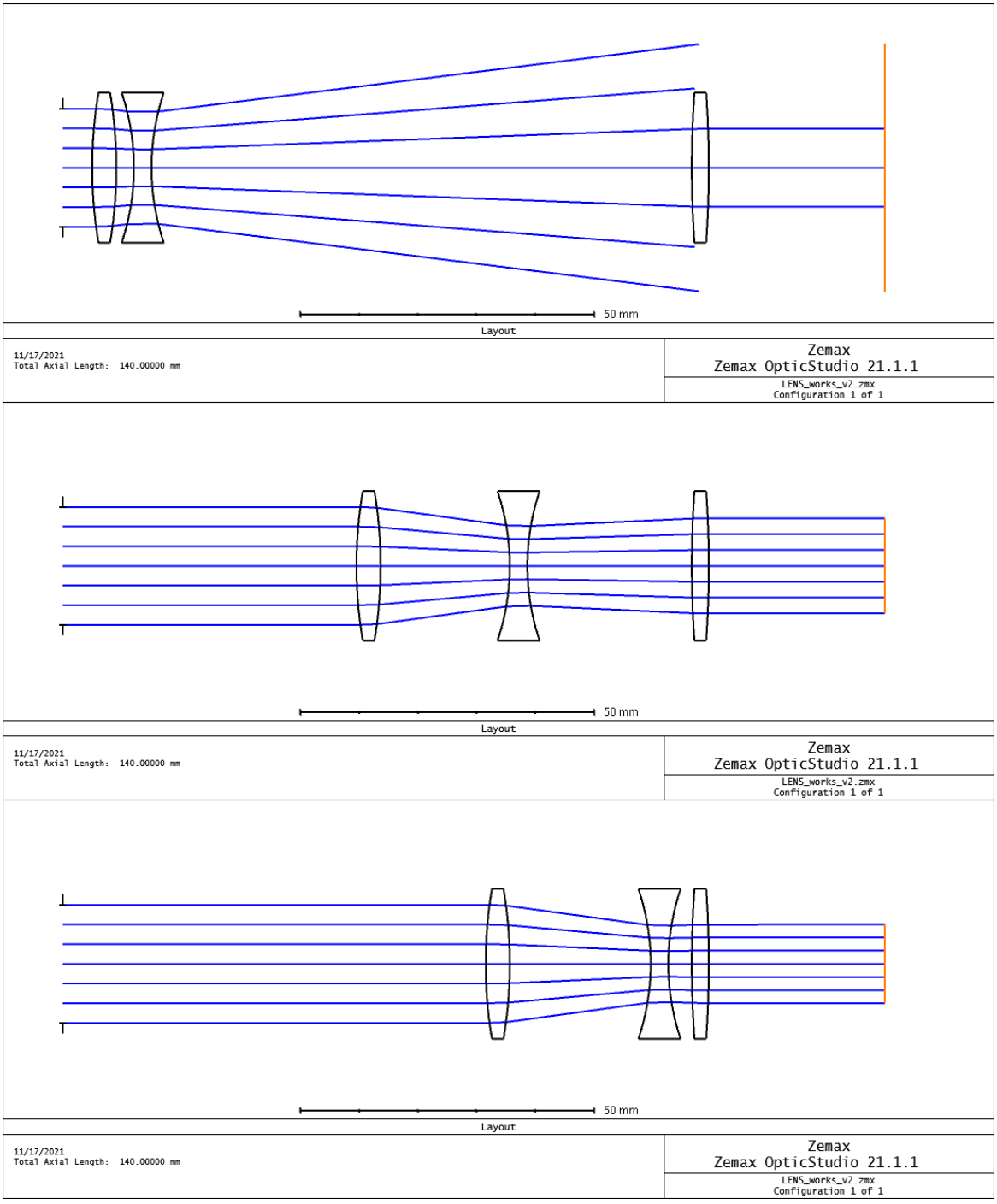

Figure 18: Simulation of afocal zoom system: Position 1, at the front of the zoom path (top). Position 2, at the center of the zoom path (center). Position 3, that the back of the zoom path (bottom). The incoming light is from the left, and outgoing light to the right, where it will hit the image plane highlighted in orange. The camera will sit at the image plane.

The Zemax simulation ran 9 positions that developed coherent output beams, mapped in figure (9). As shown in figure (9), the movement of lens A, the

biconvex lens at the front of the system (left) is nonlinear. Lens B, the biconcave lens (center) moves in a linear path. This is consistent with design principles found in preliminary research. Lens C, the biconvex lens at the back of the system (right) is stationary and stabilizes the rays on the image plane. Lens B will move at a constant rate to and away from Lens C in the zooming process. The distance Lens A moves will need to be mathematically calculated and simulated through zemax to ensure it compensates the variator lens correctly. It is essential that the image plane remains stable for a clear image to be formed.

Figure 19: Graph depicting the movement of compensator lens A, and variator lens B, relative to stationary prime lens C. Imagine lens C laying along the x axis, and each point representing a different location along the optical axis. The trend line represents the movement of the lens being linear in the case of the variator lens and nonlinear in the case of the compensator lens.

The RMS spot size is not a sufficient measure of focus in an afocal system. this is due to the parallel output beams incident to the image plane. The RMS spot size shows the entire beam diameter. This analysis, figure(10), shows the parallel rays and illustrate the zoom of the system. At position one the rays are spread out and fewer in number, as this is where the zoom will be the tightest. The smallest amount of light will be collected in this position, because it is dependent on the number of photons reflecting off the surface toward the lens system. This may mean that the closest zoom that can be obtained may not be practical or collect a sufficient amount of light to resolve an image. If this is the case, the closest zoom that can be used will be the minimum light require to be

collected to resolve an image. The second position has rays tighter together and more numerous, which is what is expected when zooming out. The third position is tighter, though has the same number of rays. The amount of light collected in position two and three are the same, due to all of the rays of light successfully traversing the lens system. this is depicted in figure (8), where some rays are angled above and below the prime lens.

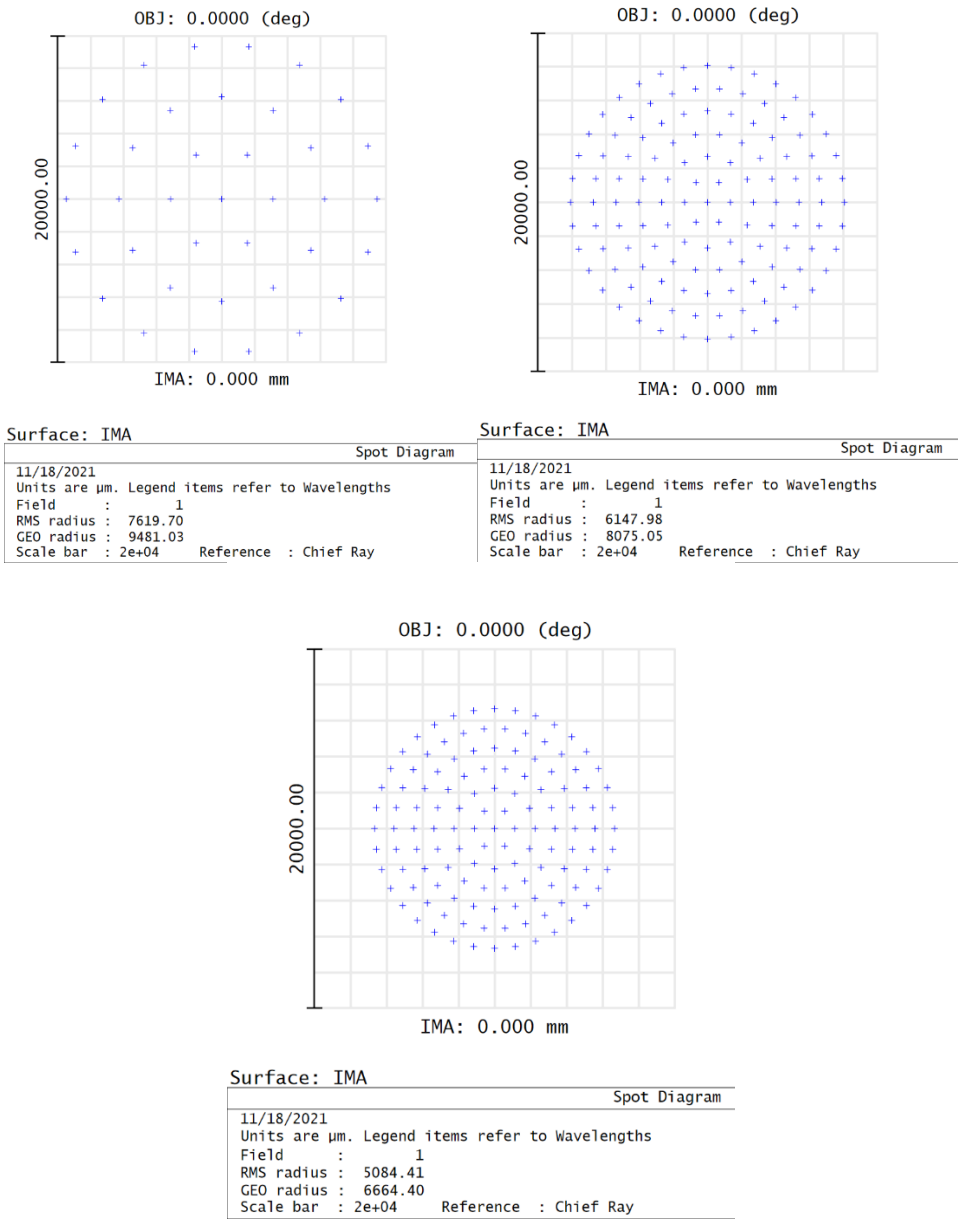

Figure 20: Spot size analysis, second simulation: Position 1, at the front of the zoom path (top left). Position 2, at the center of the zoom path (top right). Position 3, that the back of the zoom path (bottom).

Initial Zemax simulations, that did not work and were later scraped, included a split variator group design to allow for compensation of aberrations, as well as a

focal zoom system. The spit variator group led to higher complexity without great effects. It also increased the cost which impeded on budgetary constraints. The focal system is unnecessary and introduced too many aberrations to compensate for, given the limited budget.

Aberrations were a main concern when initial Zemax testing was conducted. However, adjusting the parameters and realizing that an afocal system is a simpler and cost-effective solution, aberrations are no longer a main concern. Light rays do not need to converge for the zoom system to work. This configuration with parallel rays on the image plane is common in telescopes and binoculars, which influenced the design of this system.

6.3.3 Zemax simulations (3)

The main concern from the previous simulations was that it relied on the chosen camera, the ZWO ASI 385 Color CMOS Telescope Camera, having a focusing lens built in front of the sensor. If the camera does not have a focusing lens, the need for a one will be crucial for a clear and focused image. Prior to initial lab testing, elaboration of which will occur in a future section, the camera focusing lens was not a priority. This is because typical consumer ready cameras have one built in, however lab accessible testing cameras did not, so a focusing lens is explored here. The addition of focusing lens to the design will simply require a focal point that falls incident to the camera sensor. The focusing lens would be stationary and lay between the afocal zoom and the camera. The main change that would occur if the focusing lens is needed is the length of the overall system. The current lens system design is 14 cm before the camera. The focusing lens would add that lens' focal length to systems length. The following simulations serve two purposes, proof of concept that the zoom system does in fact produce parallel light rays that then can be focused on the camera sensor, and selects a fitting focusing lens, in the case it is needed.

The requirement of the focusing lens is that it is a biconvex lens. Several focal lengths were tested, and the resulting focus is tabulated in table (4). The highlighted lens resulted in the smallest rms spot size, meaning it focused to the smallest point on the image plane, where the camera sensor will lay.

Focusing lens (ThorLabs)	*Focal length (mm)*	*Back Focal length (mm)*	*RMS spot size (μm)*	*Distance from camera - added length to the system (mm)*
LB1761	*25.4*	*22.2*	*287.8*	*19.25*
LB1471	*50.0*	*48.2*	*58.2*	*46.98*
LB1901	*75.0*	*73.6*	*14.07*	*73.09*
LB1676	*100.0*	*98.8*	*4.48*	*98.59*
LB1904	*125.0*	*123.9*	*15.9*	*123.94*

Table 6: Foucsing Lens

The simulation design uses the same afocal zoom lenses as the previous round of simulations, however, introduces a 1 in. biconvex focusing lens with a radius of curvature of 128.2 mm and focal length of 100.0 mm. The lens data and distances between each lens at each of the three positions in the simulation are shown figure (11). The entire length of the system is increased by cm to be 24.2 cm total throughout the entire simulation, which is within the design parameters for this project.

	Surface Type	Comment	Radius	Thickness	Material	Coating	Clear Semi-Dia	Chip Zone	Mech Semi-Dia	Conic	TCE x 1E-6
0	OBJECT Standard		Infinity	Infinity			0.000	0.000	0.000	0.0...	0.000
1	STOP Standard		Infinity	3.000			10.000 U	0.000	10.000	0.0...	0.000
2	(aper) Standard		76.600	4.100	N-BK7		12.700 U	0.000	12.700	0.0...	-
3	(aper) Standard		-76.600	3.000 V			12.700 U	0.000	12.700	0.0...	0.000
4	(aper) Standard		-39.600	3.000	N-BK7		12.700 U	0.000	12.700	0.0...	-
5	(aper) Standard		39.600	92.000 V			12.700 U	0.000	12.700	0.0...	0.000
6	(aper) Standard		179.800	2.900	N-BK7		12.700 U	0.000	12.700	0.0...	-
7	(aper) Standard		-179.800	30.000 V			12.700 U	0.000	12.700	0.0...	0.000
8	(aper) Standard		102.400	3.600	N-BK7		12.700 U	0.000	12.700	0.0...	-
9	(aper) Standard		-102.400	98.596			12.700 U	0.000	12.700	0.0...	0.000
10	IMAGE Standard		Infinity	-			10.000 U	0.000	10.000	0.0...	0.000

	Surface Type	Comment	Radius	Thickness	Material	Coating	Clear Semi-Dia	Chip Zone	Mech Semi-Dia	Conic	TCE x 1E-6
0	OBJECT Standard		Infinity	Infinity			0.000	0.000	0.000	0.0...	0.000
1	STOP Standard		Infinity	52.000			10.000 U	0.000	10.000	0.0...	0.000
2	(aper) Standard		76.600	4.100	N-BK7		12.700 U	0.000	12.700	0.0...	-
3	(aper) Standard		-76.600	22.000 V			12.700 U	0.000	12.700	0.0...	0.000
4	(aper) Standard		-39.600	3.000	N-BK7		12.700 U	0.000	12.700	0.0...	-
5	(aper) Standard		39.600	28.000 V			12.700 U	0.000	12.700	0.0...	0.000
6	(aper) Standard		179.800	2.900	N-BK7		12.700 U	0.000	12.700	0.0...	-
7	(aper) Standard		-179.800	30.000 V			12.700 U	0.000	12.700	0.0...	0.000
8	(aper) Standard		102.400	3.600	N-BK7		12.700 U	0.000	12.700	0.0...	-
9	(aper) Standard		-102.400	98.596			12.700 U	0.000	12.700	0.0...	0.000
10	IMAGE Standard		Infinity	-			10.000 U	0.000	10.000	0.0...	0.000

	Surface Type	Comment	Radius	Thickness	Material	Coating	Clear Semi-Dia	Chip Zone	Mech Semi-Dia	Conic	TCE x 1E-6
0	OBJECT Standard		Infinity	Infinity			0.000	0.000	0.000	0.0...	0.000
1	STOP Standard		Infinity	52.000			10.000 U	0.000	10.000	0.0...	0.000
2	(aper) Standard		76.600	4.100	N-BK7		12.700 U	0.000	12.700	0.0...	-
3	(aper) Standard		-76.600	24.000 V			12.700 U	0.000	12.700	0.0...	0.000
4	(aper) Standard		-39.600	3.000	N-BK7		12.700 U	0.000	12.700	0.0...	-
5	(aper) Standard		39.600	7.000 V			12.700 U	0.000	12.700	0.0...	0.000
6	(aper) Standard		179.800	2.900	N-BK7		12.700 U	0.000	12.700	0.0...	-
7	(aper) Standard		-179.800	30.000 V			12.700 U	0.000	12.700	0.0...	0.000
8	(aper) Standard		102.400	3.600	N-BK7		12.700 U	0.000	12.700	0.0...	-
9	(aper) Standard		-102.400	98.596			12.700 U	0.000	12.700	0.0...	0.000
10	IMAGE Standard		Infinity	-			10.000 U	0.000	10.000	0.0...	0.000

Figure 21: Table of lens data, simulation 3: Position 1, at the front of the zoom path (top). Position 2, in the middle of the zoom path, (center). Position 3, at the back of the zoom path (bottom)

As the simulation shows in figure (12), the variator moves from the front of the system to the back as it zooms. The focusing lens is the final lens before the image plane, where the camera sensor will sit, highlighted in orange. For the afocal zoom, both the incoming and outgoing light rays are focused at infinity, however are closer together as the variator lens moves closer to the image plane and the zoom increases. The lens motion is the same as the last simulation where the compensator lens moves to compensate the rays and keep the image plane stationary and the third lens group, the prime lens, does not move and fixes the image on the image plane. The final lens is the focusing lens which is stationary through the entire zoom range. At each position, the rays focus to a single point on the image plane.

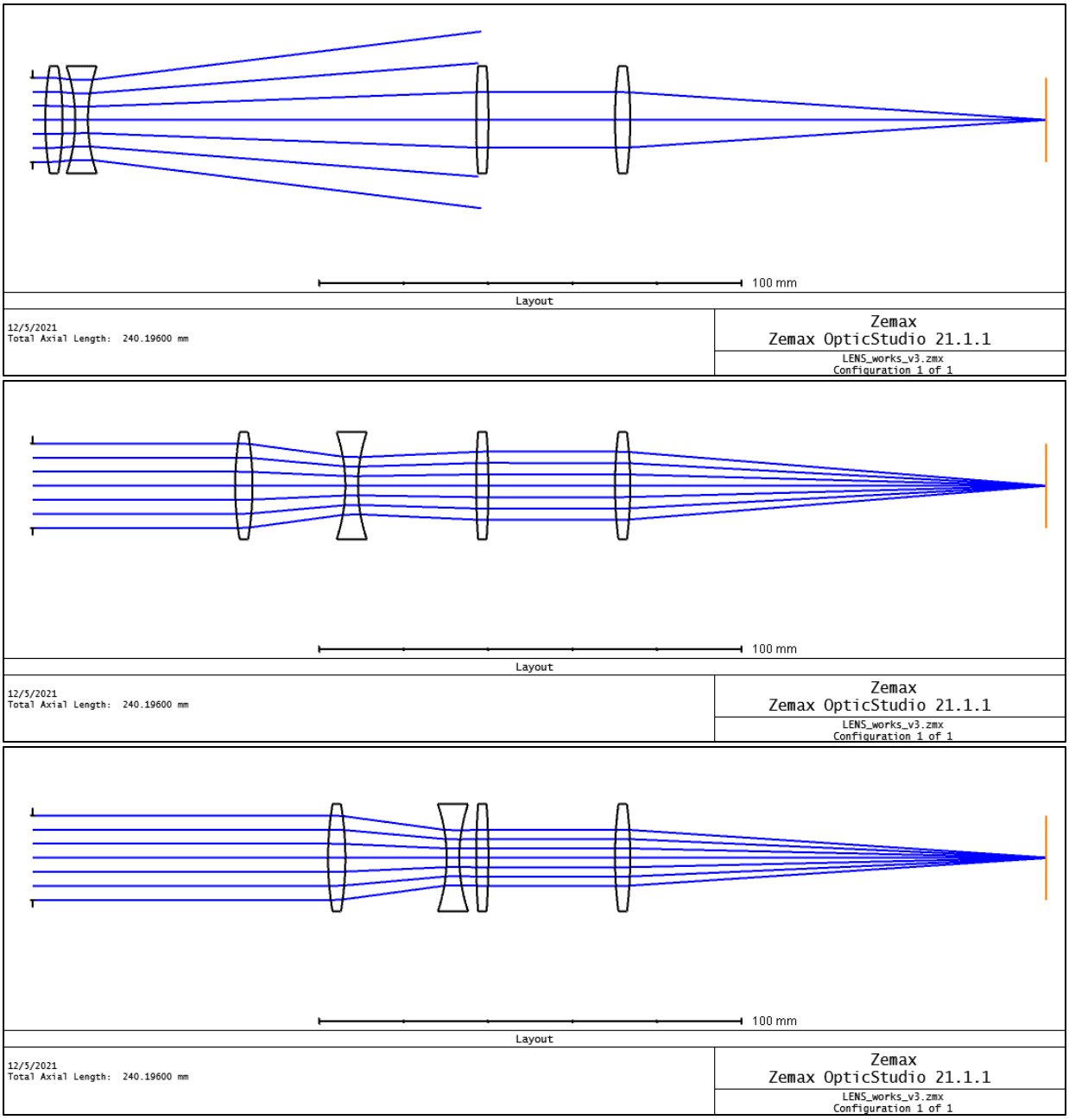

Figure 22: Simulation of focal zoom system with focusing lens: Position 1, at the front of the zoom path (top). Position 2, at the center of the zoom path (center). Position 3, that the back of the zoom path (bottom). The incoming light is from the left, and outgoing light to the right, where it will hit the image plane, highlighted in orange. The camera sensor will sit at the image plane

The simulation focuses the beam to one spot on the image plane more tightly than previous simulations. The spot size analysis shown in figure (13) shows small RMS radiuses for all three positions. The RMS radius is a sufficient measure of resolution and is used to tell if the beam is focused to one spot on the image plane. The smaller the RMS spot size, the more focused the image is. The RMS radius for the first position is 42.03 µm, while the second position is 4.486

μm, and the final position is 2.147 μm. The large RMS radius for the first is relatively small and is expected when the rays are far apart.

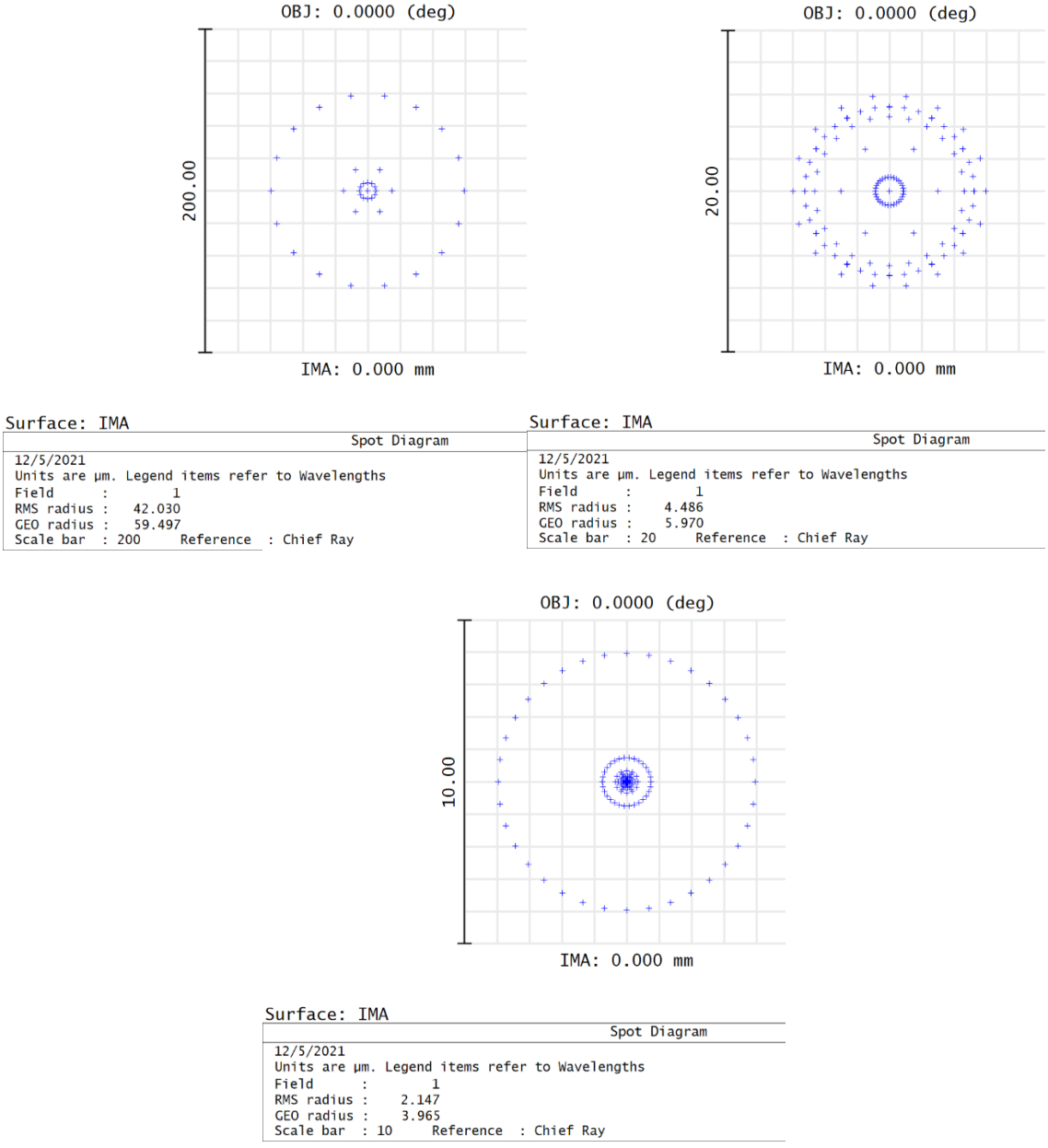

Figure 23: Spot size analysis, third simulation: Position 1, at the front of the zoom path (top left). Position 2, at the center of the zoom path (top right). Position 3, that the back of the zoom path (bottom).

6.3.4 Future Zemax simulations and design considerations

Future design considerations that need to be explored and simulated are a collection lens, a focusing lens and reintroduction of split variator group design. The need for a collecting lens must be explored because the incoming light into

the system is small. The small amount of light collected is because the light is coming from a diffused surface and at a distance. Additionally, the lenses and housing are small, around 1 inch in diameter, so there may be a need for a large collecting lens to sit in front of the zoom system to focus in as much light as possible. Also, introducing a split variator group to may be needed to account for aberrations if the addition of a collector lens or focusing lens introduces those issues.

6.3.5 Initial Lab Testing

Once the lenses were purchased, initial lab testing began to zoom in on an image using a camera provided by the university testing labs. The schematic of the experiment is depicted in figure (14). The set up consisted of an optical rail, on which an image screen is position on one end and the camera on the opposite end. On the optical rail the three lenses that make up the zoom system are positioned before the camera. The lenses are held up by lens mounts that can move along the optical rail. The test contains four positions of the front two moving lenses. Three of these four positions are used in the simulations contained in the Zemax simulation section, though all four were simulated prior to testing, and are tabulated below in table (5).

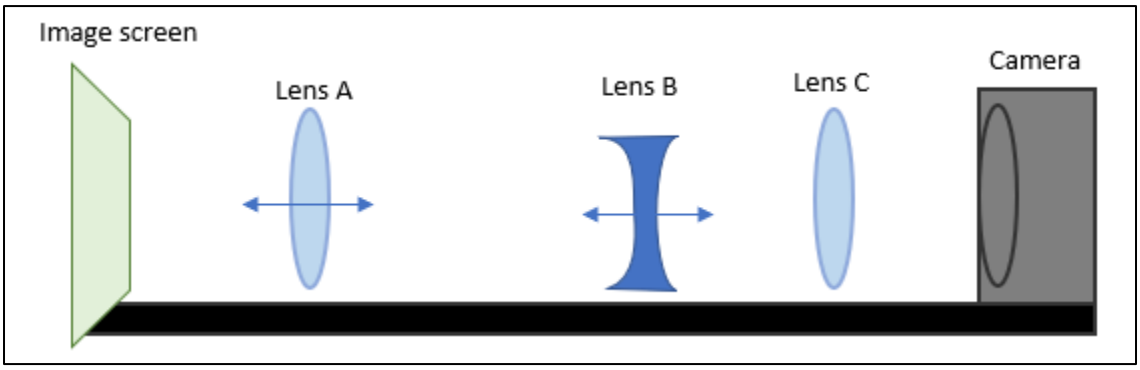

Figure 24: Zoom experiment schematic

Position	*Distance between lens A and B (mm)*	*Distance between lens B and C (mm)*	*Distance between the focusing lens and the camera (mm)*	*Simulated RMS spot size (µm)*
1	*3*	*92*	*98.6*	*42.03*
2	*18*	*53.7*	*98.6*	*0.4*
3	*22*	*28*	*98.6*	*4.48*
4	*24*	*7*	*98.6*	*1.355*

Table 6: Simulated Distances between Lenses

Several issues with the current state of the design stood out right away. The camera used does not have a focusing lens in front of the sensor and cannot develop a clear or focused image. This is not the camera that will be purchased for this project, it was a testing camera provided in the lab. However, this revelation caused additional simulations that introduced a focusing lens to occur. This issue is easily remedied by adding the lens that was optimally chosen via Zemax simulations. Another issue is that the distances between lenses, the closest of which is 3 mm at position one, is too close to be feasible while using the optical rail and lens posts. In fact, in all positions the distance between lens A and B are too close to be feasible given the current equipment available. The posts and rail sliders are too thick, and the lenses cannot get close enough to each other to successfully be in any of the four positions. Because the design relied on using the same equipment that is available to test with, several solutions need to be explored as to not waste time or money jumping to an unviable solution. To overcome the bulky equipment issue, various solutions to this problem are explored below, along with each's pros and cons.

One solution, may be the simplest, is to use different posts. Newport offers A-line Keyed guide rods and A-line fixed lens mounts which would eliminate the need for bulky mounting equipment. The mounts are designed to be self-aligning as there is a hole parallel to the optical axis through the face of the lens mount where a guide rail will run through all subsequent lens mounts. The optical axis would therefore be the guide rod rather than the optical rail in this design. The clearance of the lens mount is the only equipment that would need to be considered when testing different positions. This is the simplest solution, however, may cause an issue with movement using the motors. Additionally, all the mounting equipment would need to be purchased before further testing, as these are not readily available in university labs. However, the cost for the Newport mounts cost about half as the Thorlabs mounts that the tests were conducted with, which would also help with the budget.

Another solution would be to use translation stages in the place of an optical rail. This was a solution tested in the lab. Two translation stages positioned butt to butt are able to move at different distances, as is needed for lens A and lens B's movement paths and provide mounting holes close enough together to reach the smallest gap of 3 mm in position 1. The main issue is that translation stages are extremely expensive, and this design would employ two translation stages. For

this reason alone, though its confirmed to be a working solution that can meet all other design need and reach close distances, the price is too high and cannot be chosen.

An untested but feasible solution would be to use two rails rather than the one so that the lenses are horizontally suspended over the optical axis. To illustrate the concept, figure (15) shows the horizontal suspension. The lenses would only need to consider the clearance needed by the mounts themselves rather than the posts or slide rail mounts, which caused the main issues. The movement would be easier than with the A-line mounting rod because the motors would be able to shift the rail-mount along the fixed rail rather than the lens-mount along the rod. However, the optical axis will be hard to maintain because there will not be a rail or rod in this design to adhere the lenses to it. For this reason, it may be too difficult to maintain a proper optical axis given the nature of the device's movement in several directions and being outside.

Figure 25: Horizontally suspended lens (Image taken from ThorLabs)

Finally, the last solution, would be to redo the simulations with new lens taking into account the need for 15 mm minimum clearance for the available rail-mounting equipment. This option is a backup option and other solutions should be exhausted before this one is taken, given the amount of time required to redo the simulations.

6.4 Camera

In our beam profiler, care will be needed to balance the need for low read noise and higher frame rate. Though, as previously mentioned, a frame rate of 60+ fps is unlikely to be necessary, it is important to keep in mind any relationships that will affect the image (Andor, 2019).

In our demo we plan to use a green or red laser pointer. Because the quantum efficiency is highest in the green frequencies, it is likely that a green laser pointer is most practical for proof of concept. Also, a high quantum efficiency is high priority when choosing and comparing camera options,

especially in low power scenarios. Low power laser pointer beams will not be as easy for the camera to pick up because less photons will be diffused from the target surface. Therefore, a high peak quantum efficiency is needed in our demo (Andor, 2018).

Specification	Goal	ZWO ASI 385 Color CMOS Telescope Camera	ZWO ASI120MM-S Monochrome CMOS Astrophotography Camera	Celestron NexImage 10 Color Solar System Imager	Orion StarShoot AutoGuider
Price	<300	$350 ($299)	$179	$435.95 (274.95)	$299.99
ADC	12 bit	12 bit	12 bit	12 bit	8 bit
Back focus		12.5 mm	12.5 mm	13.1 mm	
Connection		Female M42x0.75	Female M42x0.75	C thread	1.25" Nosepiece
Color/mono		Color	Mono	Color	Mono
Dynamic range		12 stops	11.6 stops		
Frame rate (full res)	30+ fps	120 fps	60 fps	15 fps	
Frame rate (max)		120fps	254 fps	200 fps	15 fps
Full well	Large ke	18.7 ke	20 ke		
Mega pixels		2.1 mp	1.2 mp	10.1 mp	1.3 mp
Peak QE	High QE	80%	78%	39%	
Pixel array		1936 x 1096	1280 x 960	3664 x 2748	1280 x 1024
Pixel size		3.75 microns	3.75 microns	1.67 microns	5.2 microns
Read noise	Low e-	0.7 e-	6.6 e-		12 e-
Sensor diagonal		8.3 mm	6 mm	7.6 mm	8.5 mm
Sensor type	CMOS	CMOS	CMOS	CMOS	CMOS
Sensor		Sony IMX385LQR	CMOS AR0130S monochrome sensor	ON Semi MT9J003	Micron MT9M001
Weight	Low lbs		0.2 lbs		

Table 7: Camera specifications comparisons. Taken from (CMOS Cameras, 2021)

Due to the considerations mentioned above, the ZWO ASI 385 Color CMOS Telescope Camera fits the design needs the most. Key considerations included the ADC, frame rate, full well, peak QE and read noise. Ultimately, the read noise and peak QE are the parameters that this camera rose above compared to the other options and were the reason this was chosen. The frame rate and peak QE eliminated the Celestron NexImage 10 Color Solar System Imager from consideration. The read noise eliminated the ZWO ASI120MM-S Monochrome CMOS Astrophotography Camera, despite all other specifications meeting the design requirements. The read noise and frame rate of the Orion StarShoot AutoGuider were nowhere near the requirements needed for this application, and therefore eliminated this option as well.

6.5 Optical Filter

The design for this experiment will consist of two optical filters. One filter will be a long pass optical filter and the other a short pass optical filter. The two optical filter stacked will create a custom bandpass filter. The goal is to have as narrow of a bandwidth as possible only allowing in the laser wavelength being used for experimentation and blocking all other frequencies outside of the bands. These two filters will need to be compatible, have a high enough optical density to block the outer bands sufficiently, and have a high enough transmission rate of the pass band. The calculated threshold transmission rate for the design is at least 70% to have an intense enough optical signal to reach the camera. Interference filters were not chosen because of their extreme angle sensitivity. The ideal choice are absorptive filters that require no angle of incidence, and they must fall within the budget for the lenses of roughly 250.00$. For lab testing of this experimental design a high intensity laser pointer of 532 nm wavelength will be shone upon a diffused surface backboard. The diffused surface will be made of material that is used on the outdoor range for the stretch goal. The main objective of this design is to capture as much diffused laser light as possible from the diffused surface through the lens system and filter system by the camera. During lab experimentation there will be ambient light from a light source that is in the room. This light source will introduce a broad range of visible wavelengths into the system that will be considered noise and must be filtered out by an optical filter. By stacking both an optical short pass filter and an optical long pass filter a custom optical bandpass filter will be created. It is ideal to have the smallest bandwidth of allotted wavelengths being introduced to the camera for analyzing the data. After searching around on many websites, to name a few, Newport, OmegaFilters, OceanInsight, Alluxa, OpticalfiltersUS, EdmundsOptics, many optical filters and design combinations are available on the market. The

prices of each optical filter and there working properties ranges from as low as forty dollars US to as high as a few thousand dollars. The price difference is due primarily to the types of materials, the thickness of the optical lens, the type of filter, and the working properties. Many rare metal coatings on optical filters will give the optical filter unique transmission windows, but in turn significantly increase the costs. There are many optical filters online that are the exact transmission spectrum with the required central wavelength for this experiment, but unfortunately the cost makes them unrealistic to add to the budget. These types of optical filters are traditionally used in specialized experimentation. The option to design an optical filter on many of the websites is also available for the company will create the necessary lens per specification. This process through shopping around is quite costly and can potentially be even more than purchasing all other components individually for the design. Instead of purchasing an expensive optical filter for the experiment or just buying a bandpass filter that is centered at the 532 nm, the approach taken is to create an optical bandpass filter using both an optical short pass filter and optical long pass filter. By stacking these two types of optical filter a unique bandpass filter will be created and will allow the proper range of spectrum to travel through the optical system designed. Below is a table of many combinations of optical filters that were attempted.

For the stretch goal a similar approach can be attempted to build a band pass filter with a narrow transmission band allowing only the desired 800 nm frequency transmitted. After having already looked at multiple websites to find a similar design for the stretch goal it has been challenging to find a combination that narrows the bandwidth as small as that with the 532 nm design. The smallest bandwidth combination found was larger than thirty nanometers which is not ideal. This stack combination also was much more expensive than that of the filters being used for the green laser experimentation. In compassion to the 156.00$ of the green filter design the 800 nm design costs nearly double. Through looking on many different optical filter websites there are multiple band pass filters already on the market which are quite affordable. When it comes to the stretch goal instead of designing a bandpass filter it may be the most reasonable decision to just purchase an already prefabricated 800 nm central bandwidth filter.

Manufacturer	Long Pass Optical Filter	Short Pass Optical Filter	Peak Transmission Bandwidth	Cost
Edmunds	#49-026 D = 12.50 mm Cut on 500 nm Transmission: 520 – 2000 nm > 85% @ 532 OD = 2 Angle of Incidence: 0	#47-813 D = 12.50 mm Cut off 550 nm Transmission: 400 – 535 nm > 85% @ 532 OD = 2 Angle of Incidence: 0	520 – 535 nm	LP = 64.75 $ SP = 92.50$ Total = 157.25$
Omegafilters	SKU: W4583 501AELP D = 12.50 mm Cut on 501 nm Transmission: 505 – 600 nm > 90% @ 532 OD = 4 (484 – 492 nm) Angle of Incidence: 0	SKU: W6045 540SP D = 12.50 mm Cut off 805 nm Transmission: 432 – 538 nm > 90% @ 532 OD = 4 (540 - 1100 nm) Angle of Incidence: 0	505 – 538 nm	N/A Requested Quotes.
Thorlabs	FEL0500 D = 25.4 mm Cut on 500 nm Transmission: 502 - 2200 nm > 88% @ 532 OD = 2: (200 – 502 nm) Angle of Incidence: 0	FES0550 D = 25.4 mm Cut off 550 nm Transmission: 380 – 550 nm > 85% @ 532 OD = 2: (560 – 2200 nm) Angle of Incidence: 0	502 – 548 nm	LP = 80.62$ SP = 80.62$ Total = 161.24$
Dyanasil	LP-500-25 D = 25 mm Cut on 500 nm Transmission: 500 – 2200 nm > 80% @ 532 Angle of Incidence: 0	SP-550-25 D = 25.4 mm Cut off 550 nm Transmission: 400 – 550 nm > 80% @ 532 Angle of Incidence: 0	505 - 545	LP = 70.00$ SP = 70.00$ Total = 140.00$

Table 8: Filter Comparison

Choosing which combination is both the best for application as well as for cost efficiency the The Edmunds set of edge filters will give the narrowest bandwidth, and the transmission is 72.25% (above the 70% threshold sought for design). The optical density will be a little higher than two for the band reject region and the price is within budget. The omegafilters have the highest transmission rate of 81% and the highest band reject region with optical density of a bit more than four when stacked. These two optical filters have an acceptable bandpass window, but without knowing the pricing it is hard to say if

they are within the budget. The Thorlabs short pass and long pass optical filters have an acceptable bandpass transmission of 74.80%. The optical density of for the band reject region will be just above two. The pricing is comparable to the Edmunds but the bandpass transmission window is a little wider than desired for the design. The Dyanasil edge filters have a bandpass transmission of 64%. The bandpass region is also the broadest of the four filters compared. The pricing is reasonable but because of the wide bandpass region and the transmission lower than the desired 70% threshold this option will not be chosen. It is in the best interest of the design to have the highest possible transmission rate. The laser light signal will already be lower intensity as it will be diffused light, and highly attenuated by the optical lens system design. These two factors will make it harder to get quality data. If the pricing for the omegafilters optics are comparable to that of the Edmunds than those may be the stack combination of choice choice. These optical filters have a higher bandpass transmission rate as well as a higher optical density to block out the undesired frequencies Currently the bandpass filter design combination of choice is the Edmunds set. The total transmission of the stack is 72.25% which is what is being sought (over the 70% threshold mark). Also, the cost of the filters is reasonable and within budget. The optical density reject region is high enough to block out the undesired frequencies from entering the camera. If the pricing for the omegafilters optics are comparable to that of the Edmunds than those may be chosen. These optical filters have a higher bandpass transmission rate as well as a higher optical density to block out the undesired frequencies The images below show the spectrum of both the Edmunds #47-813 short pass filter and the Edmunds #49-026 long pass filter.

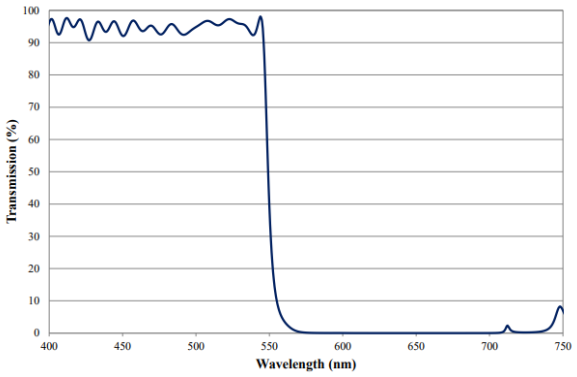

Spectrum of short pass filter used in device
Edmunds #49-026
Picture taken from Edmunds website

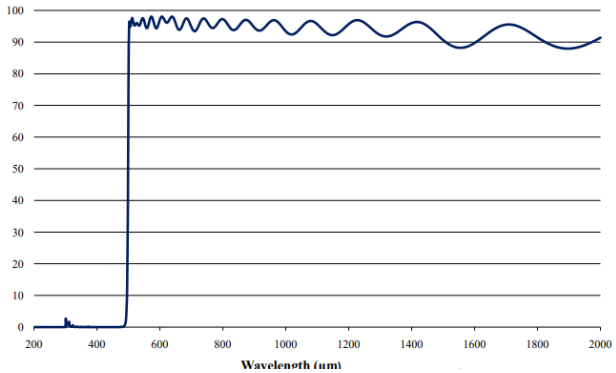

Spectrum of long pass filter used in device
Edmunds #49-026
Picture taken from Edmunds website

Figure 26: Short Pass and Long Pass filter acceptance band

The stacking of these two filters will be the linear multiplication of the two filters which can be written as a unit stepwise function. Let H_1 be the long pass optical filter dimensions and let H_2 be the short pass optical filter dimensions. Below the unit stepwise function of the designed bandpass filter

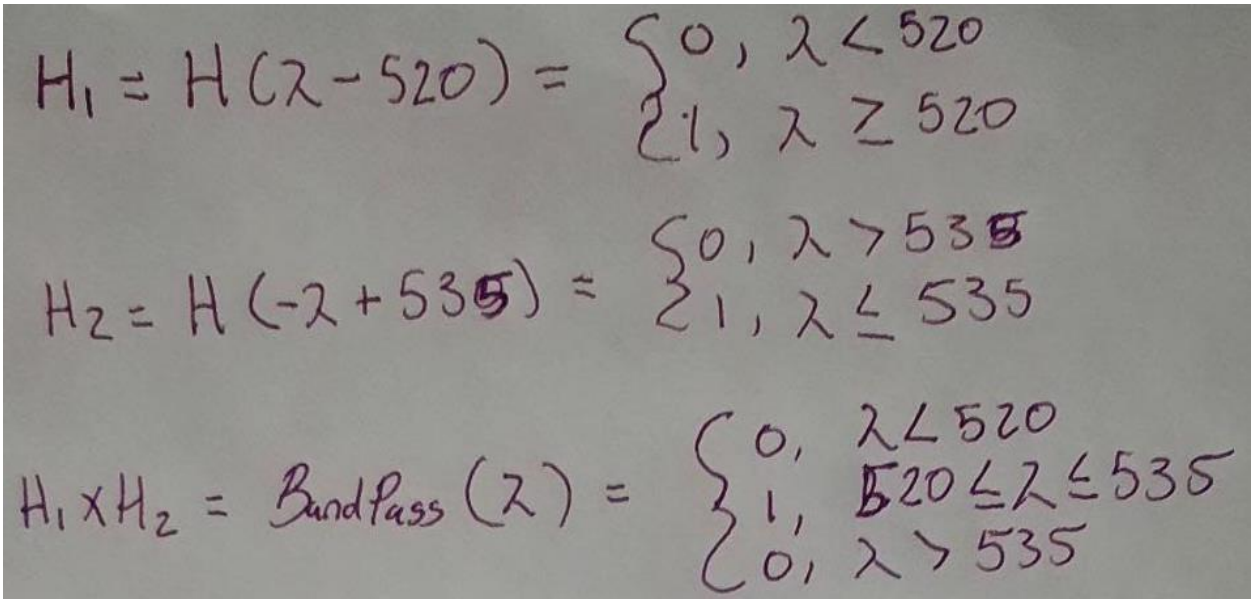

Figure 27: Stepwise function for bandpass filter design
Depicts the linearity of stacking a short pass and long pass optical filter to create a unique band pass optical filter

For the stretch goal of working with the 800 nm laser a similar approach with the filter design can be achieved. There are many band pass optical filters on the market that are made with a central wavelength of 800 nm. Doing the same process as before searching low pass and long pass optical filters online there are many combinations from different optical lens distributers that can be stacked to achieve a narrow bandpass linewidth for the 800 nm laser. The problem with these combinations is that the optical lenses are a bit more expensive than that of the ones used for the 532 nm optical band pass design. The types of optical filter materials used to reach this infra-red region are what add onto the additional cost making them out of budget. For the stretch goal it will be much cheaper to buy one of the already fabricated optical bandpass filters designed for this bandwidth.

6.6 Ambient Light Sensor (PIN Photodiode)

The proper photodiode for this experimentation is a silicon PIN photodiode that is sensitive to both visible light and near IR. Below is a list of the many different PIN photodiodes on the market that have been researched for the design.

Brand	Model	Operating Voltage	Functioning Temperature	Cost	Response Time	Spectral Range
CivilLaser	1.2mm Si PIN Photodiode	0 – 15 V	-40 – 85 C	20.00 $	8 ns	200 – 1100 nm
Osram Opto	SFH2704	0 – 5V	-40 – 85 C	0.65 $	46 ns	400 – 1100 nm
Advanced Photonix	PDB-C152SM	0 – 10 V	-40 – 105 C	1.97 $	50 ns	400 – 1100 nm
Advanced Photonix	PDB – C154SM	0 – 10 V	-40 – 80 C	1.47 $	10 ns	400 – 1100 nm
CivilLaser	3.2mm Si PIN Photodiode	0 – 15 V	-40 – 85 C	11.00 $	6 ns	400 – 1100 nm
CivilLaser	3mm Si PIN Photodiode	0 – 10 V	-25 – 85 C	6.00 $	15 ns	300 – 1200 nm

Table 9: Photodiode Comparison

The Civil Laser 3mm SI PIN photodiode seems to be the appropriate photodetector for the ambient light measurements for the design. This light sensor has a relatively quick response time of 15 ns and will be able to be operated with a low voltage of 5 volts. This photodiode was chosen over the other because it does have a much broader bandwidth reaching into the UV. This photodiode will be used to measure the intensity of the full spectrum light source as well as the sun for the stretch goal. The ability to get an accurate full spectrum intensity profile of the ambient light will allow for the true intensity profile of the laser beam being measured to be calculated by neglecting the ambient light of the same intensity as the laser source. This photodiode has the highest responsivity to the 532 nm spectrum as well so an additional photodiode within the system can be used to aid in determining the intensity of the diffused light travelling through the system. This photodiode also has a relatively low dark current (V_R = 10V) of 10 nA. The cheaper options are still being investigated but unfortunately were not in stock or had a delivery time that would be way outside the window of building the project. The only drawback is to order these photodiodes they must be purchased with a minimum of ten per order which places the cost at 60.00$. This cost is not necessarily out of budget but would be ideal to find cheaper photodiodes that can be ordered in smaller batches. As of right now it seems this photodiode will be the appropriate fit and with having multiple there is room for mistakes in case one burns out in testing. Below is the spectral profile of the photodiode in operation.

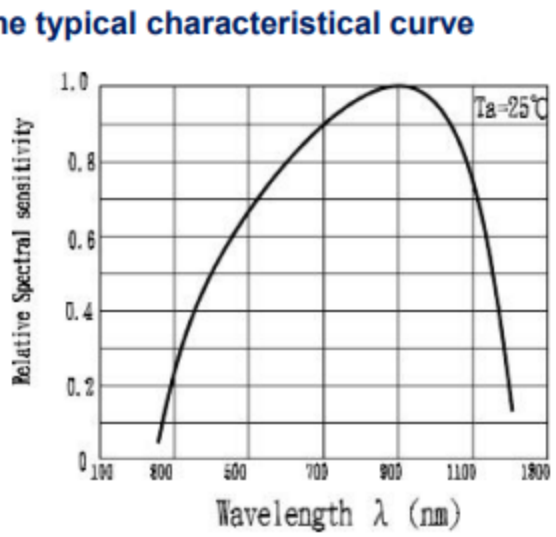

Figure 28: PIN photodiode sensitivity graph (taken from civillaser.com)

The stretch goal is to be able to block out the undesired wavelengths of light through the optical system and then sense, how much of the wavelength is actually being measured from the 800 nm laser versus the full spectrum visible light source. In the lab setting it is possible set a control variable when the lights are off compared with when the full spectrum light is on. Since there is no way to get a true control outside in the sun the device will need to be able to differentiate the blackbody radiation through the optical filter from the diffused laser light. The problem with this is the inconsistent fluctuation of light intensity as the brightness, cloud coverage, and position of the sun changes. This means that every time a test is run the results will be unique to the weather conditions at that time. Since the light intensity is affected by a multitude of factors relating to weather the system needs to be able to record the data and by design differentiate the diffused wavefronts of the laser from the infrared black body radiation of the sun. This approach is still being worked out to find the most effective sensor and approach to single out only the diffused laser light for the stretch goal outdoor laser testing.

6.7 Power Supply and Distribution

A design for a power supply is needed for the system. Batteries of a range of 12-24 volts will be compared along with the chemical composition of the battery. Calculating a comfortable amount of output power for the overall load of our system, allows us to find the right battery’s amps per hour which will allow the system to run without any interruptions or damage. Our system does not require

a high voltage as a power supply, but it does require the right distribution of power to the components making up the system. Since our system powers a number of different components (i.e., motors, cooling fans, sensors), DC-to-DC converters will be designed using TI's Webench software, in order to provide a stable voltage and current to the component. Providing power to the motors will be the biggest challenge in terms of providing power to the system. There are three motors providing three movements, with each movement holding a different weight. Comparing types of motors, as well as an understanding of each motors' rated values (voltage, current and torque) is key to be able to combine supplied power given to the motor, and output work from the motor. Since the system will be protected by a waterproof casing, fans will be installed around areas with the highest risk of temperature increase. Although the microcontroller needs power to operate, the controller will be connected to a laptop in order to read values from the camera, as well as powering it. The microcontroller will be connected to the couple of temperature sensors, and the motors in order to move them when needed for calibration.

6.7.1 Power Supply

The total amount of power consumption based on each component of our system was calculated. Carefully detecting what components consumed the most power from the system is key, then moving on the rest of the components that will need to be powered by the battery. Our system is implemented with three stepper motors, two of them will work to hold the overall weight of the system and will be in charge of displacing the weight when our camera needs to adjust and find the refracted laser from the target. These two motors are chosen to be the most powerful, bringing a higher holding torque, with an acceptable speed. Being powerful motors, they will also consume the most energy, which means we will design a capable power supply that can provide the right currents in order to run with no errors.

Our system requires a variety of magnitudes for voltages and currents, which is not possible by just connecting the battery to these components. DC-to-DC conversion is required to be designed, in order to distribute and amplify the power going through these components. The motors for instance, which are our heaviest component required currents that range from 1.4 amps to 3.0 amps. In the figure below, Webench was utilized in order to get an acceptable circuit schematic for an input voltage ranging from 11.3 V to 12 V. This circuit design results in an output of 13.8 V and 3.0 A.

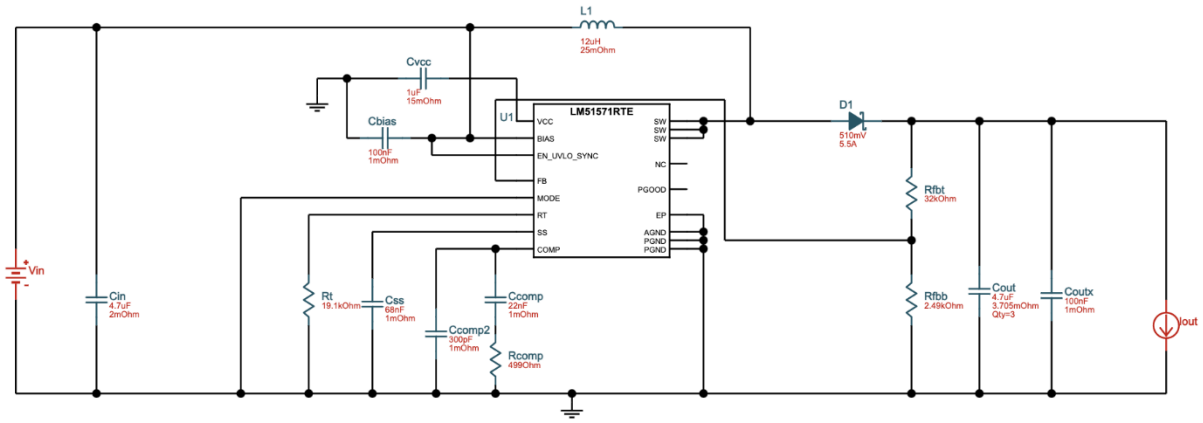

Figure 29: Webench Circuit Design

6.7.1.1 Battery

It is important to size the battery with enough capacity, that it could keep running for longer than what it expected. One of the main parameters is the length at which the system will be in use. For our system, each session will last around ten minutes, leaving enough room for error when it comes to the battery charging and discharging. It is important to understand how much power the system is estimated to consume, this value is 111.94 W which is mainly added from M1 and M2 holding the large load which is the rectangular casing surrounding the electronics. Knowing the total power conceded by the system, the capacity of the system can be calculated and compared to see if we have enough energy. Another key component is the discharge time. For our system, it will be tested outside, where the environment can affect certain components. The battery is one of those components that our group has to pay attention to. At this moment, our group has decided to power the system with an Eco-worth Lithium iron battery, which is rated at 12 volts, with 20 Ah. Its temperature ranges from 0 - 55 Celsius, and for discharge temperatures ranges from -20 - 55 Celcius.

As we make a decision for a battery of the right size, figure 30 illustrates a schematic where a 12 volt battery energizes each component. Our system has four motors, each pair in charge of doing similar tasks and carrying the same load. For that reason, the schematic illustrates one of each of the connections. As it can be seen, after the microcontroller is powered by the battery, the stepper driver MP6500 is connected to the microcontroller at one end, and at the other end is connected to the coils of the motor. Another component from the figure, is DC-to-DC converters which will scale down the voltage coming from the battery and allow the voltage to be more managle. Even though there are two motors, the implementation for the other two is identical. One of the motors, M1 as can be seen below, will take as an input 4.0 volts, from the DC-to-DC converter

output. This converter described in earlier sections will scale down the battery voltage three times its size. For the other motor M3, a separate DC-to-DC converter is displayed, where it will scale down the battery's voltage four times its own. As our group looks to start gathering all the components and deciding on what implementation of electronics to go about, the PCB designed, was held to be shown since our schematic implementation might be adjusted, when building the system. Our PCB design will be designed through fusion 360, and for the moment and the price, we will be sending our final design to JLCPCB.

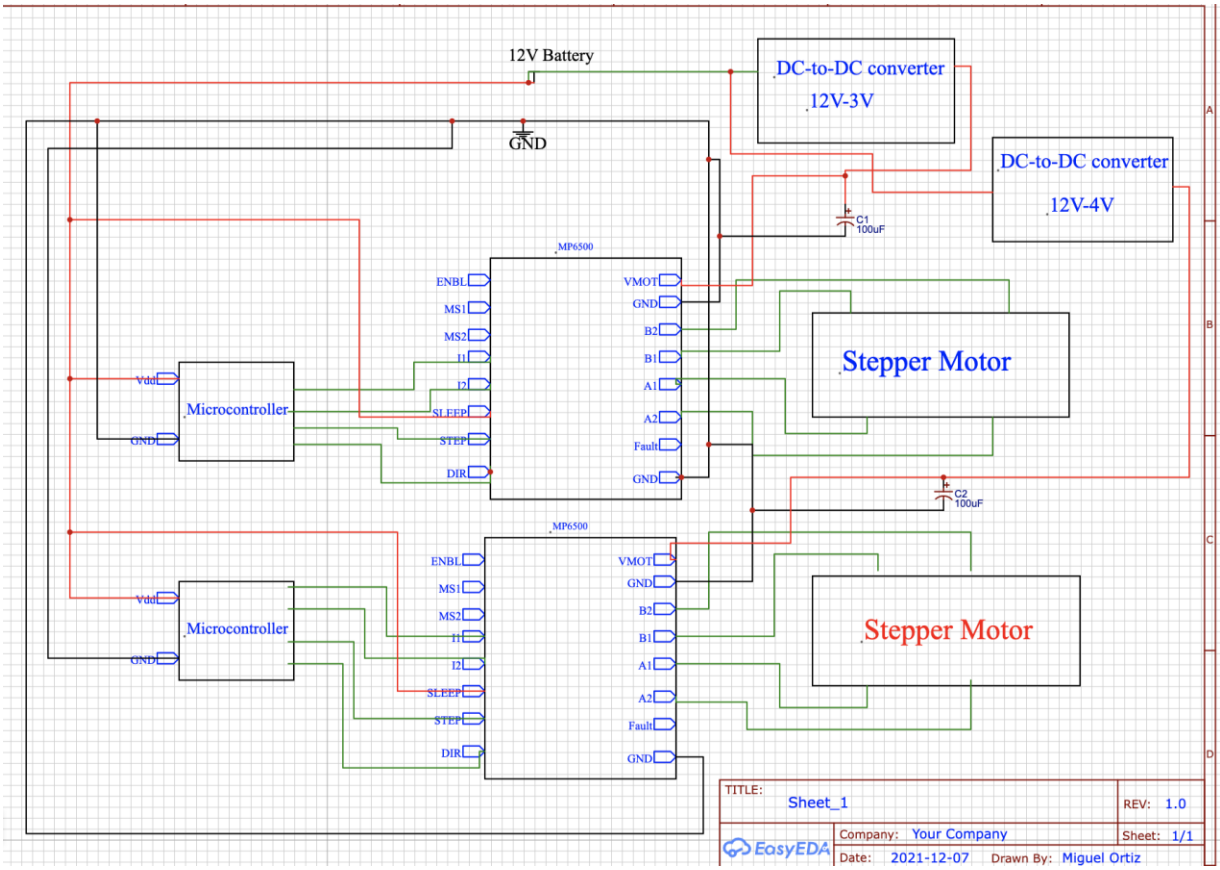

Figure 30: Schematic

On the table below, we have listed batteries which are an option for our system. We can see that the list consists of 12 volts, but the capacity of each battery varies. The capacity is important to note, because our motors will require a constant amount of current in order to work without any interruption or failures.

Name	Type	Voltage	Capacity(ah)	Power (w)
ExpertPower	Sealed lead acid	12	7	84
MightyWax	AGM Deep Cycle	12	12	144
Weize	SLA AGM	12	18	216
Weize	Lead Acid	12	20	240
Weize	Lead Acid	12	100	1200
Lossigy	Lithium ion	12	8	96
Miady	Lithium ion phosphate	12	6	72
ECO-Worthy	Lithium ion phosphate	12	20	240

Table 10: Battery Comparison

6.7.2 Motor Consumption

As mentioned before, the system will create motion utilizing three different motors. We will implement stepper motors to create these motions. Looking independently to each motor we will be able to make a decision for how much power each motor requires from the battery. As we can see one motor will implement a left/right movement to the entire system. As shown in the figure it can be seen that the motor needs to hold the gravitational force, which is produced by the arm, or filter system which extends away from the camera. The second motor is shown in figure 1.6, as you can see, this motor is in charge of the up/down movement of the entire system. As the previous motor described, this motor is one of strongest motors used in our system, since it has to be able to produce a holding torque strong enough to work against gravitational torque, but it also has to produce enough angular velocity to move the arm, or filter system up and down. The last motor used to create movement to our system is shown below this motor allows movement to the filter within our subsystem. The filter subsystem contains one filter which will move linearly between two other stationary filters. One of the filters will be at the end of the camera lens, which is the start of the filter subsystem, and the other at the end of the filter subsystem.

6.7.3 Horizontal and Vertical Motion Motors

As mentioned before, the motor used for the horizontal motion will be chosen to have a greater torque than other motors used for our system. Conducting engineering investigation, we sought a few stepper motors which range from 31 oz.in to 63.74 oz.in of torque. Two motors from both sides of the spectrum will be chosen for testing. These motors will go through simulation, where an estimate of 4,535 grams will simulate the overall weight of the system. Our group will record the response of these motors when using enough weight to make the motor stall. Knowing at what weight the stepper motor will stall is

essential to know when we have obtained a motor with or without enough power for our final system.
Similar to the motor creating the horizontal motion, our system will implement a stepper motor of similar specs. Careful calculation must be done, because even though the vertical stepper motor will manage an equal amount of weight as the horizontal motor, the vertical torque required may increase as the gravitational force increases, since the ‘arm’ of the system will extend away from the center of mass and axis of rotation. When designing our system’s arm, which is where our filtering system will be contained, length between the camera lens and the edge of the arm will be carefully calculated in order to keep our required torque as low as possible. In the prototype phase, different arm lengths will be tested, in order to obtain an acceptable length for the sliding rail which is also inside the ‘arm’.

6.7.4 Filter System Motion Motors

Inside the ‘arm’ of our system, as detailed in previous sections a filter subsystem will be implemented. Careful calculations being conducted describe the lengths each non-static filter will move, inside the ‘arm’. As described earlier, the filters will be light weight (ranges of 50 to 100 grams). With this in mind, a high torque is not the main priority to implement for this subsystem, since the weight of the filters is low. An important characteristic for these two motors is the weight of the motors themselves, by searching for stepper motors of around 140 to 180 grams, will allow our other two motors (horizontal & vertical) to handle gravitational and angular force much easier, allowing the system to run without failure.

Below, table provides a few of the options that are out in the market. As it can be seen there are a range of stepper motors with a wide variety of torque created, as well as weight of each individual motor. Two servo motors are also shown in the table below, the table shows that servo motors can produce a large torque within one motor, which also gives the group an option to utilize both motors in the system. A stepper motor can be a greater option for our system’s vertical and horizontal motion, since a bigger stepper motor can be found at a more affordable price. Where a servo motor can be utilized for the filter system, where precision and accuracy are more crucial than a high torque.

Name	Type	Torque (Oz.in)	Voltage	Current (Amp)	Weight(g)	Dimensions(mm)
Nema 17	Stepper	18.4	2.9	1.4	180	42x42x25
Nema 17	Stepper	22.6	3.7	2.0	140	42x42x20
Nema 17	Stepper	63.74	13.8	3.0	280	42x42x39
LD-20Mg Digital	Servo	277.6	7.4	1	66	54.5x20x47.5
Deego-FPV	Servo	11.65	7.2	1.0	55	40.7x19.7x42.9

Table 11: Motor Motion Comparison

6.7.5 Torque

For our system, we understand that the correct torque will be calculated from effects of both gravitational force and angular acceleration. A point to consider is that commonly the torque needed for gravitational force is notably higher than the torque needed to opposite angular acceleration. This gives us guidance to look into the design of our case, which inside holds the filter system including rails, a motor and other electronic connection between components. The overall system's weight and the length between the end of the filter and the axis of rotation, will dictate the size of the motor needed for the up/down movement. The next step for sizing the motors implemented for our system is calculating Torque. Torque will be calculated into two, load torque and acceleration torque. Load torque is the energy used to hold our system, or the load. The load held by the load torque can be split into two categories, gravitational and frictional loads. For the vertical and horizontal motion, which are provided by motors M1 and M2, gravitational load results from the effects of the overall weight of the rectangular casing and the earth's gravitational acceleration. With that being said, M1 and M2 will not experience any frictional load, since the rectangular casing will not be sliding. Both gravitational and frictional loads will be found in the filtering subsystem, where the motion of the filters is linear. Acceleration torque only exists when there is a need for our system's body to move from a stationary position, or stop the body to a stationary position. Acceleration torque is very dependent on the moment of inertia, so as we previously calculated, high attention should be paid to the vertical and horizontal motors M1 and M2, since the extension of the 'arm', along with its dimensions result in a large moment of inertia. For the linear motors M3 and M4, the acceleration torque will be more manageable than the other two motors. Acceleration will be easier to achieve, having to move significantly lighter loads than M1 and M2. The following will calculate both load and acceleration torque, it will also illustrate the system with each torque being clearly labeled.

6.7.6 Load Torque

The total weight of the system will be at around 4.5 kg, and the axis of rotation will be located at around 26 cm from the body center of mass. Figure 5.1.3 shows a prototype of the system, as shown in the figure, the motor will be installed on the right side of the body of the system. The figure shows the distance between the center of mass and the motor, which is located on the axis of rotation. In order to find the Load torque of our system's body, we calculate the force needed for M1 to hold the weight at any position, with movement from 0 to 90 degrees clockwise. We calculate the gravitational force of the body by using the equation given in previous sections;

$$F = m * g$$

Where, m is the body of our system, and g is the gravitational force. As mentioned before, our system's mass will be around 4.5 kg. We also know that gravitational force is 9.8 m/s^2, which by multiplying these two, our system's body requires a force of 44.45 N in order to at least hold the gravitational force or acceleration. For the vertical motor M2, the gravitational acceleration will also equal 44.45 N. One point to have in mind is that M1 will be the motor with enough holding torque to offset the gravitational acceleration due to the rectangular casing.

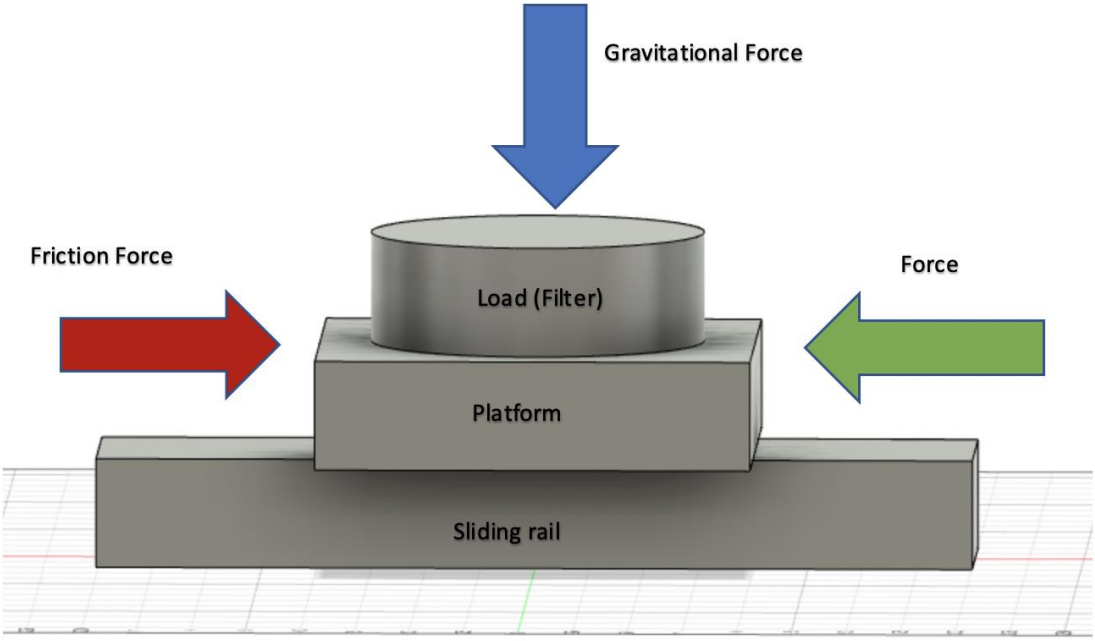

Figure 31: Gravitational and friction force acting on the load and rail

Force (N)	Diameter (m)	Efficiency	Gear ratio	Load Torque (Nm)
0.098	0.0381	0.85	10	2.2×10^{-4}
0.098	0.0508	0.85	5	5.86×10^{-4}
0.098	0.0635	0.85	5	7.32×10^{-4}

Table 12: Load torque with different gear diameter and ratios

Looking into motors M3 and M4, we focused on the filtering subsystem, constructed by a linear rail connected to a platform, which will slide back and forth in a linear motion. Before calculating the load torque, each external force must be recognized. Figure 31 illustrates the two forces that result in load torque, gravitational and frictional force. Illustrated in the image, the vertical arrows show the gravitational force acting on the body of the system, and the rail creating friction. The arrows going in a horizontal direction depicts the frictional force acting on the platform and the load it is carrying. Gravitational force is calculated by utilizing the formula used earlier, which multiplies the mass of the load at around 5 grams with the gravitational acceleration of 9.8 m/s^2. This results in a gravitational force of 0.049 N, which is the body of the system pushing against the platform and rail. Frictional force must be calculated for this type of motion, but at this point our group has not made a decision of what material to implement for our railing system. A timing belt along with a gear reduction strategy will be utilized, in order to create motion for the two filters along the rail. Having that in mind, use of the load torque formula mentioned is as follows;

$$T_L = (F * D)/(2 * \eta * i),$$

Where F is the force needed move the load, D is the pulley diameter, η is the efficiency of the system, and i is the gear ratio. We can estimate a set of diameters and gear ratios in order to obtain the load torque. The following formula is also utilize, in order to find the force that acting on the filters;

$$F = F_{fric} + F_{grav},$$

Where F_{fric} is the friction force acting on the platform when sliding, and F_{grav} is the gravitational force acting vertically on the rectangular casign, which was calculated above. Since the material of the sliding rail has not been confirmed, our group will double the gravitational force in order to calculate with room for error. Table 12 calculates a load torque varying gear dimension, and gear ratio. From the table it can be seen that as the diameter of the output gear increases,

the load torque also increases. On the other side, it is also possible to design a gear reduction system, which will result in a gear ratio large enough that will help reduce the overall force needed to move the rectangular casing.

6.7.7 Acceleration Torque

Now we focus on the torque which is responsible to accelerate and decelerate a body of mass. In our system we have four moving parts, where acceleration torque is needed. As mentioned before acceleration torque is linearly affected by the moment of inertia given by the mass needed to be moved. For our system, the moment of inertia for the rectangular casing and the filters inside the subsystem was calculated earlier. Having this results, acceleration torque is calculated by using the formula described in previous sections which equals,

$$T_a = J * A,$$

Where J is the moment of inertia, body of mass, and A is the acceleration rate to start moving the body of the rectangular casing. Plugging in the values for the moment of inertia for the rectangular casing, and an acceleration rate of 0.20944 rad/ s^2, results in an acceleration torque of 0.00697 Nm. Even Though, a majority of the usage of the system will be stationary making readings and obtaining data from the incoming laser beam, once the system starts moving searching for the beam, acceleration torque will be used very consistently, till the laser is finally captured. Calculating the acceleration torque for the loads inside the filtering subsystem, with two filters of an estimated weight of 5 grams each. Using an acceleration rate of 0.0762 m/s^2, and the moment of inertia from each filter of 0.0007958 $kg\text{-}m^2$ results in an acceleration torque of 6.064×10^{-5} Nm.

As it can be seen in this section, The moment of inertia affects the acceleration torque resulting on motors M1 and M2, to produce a torque large enough that will compensate for the torque needed to accelerate and decelerate the rectangular casing. Motors M3 and M4, will also need to produce a torque large enough that will cover the acceleration torque, when the filters need to be adjusted. Below, table 5.1.3 calculates the acceleration torque with varying moment of inertia, and acceleration rates. The table shows that by reducing the moment of inertia, acceleration torque can be affected linearly, but as our system extends to house the filtering subsystem, it will be very difficult to adjust the dimensions of the overall body of the system. Another option to reduce the acceleration torque is to reduce the acceleration rate, which will be affected when choosing the right implementation for the gear reduction system. Figure 5.1.5 illustrates the acceleration and speed graph for our system. It visually labels the acceleration rate increasing at a time (s), till it reaches constant speed, and finally decelerates till it gets to a speed of zero.

Moment of inertia	Acceleration rate	Acceleration Torque (Nm)
0.033	0.209	0.0069
0.033	0.109	0.0036
0.0008	0.076	6.08×10^{-5}
0.0008	0.096	7.68×10^{-5}

Table 13: Acceleration torque from inertia and acceleration rate

6.8 Gear reduction and motor selection

After calculating all different types of torques for our system, the required torque is calculated by using the formula mentioned in earlier sections which is;

$$T_M = (T_L + T_a) \times S_f$$

Where, T_L is the load torque, T_a is the acceleration torque found earlier, and S_f is the safety factor which will be defined as 0.85. First solving for the required torque for which M1 and M2 must reach, the load torque of 44.45 Nm found in the previous sections is plugged into the equation above, along with an acceleration torque of 0.00697 Nm. The resulting required torque is 0.263 Nm, which is a manageable amount of torque which will avoid having to purchase an expensive motor. For the filtering subsystem, as mentioned before in the load torque section, we use the formula where we double the gravitational force acting on each filter. Also, a diameter of 0.0382 meter for the output gear, along with an efficiency of 85% and designing a pair of gears which give a gear ratio of 5. Plugging this into the equation above, the load torque for motors M3 and M4 is 2.20×10^{-4} Nm. Now combining the load torque with acceleration torque of 6.064×10^{-5} Nm and a safety factor of 0.85, results in a required torque of 1.33×10^{-8} Nm.

Figures 31 and 32 below, shows the prototype of the four gears which are going to be used to increase the torque given to the system in order to change positions. The figure illustrates two driver gears and two driven or output gears. The driver gear will have an estimate of eight teeth, and will drive power to two driven gears which have a diameter of 1.5 inches or 0.0381 meters. In this section it can be seen that due to the dimensions of our system, by having a extension or an ‘arm’, it creates a large moment of inertia, which our group had to think of strategies to overcome a large load torque, due to the weight and distance from the axis of rotation and center of mass. One of the most common strategies is gear reduction, which by connecting a driver gear of a smaller

diameter at higher speeds, will transfer power to a driven gear which has a larger diameter. This transfer of power increases the torque given by the motor and will allow for our motors M1 and M2 to hold and rotate the loads comfortably. For motors M3 and M4, not much torque is required, since the dimensions and weights of the loads inside the filtering subsystem are small. It is important to realize that a gear reduction in the filtering subsystem will help our group to purchase smaller and lighter motors. Our system can benefit from implementing small motors for the subsystem, since the motors will be adding weight to the overall load both M1 and M2 will be holding. As we talk about torque and gear reduction, it is important to have an understanding of the motor's speed effects over its torque.

Illustrating the effects of the increase of speed to the torque, which are available on the motors datasheet. We could see that as we increase the speed, the motor starts to lose torque. This highlights the importance of keeping a balance over speed and torque when selecting the motor. The table also gives different implementations for the gear reduction system. Adjust the diameter of a gear, or changing the gear ratio affects the load torque needed for the motor to overcome

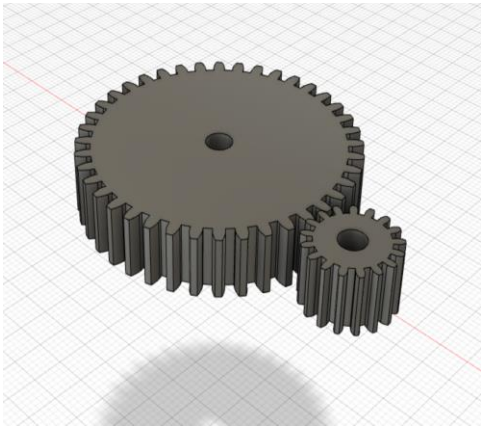

Figure 32a: Gear reduction system using Spur gears

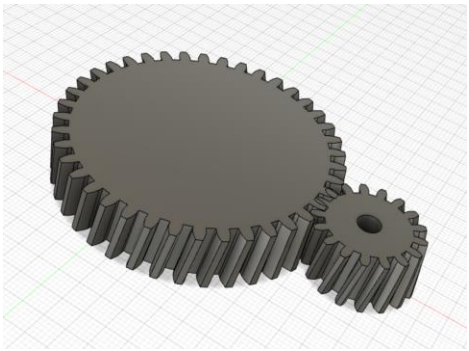

Figure 32b: Gear reduction system using Double helical gears

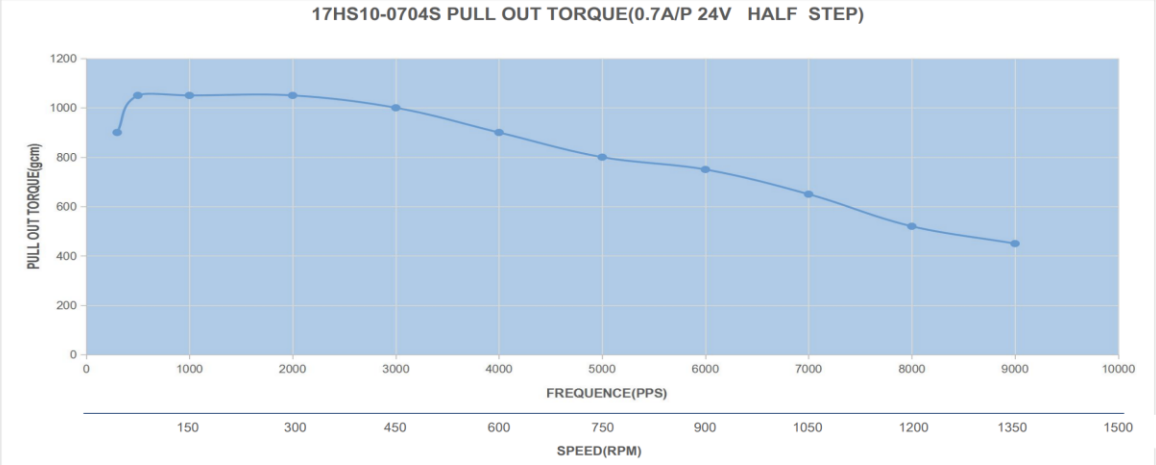

Figure 33: Effect of speed over torque for Nema 17 (18.4 oz. in)

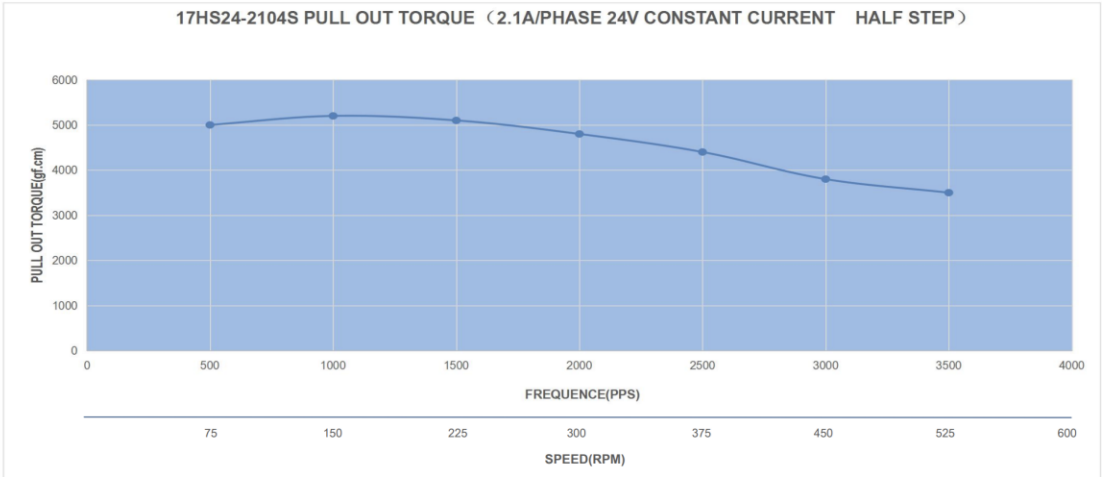

Figure 34: Effect of speed over torque for Nema 17 (92 oz. in)

6.9 Sliding Rail

In order to provide a platform that provides movement to the filters, a sliding rail will be implemented to our system. Both types of filters, motion and motionless will sit on the rail. F1 and F2 will sit stationary at each end of the system. F3 and F4 will be attached to two sliding platforms attached to the sliding rail. Each filter's motor will be sized in order to consume the least power, add the least weight to the system and be as precise as possible. The filters, by having a light weight it is very promising to find two motors which will allow us to find small size motors. As mentioned previously, the sliding rail is an estimate of 31 cm, which will be mostly covered by F4. Having this in mind, the motors have to be

sized correctly in order to give the right amount of power and provide enough torque to move the middle filters smoothly through the sliding rail.
What makes our system unique from another laser profiler besides being controlled electronically, is the fact that a filter system is implemented in order to capture the refracted laser beam from the target accurately. From the engineering investigation that our group conducted, the distance for the extension starting from the lens of the camera will be around 31 cm. Having this in mind, we can find a more accurate estimate for the overall weight of the 'arm', where our filter system will sit. Four lightweight filters will compose the filter system, which will sit on a sliding rail. Two of the filters will be stationary at the end of the 'arm', where the other two filters will have motion. Figure 3.1 below, shows the filter system, showing the two middle filters and the motor that allows motion for each. Next, we will break down the filter system, and go over each component's requirements and characteristics which then gives the group a clear vision towards what type of motors our filter system needs.

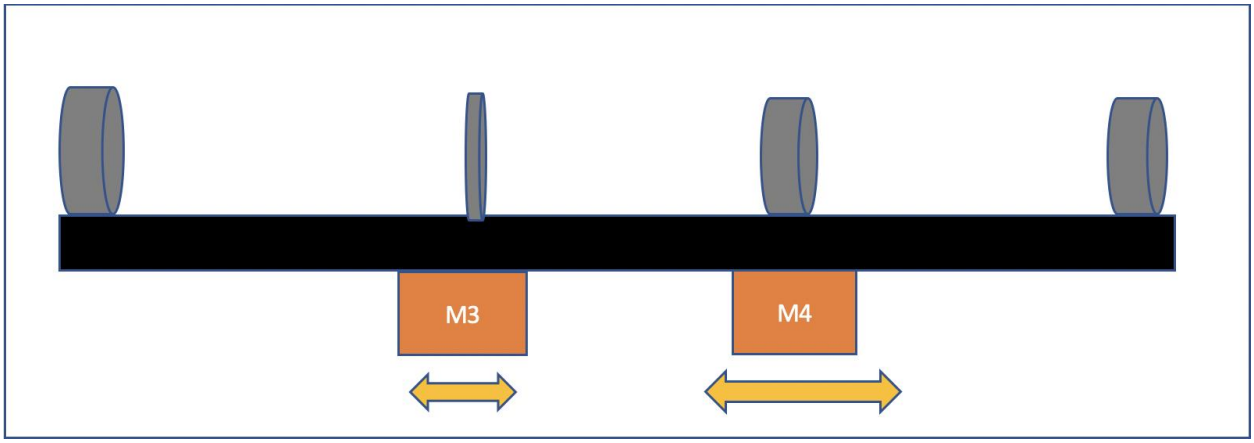

Figure 35: Lens Sliding Rail

As seen in the figure above, the two filters that have motion will be named F3 and F4, where it's an abbreviation for filter three and filter four. The specific purpose was described (above/below). Understanding that F3 does not cover a large distance compared to F4, but the motion needs to be more precise will point the group into looking for a more precise motor than the other three.
For the other middle filter F4, the distance cover is larger than F3. By covering a larger area, accuracy might not have to be as accurate as F3, meaning we can find a smaller and more affordable motor. This will reduce the overall weight of the 'arm', reducing the overall weight of the system.

6.9.1 3D Camera Pan Tilt Mount

A project by Isaac Chasteau who built a camera pan tilt mount that is electronically controlled by a xbox one controller was a great example and guide for our group to look into. Our group was interested in this project since this mount provides two of the motions that our system will be implemented to have. As we can see in figure below, he created two different mounts, one is a panoramic that moves horizontally and the other moves vertically. These motions are created by using two different motors, located on the bottom of the mount under the camera. He also had the gears used for this project 3D printed which allowed him to adjust any measurement he needed. The overall system is built in a very compact structure which caught the attention of the group, since our goal is to make our system as small and lightweight as possible in order to be able to move around the lab easily. As it can be seen in the figure below, Isaac has all electrical connections between the horizontal gear and the camera, making the overall system very organized. This system is built to give motion to a canon camera weighting around 449 grams, which compared to our CMOS camera weighting around 91 grams is significantly heavier. This project is a great example of a system that adds two of the motions that our group is looking to implement into our system. In the next section, we will show an extension of this project where Isaac builds a linear motion for this pan tilt mount, in order to extend the camera's range.

6.9.2 3 – Axis Camera Slider

As a continuation of the previous section, the 3-Axis camera slider is an addition to the 3D pan tilt mount where Isaac created a system which created a linear motion using a third motor. As shown below in figure below, the third motor is implemented between the original mount mentioned above and the rail. Once again, Isaac 3D printed all the necessary parts in yellow, including mounts and gears. A key feature from the project shown below is the sliding rail implementation, created by building a small pulley system. Isaac implements a 2GT timing belt, which is used for converting rotational motion into linear motion. A 2GT pulley with 36 teeth is combined with the timing belt, giving the right amount of tension without losing motion by slippage of the timing belt.

Figure 36: Example of design mount

6.10 Camera Control Setup

The camera control setup will consist of the following systems:

- Lens Control System
- Camera Position Adjustment System

To make things more concise the lens control system and the camera position adjustment system will be reduced to the Camera Adjustment System (CAS). The CAS will operate with 3 motors, 1 adjusting the lens focus and 2 adjusting the direction the camera is pointing along the horizontal and vertical axes. To operate the set up an MCU will be needed locally to process commands from the control device. There will also need to be a means for the input of the camera to be sent out to the control device that will allow for the control device operator to properly determine what adjustment need to be made and to allow for analysis of the laser beam profile. All these things also need to fit in a device that is at most $4ft^3$ and handle operation in a weatherproofed container and handle the intense Florida heat.

6.11 Control Module Selection

Many cheap and available RF control modules can be used for wireless communications between multiple microcontrollers for extended ranges, with different configurations having maximum ranges varying from 100 meters to 1100 meters.

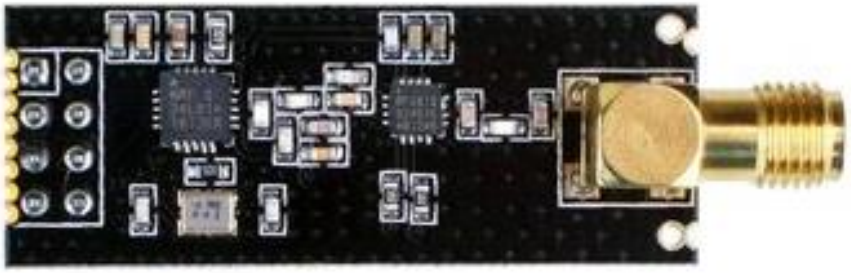

Figure 37: nRF24L01+ RF receiver module

The module used will likely be the nRF24L01+, a RF receiver module developed by Nordic Semiconductor. The module is a popular choice for longer range wireless communications between microcontrollers for its extensive range and cost as low as less than $4 for the module with an included antenna for longer range communications. The device works as a SPI slave device for the MCU.

Frequency Range	2.4 GHz ISM band
Air Data Rates	250kbps, 1Mbps, 2Mbps
Maximum Output Power	0dBm
Supply Range	1.9 - 3.6V
Standby Mode Current (Minimum Operating Current)	26µA
Maximum Operating Current	13.5mA
Input tolerance	5V
Operating Temperature	-40°C - 85°C
Communication Range	>800m
Serial Interface	SPI
Modulation	GFSK

Table 14: Specifications of Nordic Semiconductor ASA nRF24L01+ (Last Minute Engineers, 2020), (Nordic Semiconductor ASA, 2008)

6.12 Single Board Computer

The device that will serve as the controller for the camera adjustment system and will also receive the video feed from the camera to allow for the operator to view the adjustments being made and the laser profile over time. This

portion of the project has a lot of potential customization and for further development later, such as means to auto-track the beam in real-time and automatically identify certain characteristics of the beam. The main considerations for this project for now though are simply to 1) receive the imaging data of the laser beam profile from 3 meters away to track the beam position and determine its characteristics, and 2) to send signals to the Camera Adjustment System to make the necessary adjustments to best attain the necessary imaging data. For this device the following options are considered: Option 1) use separate controller and display devices used in conjunction to perform the necessary operations, Option 2) utilize some already existing device such as tablet and develop software to operate the CAS, or Option 3) utilize a single board computer (SBC) to develop a customized device with the necessary communications, control peripherals, and software.

Option 1 is the absolute bare minimum for the goals specified for this project and is likely one of the cheaper possible solutions but doesn't necessarily impress anyone and can be seen as a weak work around for achieving the basic requirements and doesn't provide much in the way of future development for this project should the need arise.

Option 2 is a possibly less time-consuming and cheaper option as the hardware of the device is already selected. There is also the possibility of already existing applications for the device that can be used for some of the more advanced features that would need to be developed for the device in later stretch goals. The downsides however are that the development may be limited depending on the operating system of the device, as software developed for a device running on Android is incompatible with a device running iOS. There are also different hurdles for application development depending on which operating system is developed for, such as which programs can be used for development and testing, curation (especially if developing for iOS and needing to release the app publicly), and limitations on what hardware can be used for development in the first place (iOS development can only be done using hardware using MacOS). There is also no guarantee that the hardware will have all the necessary capabilities for the project without having to invest in a more extensive MCU for the CAS, leading to other issues on that end. Regarding the project developing a long-term solution, this option may lead to issues with the application over time, as updates to the OS software of the device and changes to newer devices may at some point lead to compatibility issues with the older application software. This would require the software to be continuously updated, lest development become dormant, and the project become defunct well before its time due to planned obsolescence.

Moving onto Option 3, although this requires more development on the hardware end, covering the base requirements the software development may not be as extensive as Option 2. This option also allows for more customization for the device to cover all the necessary specifications and depending on what hardware is used can allow for more extensive development in the future depending on if the client wants it. If components are chosen carefully the device may come out to be relatively cheap to put together and depending on the

compatibility of the components, they may be relatively simple to implement in software. As this device would not be varied like in Option 2, the issues of having to constantly update the software to ensure compatibility of the device would be as much of an issue. Ultimately, Option 3 appears to be the best option weighing all factors.

For the implementation of the control device, there are various options for the SBC depending on a variety of factors including:

- having the capability to run both the video processing from the receiver and the control
- having a means to iterate further for automated analysis of the beam profile
- being able to do all of that still run well

6.12.1 Single Board Computer Options

For the SBC there exist various options at equally varied price ranges. The ones considered below are selected due to aspects such as price to performance, size, and power considerations.These boards also have their own additional draws that will make their use in the project easier to implement.

6.12.1.1 NVIDIA Jetson Nano

Figure 38: NVIDIA Jetson Nano (NVIDIA Corporation, 2021)

The Jetson Nano Development Kit from NVIDIA Corporation is an SBC that is designed for use in Artificial Intelligence applications, having “the performance and capabilities needed to run modern AI workloads” according to the User Guide (ssheshadri, 2019). This board utilizes a GPU that compared to other SBCs in this price range ($60-$118.75 depending on model) is much more

powerful, making the calculations necessary in AI based operations and machine learning quicker.

The specs for the board are displayed in the table below:

Architecture	Quad-core 64-bit ARM
Clock	1.43 GHz
GPU	128-core NVIDIA Maxwell GPU
Memory	4 GB
Display	HDMI/DisplayPort
GPIO Pins	28
UART	2
I2C	6
SPI	2
I/O	4x USB3.0, USB 2.0 Micro-B
Power Requirement	5V, 2A
Temperature Tolerance	-25-80°C

Table 15: Board Specs

6.12.1.2 Raspberry Pi 4 Model B

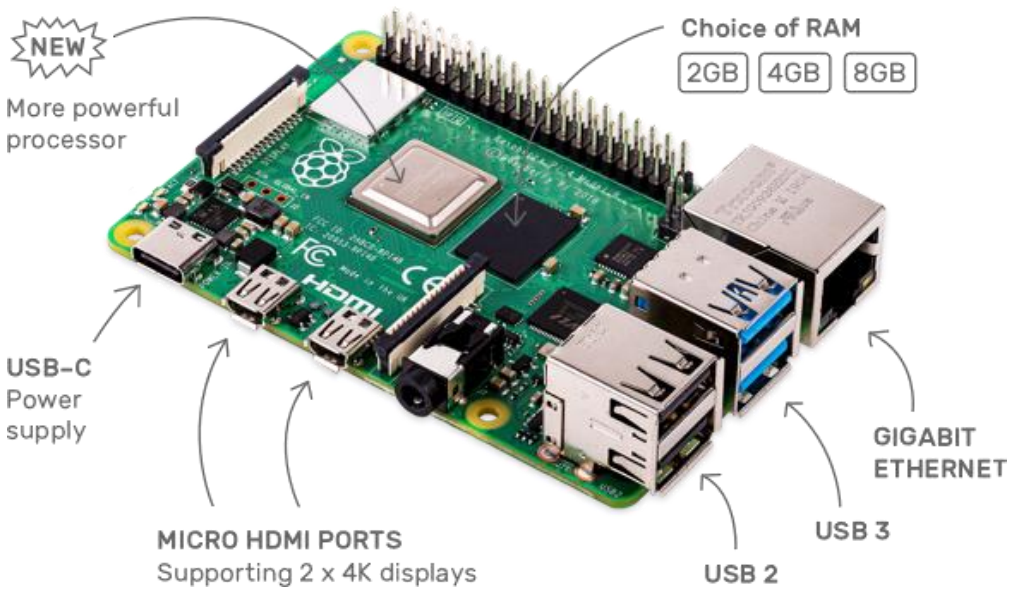

Figure 39: Promotional diagram of the Raspberry Pi 4 (Raspberry Pi Trading Ltd., 2021)

The Raspberry Pi 4 Model B (from this point just referred to as the Raspberry Pi 4) is the newest and most powerful of the popular lineup of SBCs developed by Raspberry Pi Trading Ltd. Like the board's predecessors this board has plenty of power to run the expected applications while remaining relatively inexpensive with the low end model being $35 and the highest end at $75. The specifications of the device are as follows:

Architecture	Quad-core 64-bit ARM
Clock	1.5GHz
GPU	VideoCore VI 3D Graphics
Memory Options	2, 4, 8 GB
Display	2 micro-HDMI
GPIO Pins	28
UART	6
I2C	6
SPI	5
I/O	2xUSB2, 2xUSB3
Power Requirement	5V, 3A
Temperature Tolerance	0-50°C (do not exceed 85°C)

Table 16: Raspberry Pi 4 Model B specifications (Raspberry Pi Trading Ltd., 2019)

As the specifications show this SBC should have adequate processing power to run the required applications, although while also requiring a considerable amount of power. As the control device is not the device in this project being left out outside in the elements the middling temperature tolerance is not a deal breaker and is expected given the possible applications of the SBC being a miniature desktop computer. Along with the prior computers in this series this computer has extensive community support, especially when it comes to customization for the interface.

6.12.1.3 Single Board Computer Comparison

In comparing hardware, the boards are evenly matched, each having the same 40 pin-out set up (allowing interoperability with components designed for the Raspberry Pi to work with the Jetson Nano), similar specs regarding I/O and in power requirements. The Raspberry Pi has the better CPU, being able to run at a higher clock speed than the Jetson Nano, as well as having the option for an 8GB memory model whereas the Jetson maxes at a 4 GB model. The Jetson Nano is also much larger in comparison, with the board dimensions for each being 3.9 x 3.1 x 1.1 inches for the Nano and 3.74 x 2.76 x 1.1 inches for the Raspberry Pi. This all comes with the top spec versions of each board coming out to $75 for the Raspberry Pi 4B 8GB and $99 for the 4 GB Jetsun Nano. What

the Jetson Nano does have going for it is its much more powerful GPU as highlighted in Stephen Cass's article for IEEE Spectrum (2021) that makes the board much better suited for AI and ML applications. That proficiency in AI and ML makes the board a very compelling option for this project.

6.12.1.4 Single Board Computer Selection

The selection for the SBC is ultimately the Raspberry Pi 4B 8 GB. This selection is made as a result of issues regarding availability for both boards, especially at MSRP. Neither is available for purchase at the moment of writing, with the Raspberry Pi not being available until mid-February according to all vendors and the Jetson Nano not having a set date for restock.. As a result, the choice is whatever board is available on hand or can be attained easily second-hand. Therefore, the Raspberry Pi 4B 8GB that one of the members of the team had on hand is the resulting choice.

6.13 Controller

Regardless of what SBC is utilized in the final design, the given specifications set for the device it already has the following requirements set:

- Display the video input of the camera
- Adjust the camera position and focus to best capture the laser beam profile.

Given these requirements, what is ultimately done regarding the interface ultimately comes down to a balancing act between what is easy to implement for the controller, what is easy for the end user to utilize, and what knowledge is required for development. As such, to best meet the base specifications the physical interface for the device should be to be as simple as possible, utilizing minimal physical inputs from the user to allow for quick understanding of the controls of the adjustment system. This could entail button and/or joystick inputs that can be implemented in such a way that would make the functions of the camera adjustments feel more natural.

6.14 Software

For software there are two aspects that need to be coded for: 1) the operation of the motors for the adjustment of the camera, and 2) the tracking of

the beam profile. For the motor operation a microcontroller will be used to operate the motors themselves and a separate SBC will be utilized to transmit directions for the microcontroller. For the beam profile tracking the same SBC from before will also be utilized to perform analysis on the beam profile based on video transmitted back to it from the camera

6.14.1 Development Tools

For the development of software there are necessary tools to aid in the process of development in order to make development simpler and to not lose progress. As such, integrated development environments will be utilized for writing and testing code, and a version control system will be utilized to hold records for the design process.

6.14.1.1 IDE and Text Editor

Programming for the Arduino board used for the microcontroller operating the motors will be handled in the Arduino IDE. The Arduino IDE is an open-source IDE that is the official software developed by Arduino.cc for code composition for the Arduino devices, which have native support with the software. The IDE is notable for its ease of use for those who have no prior knowledge in development. This user friendliness makes is aided by the extensive free libraries available for Arduino devices. This IDE also contains the necessary tools to program for other microcontrollers. This makes this a prime option for development as the software developed initially for Arduino boards can later be used in custom boards utilizing the same controller.

Software development using the Arduino IDE as described before is simple for development. It allows for development using files referred to as *sketches* that can be written in a C/C++ derived Arduino language. Given the team member in charge of the programming of the microcontroller used in this project has plenty of experience in C programming this is quite convenient. The newcomer friendliness in this IDE is shown in the sample code that exists for various supported Arduino boards, making this welcoming for those who have never coded for Arduino, much less coded ever. As Arduino is not something that the team member in charge of coding is completely familiar with, this is especially helpful. Between the built-in sample code and the code available for reference from various projects performing similar applications from the extensive community around Arduino the software development for the microcontroller will be a much less daunting task.

For programming the SBC used to send the RF signals for controlling the motors, receive the signal for video from the camera, and perform the tracking of

the laser beam profile an adequate text editor for writing and evaluating the Python code will be needed. As such Visual Studio Code, or VSCode for short, will be used. VSCode is a text editor developed by Microsoft that has features such as debugging, syntax highlighting, code completion, and source control support through Git. VSCode is designed to make coding more streamlined and configurable for the use of the developer through extensive customization and numerous available extensions.

6.14.1.2 Version Control System

As with any major software development project, having a version control system is a must. A version control system (VCS) is an application such as Git that tracks the changes in source files in development in order to better allow for data integrity and coordination in collaboration between software developers, as well as make the process quicker, according to the creator of Git Linus Torvalds (2005). A VCS achieves this by having the code hosted in a repository that is stored in a cloud-based system. To develop to the source code the developer must clone, or “pull”, the repository to their local machine to have the most up to date version of the available code (which also acts as a means of backing up the repository) to develop on. When the developer is done making their changes to the code they will upload, or “push”, their changes to the code to the repository which will allow the latest version of the code to be used from the repository as well as logging what changes are made in. Tracking what changes are made to a file allows users to review the changes and to revert to a prior version of the code if needed for the project, as well as possibly allowing collaborators to scrutinize the work of a given developer and hold their team members accountable.

Git will be utilized as the VCS for this project with GitHub being utilized as the platform to host the repository of the software developed. GitHub is an internet hosting platform used for version control through Git, which is an open-source VCS. GitHub is used extensively in the field of software development as it allows for web-based VCS between many collaborators and is ubiquitous amongst developers of open-source projects. GitHub also allows for private repositories for developers working on projects that cannot be made public to other users for any reason, as well as certain security features depending on if the users working on the repository are using a paid membership (some security features are also available to users that have the “GitHub Student Developer Pack” that allows students to have access to professional tools at no cost).

6.14.2 Camera Adjustment System

The camera adjustment system will take commands from the controller and execute the movements for the motors to adjust the view of the camera for

purposes of tracking the laser beam profile. The microcontroller operating this system will be programmed to perform the following:

- Initialize the setup of the camera adjustment system
- Receive transmissions from the transceiver
- Execute the commands broadcast to the device
- Wait for further transmission

6.14.3 Control Device

The control device containing the SBC and the necessary transmission modules as well as the controller interface. The software functions can be split based on their purpose: operating as an RF controller and operating as an Object Tracking System.

6.14.3.1 RF Controller

For the RF controller aspect of the SBC, the will communicate with the camera adjustment system via RF communications to dictate the commands input by the user. As such, the SBU for this function shall be programmed to perform the following:

- Initialize the setup of the controller and the RF communication system
- Establish a connection to the camera adjustment system
- Accept inputs from the user
- Transmit signals to the camera adjustment system
- Wait for further inputs from the user

6.14.3.2 Object Tracking System

For the tracking system the SBC will utilize the OpenCV library for Python, “an open source computer vision and machine learning software library… built to provide a common infrastructure for computer vision applications” (OpenCV Team, 2020). The OpenCV library is able to be used for object detection by reading the image to detect features it is trained to identify through the utilization of HAAR features, “rectangular features with regions of bright and dark pixels” (Kumar, 2020). Paraphrasing from Kumar’s article, the algorithm utilizes the calculated pixel difference between darker regions of an image from the lighter regions to identify certain features it is trained to associate with a certain object. The individual features it singles out are referred to a “weak figures,” and with a

determined sum of these figures within a certain region in a particular configuration the algorithm can identify some given object. Given this, we can train the SBC to identify the beam profile from the video feed coming in from the camera and track the movement of the beam over time.

6.15 Prototyping

To sort out what remaining design considerations exist there will be a process of prototyping. The prototypes will aid in determining what is necessary in the end design that will be used in the demonstration at the end of Senior Design 2. It will also help in determining if there are any major design considerations that need to be redone if some portion of the current ones prove to be ineffective or unreliable.

6.15.1 Controller Interface Design

For the design of the main controller for the camera adjustment system there will be a process of prototyping to determine what works best for functionality and in simple design. The controller interface will need to perform the adjustments for the camera by communicating to the MCU used to operate the motors adjusting the camera's view in the horizontal and vertical axes as well as adjusting the lens positioning to change the magnification. The interface is also going to need a means to see what the camera is viewing in order to have the camera positioned correctly and allow for a means to see how the SBC is tracking.

There are two items that regardless of how other parts of the controller implemented will need to be included as a result of the nature of the project:

- Radio Frequency Control module (Nordic Semiconductor nRF24L01+ RF)
- Long distance video transmission module

These components have to be used to allow for the "Remotely Controlled" aspect of the project to work, and therefore aren't negotiable in whether or not they are implemented unlike the other components. This still leaves much to be explored in how we can implement an effective controller interface that works satisfactorily for our project.

For the user input portion of the controller, there are a few options to be considered. One of these options is the use of physical analog controls (such as Joystick controls). This can be used to control the motors responsible for the horizontal and vertical angle adjustments in a way that is simple to learn and easy to operate. Using an analog control mechanism will also allow for some variance in how the adjustments are made, possibly making it easier to get the camera's frame just right to capture the reflection surface and make the set up

quicker and easier. An additional plus for this is that it is not expected to be all that difficult to implement, as there are likely to be methods and files that already exist to be referenced that would allow for this to be an easy means to control the motors. The only part that would be time intensive is narrowing in on the calibration of how the joystick input translates into motor adjustment. The joystick may also be used for the zoom lens adjustment as well if the implementation can be shown to be useful. A downside for the joystick in how this project is meant to be implemented is how to keep the joystick mechanism free of debris that can inhibit the function of the joystick, as this device is expected to be used outside where such things can be unavoidable. Solutions my already exist that can be implemented, or we may have to come up with ways to handle this scenario. Another is that accidental movement of the joystick when the tracking of the beam profile is already occurring can throw off the data as the whole fame of view of the camera is thrown off if there is not a way to disable joystick inputs after the adjustments are dialed in implemented.

Another option for physical inputs is the use of physical buttons for the interface. Regarding implementation this is probably the easiest as it can operate on Boolean logic to determine what action is to occur. This may be the more versatile physical input for what it can be used for, as they can be implemented for various purposes and individual buttons can work in multiple operations. A duo of buttons can be used for the camera lens zoom, which works quite well as there are only two options for that mode of camera adjustment: zoom in and zoom out. A set of four of them can be utilized as a directional pad that can be an alternative to the joystick discussed prior, although you do lose the benefit of more adjustability in movement that the joystick allows for. Buttons can also be used for other potential functions that can be easily programmed for that something like a joystick would likely be locked out of, such as confirmation or denial of certain functions.

For the ability to control the camera remotely it’s quite important to know what is currently in the view of the camera. For this reason, a screen is a necessity for implementation. Aside from being just being the interface to help make the necessary adjustments for the camera system, the screen can also be used as another means of implementing controls if the screen used is a touch screen. While it lacks the physical, tactile feeling of adjustment for the system and depending on implementation may also lack the degree of adjustability that the joystick allows for, it does allow for a simpler but more full-fledged interface that can replace the need for any additional physical interface. For the other physical interface options discussed prior, a combination of the two would likely be required for either of the parts to be able to be useful in implementation. If implemented properly the touch screen can work standalone as an interface for the user. Speaking of implementation, it may be a bit more intensive than the other options discussed. It would also be a much more expensive implementation than the other options as well. Another potential issue will be discussed later in this document.

Another possibility to explore regarding interface is the utilization of USB peripherals such as a mouse and keyboard. As the interface is expected to be

connected to a computer implementing USB peripheral devices shouldn't be too difficult aside from establishing the input assignments for the applications used for the project. This is mainly for the use of the SBC, as there is not much additional utility in implementing these peripherals just for the camera adjustments. Rather this would be for easier access to the functions of the SBC and to allow for more extensive control over the tracking application.

There is another important consideration to make regarding the design of the controller interface that will likely lead to some other adjustments in how the project would go forward. If the video signal does not appear to be adequate for accurate tracking and analysis, a way this can be solved is by placing the SBC on the camera adjustment end of the project and just use the screen in collaboration with the microcontroller to do the adjustments needed and then authorize the tracking to begin. This would allow for the SBC to get the full resolution of the camera to make the necessary tracking calculations which could make the identification and tracking of the laser beam profile much more accurate. It could also possibly simplify the needs of the remote-control device for the camera adjustment system as it would just need an additional microcontroller to conduct the motor adjustments that are previously assigned to the SBC. The additional microcontroller would be hooked up to the communications module that was set for the SBC to be used. For the video transmission there would be some further considerations to be made. It could be possible to connect the video transmitter to the SBC which would allow for the user to still see what the SBC is able to track in real time, although if this implementation is shown to still cause issues it is possible that we can find a means to tap into the camera feed separately and rely on the machine learning algorithm used by the SBC to be accurate enough to be trusted to act alone. This would also mean we'd need to have the SBC connected to some storage device where the tracking files can be stored so the research team can collect the data after the fact.

6.16 Cooling Fans

As in all electrical systems, heat is one of the most important characteristics to note. Being able to measure and control is very important for our system, in order to avoid any malfunction or damage to the components. Having that in mind, our system will utilize four motors, sensors among other electrical components. These components when running at the same time, will produce heat, which our system needs to react and respond. Engineering investigation was done into cooling fans. These fans will allow for our system to cool down our components and avoid reaching a temperature limit.

7. Design Diagrams

This section contains visual diagrams for the proposed designs of the project in its various areas spanning from photonics to software.

7.1 Optical System

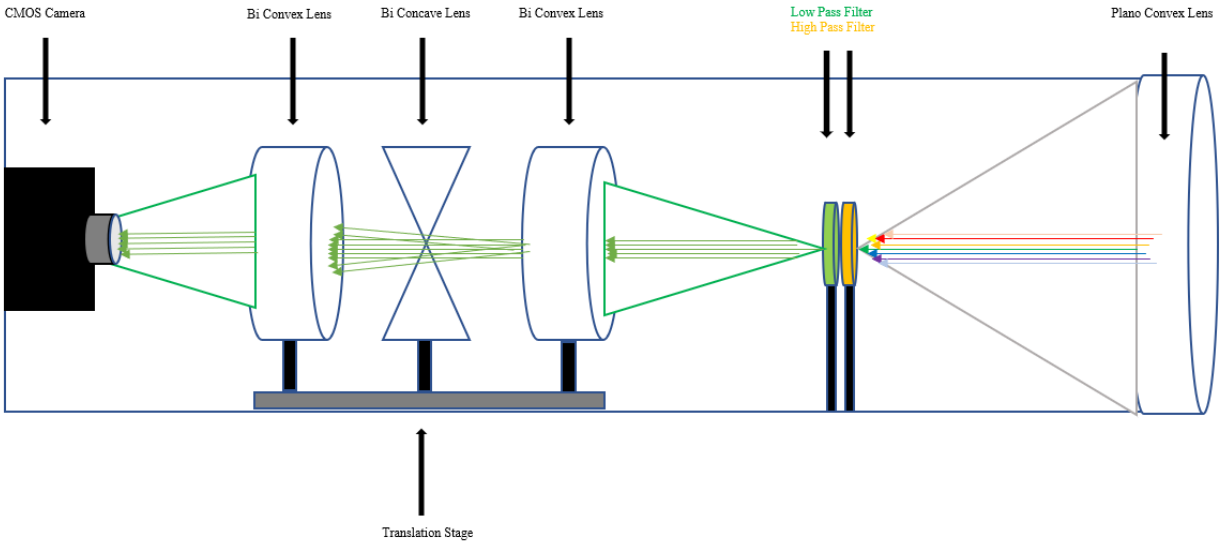

Figure 40: First design of optical cavity for device

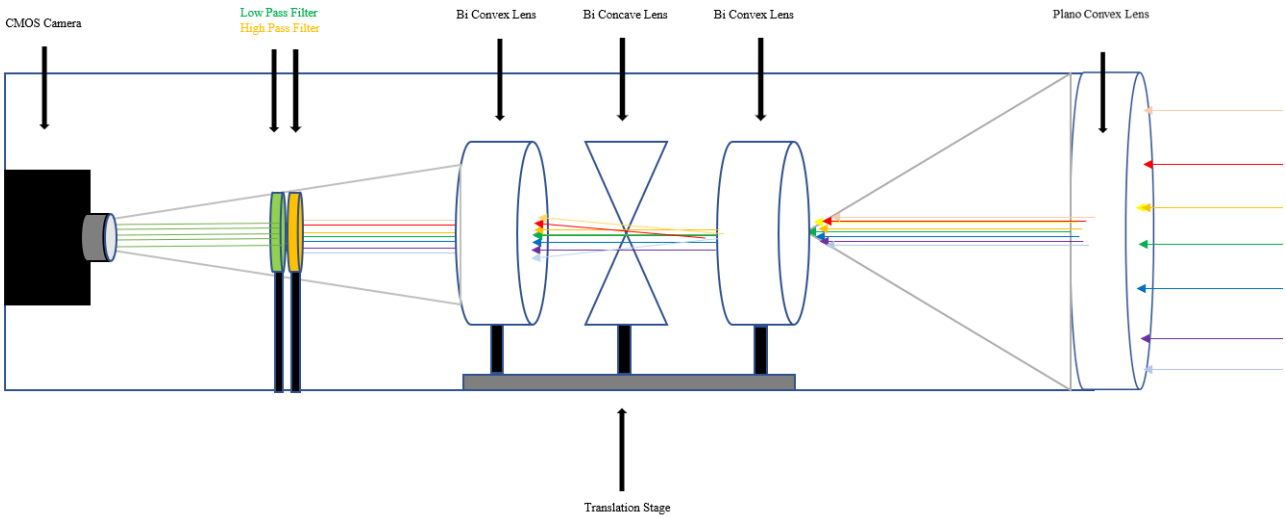

Figure 41: Second design of optical cavity for device (current project design)

7.2 Camera Adjustment System

Figure 42: RC receiver flowchart

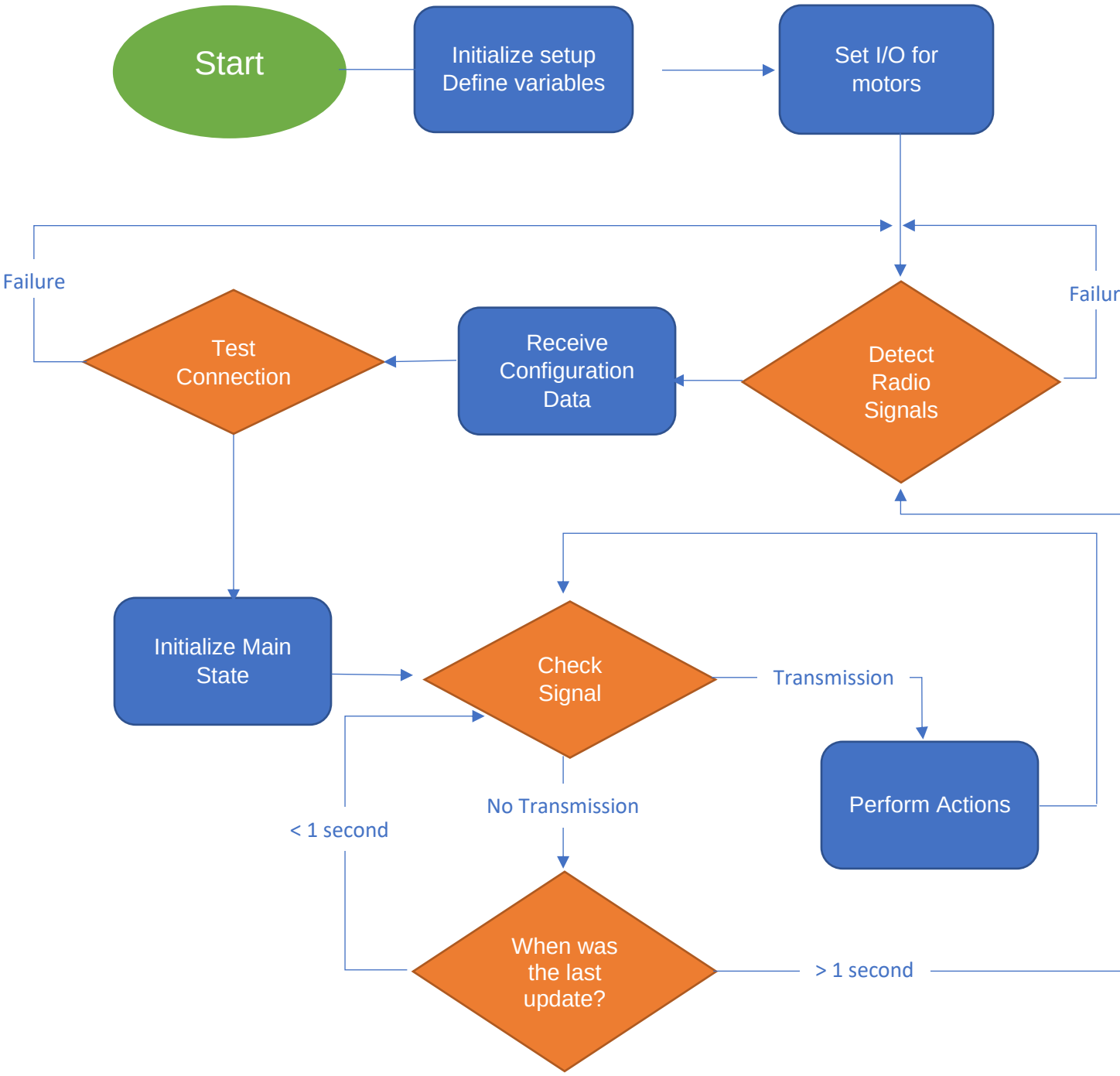

7.3 RC Controller

Figure 43: Flowchart for directing controls

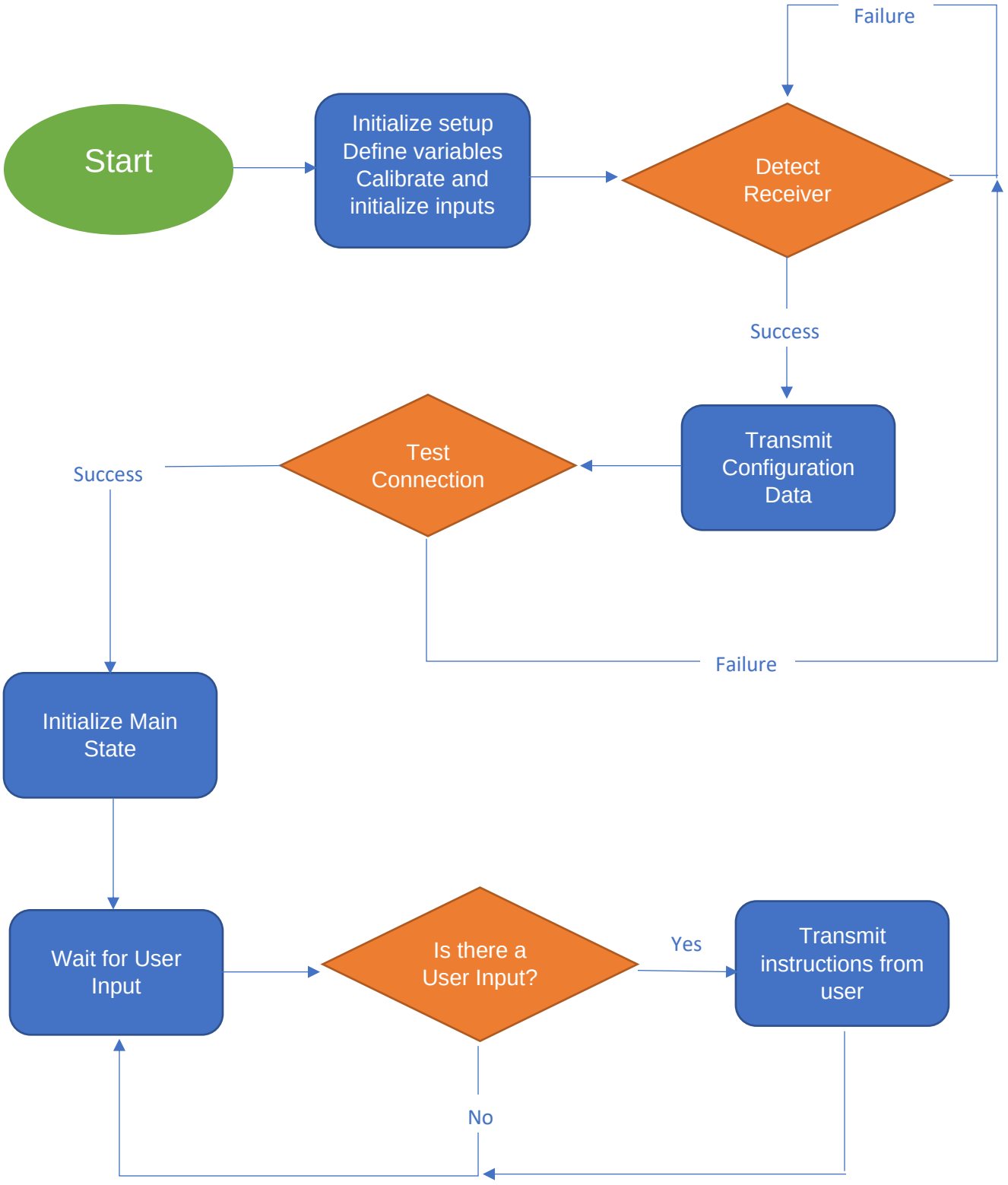

7.4 Object Tracking

Figure 44: Tracking flowchart

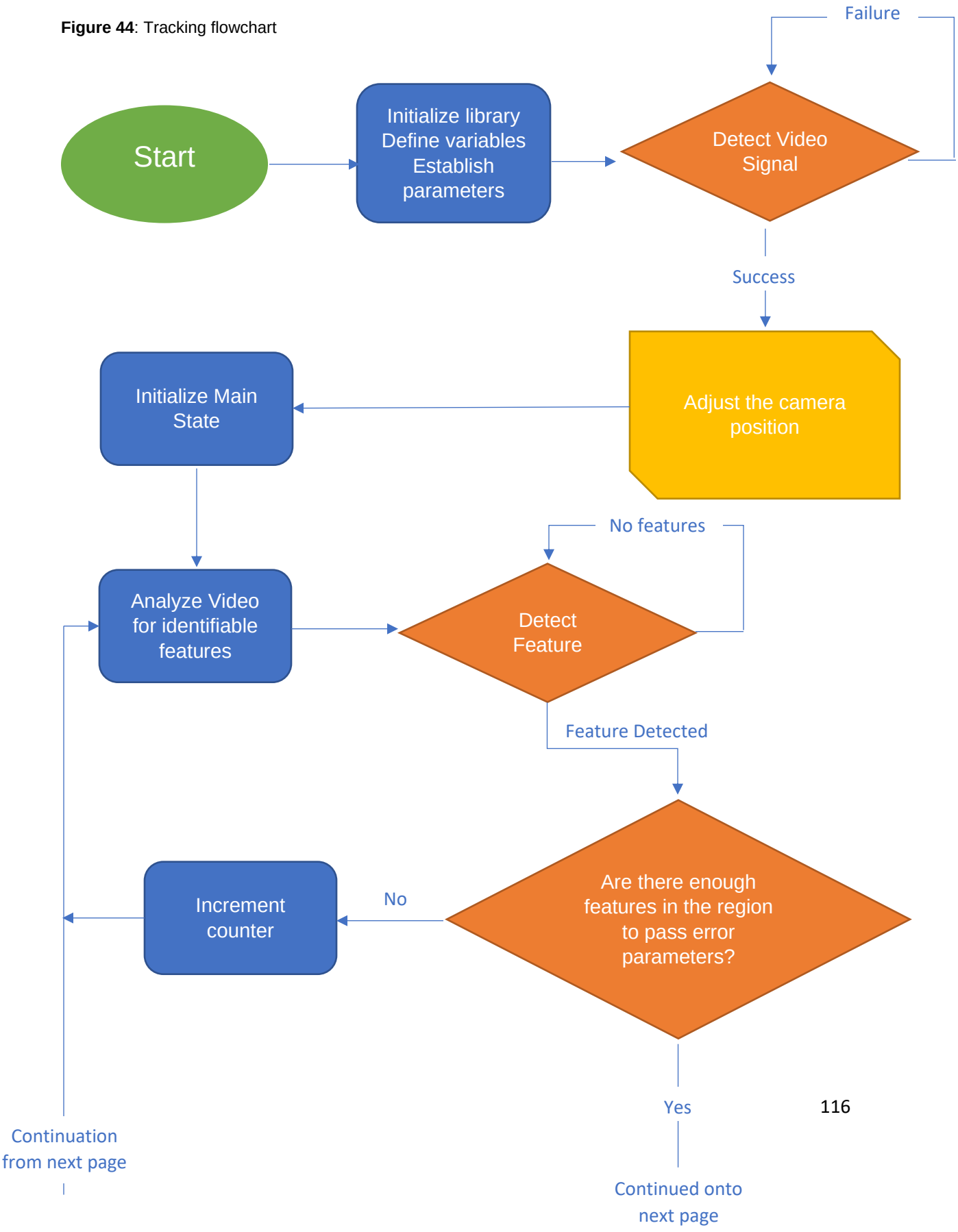

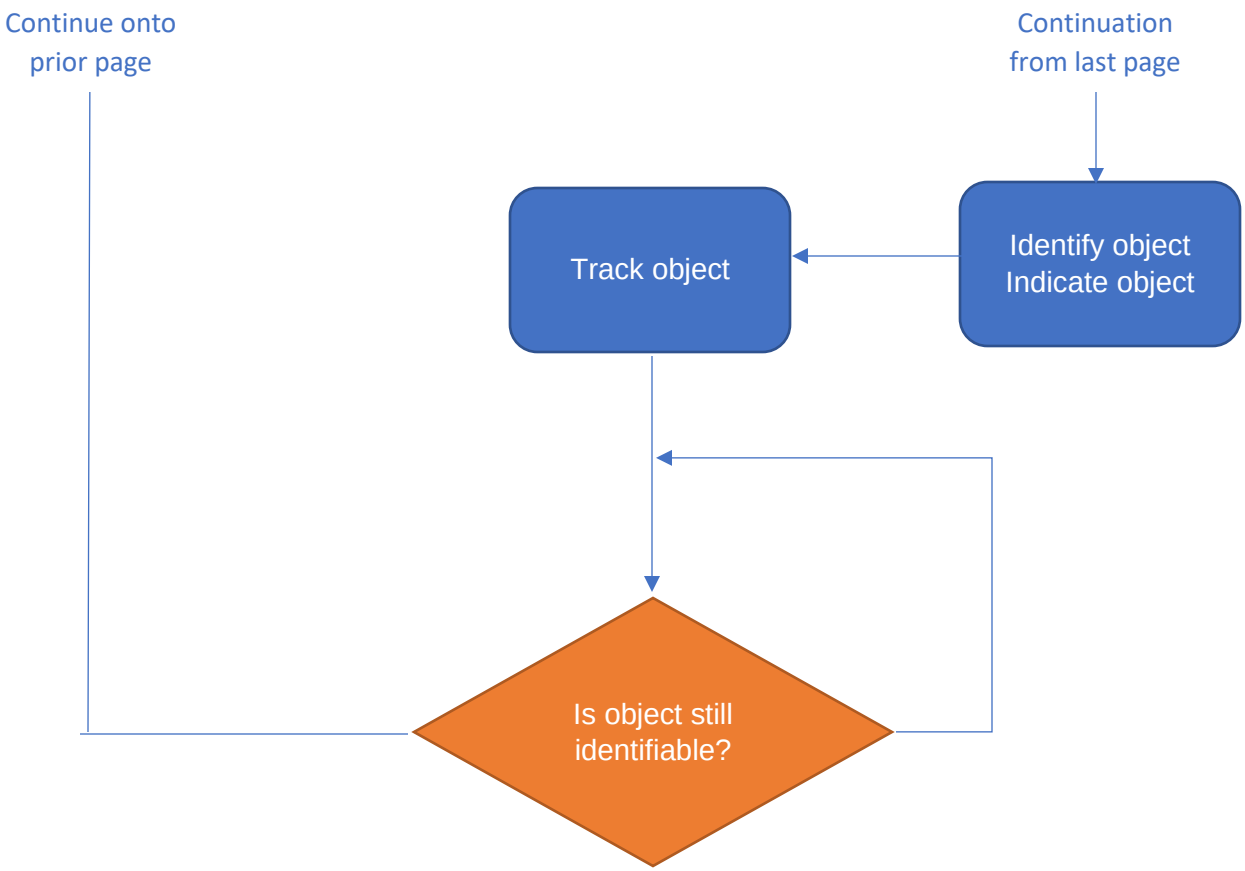
Continue onto
prior page
Continuation
from last page
Track object
Identify object
Indicate object
Is object still
identifiable?

7.5 Power Diagram

Figure 45: Battery and power consumption flowchart

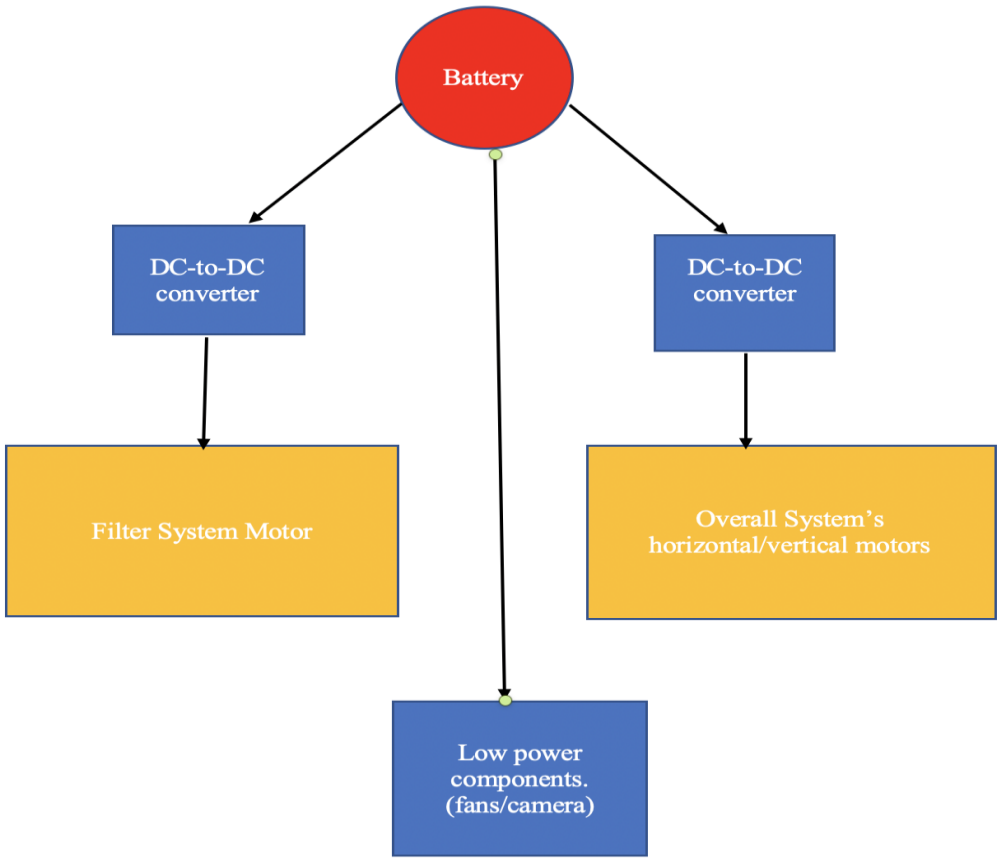

8. Testing

To ensure the end result of the project is that of a demoable product tests will need to be done in various areas to guarantee that the design and the materials used are all sound.

8.1 Hardware

Testing of hardware will be a necessary part of guaranteeing the functionality of the components of the project and of the project. Testing will carry out as described in the following section.

8.1.1 Microcontrollers

For the testing of the microcontroller hardware there are a few areas that need to be tested in order to verify the integrity of the microcontroller and its functionality: the functionality of the I/O pins, the power draw of the controller, and its ability to physically operate with other devices.
For the microcontroller the functionality of the pins is obviously quite necessary for the ability to be implemented into the project. There are many reasons why the pins may not be operable, either there is an issue with the connection due to how either the microcontroller or the pins are soldered that may just need to be resoldered, or it could be a manufacturing defect on the chip of the microcontroller that may require the microcontroller to be replaced, which can be a major setback if not handled early. Using a simple circuit, a multimeter, and some code that can be uploaded to the microcontroller the pins can be tested for functionality. Pin testing will be necessary not only for the initial test board but also the final PCB implementation.
The microcontroller also needs to be tested for power consumption, especially based on clock speeds to verify the manufacturer's specifications and to also guarantee the functionality of the board. For this just a power supply and a multimeter are necessary for measurements themselves, with a computer needed to upload the necessary code to test at the clock speeds to be tested at. The board will be tested for the power consumption at the available clock speeds it can run at, and the results will be compared to those in the user's guide for the microcontroller to verify how the board functions and to gather our own understanding of what considerations need to be made regarding power for the system.
The microcontroller also needs to be tested with the Radio Control Transmitter module to verify the setup of the module, the interoperability between module

and microcontroller, and the ability of the communication module used for the microcontroller to communicate with the other module. The means by which this will be achieved are covered in the section on the testing of the Radio Control Transmitter.

8.1.2 SBC

For the SBC, the tests done will be similar to that of the tests used for the microcontroller, with the areas tested being the functionality of the I/O pins, the power draw of the SBC, and its ability to physically operate with other devices. For the testing of the functionality of the pins of the SBC, the tests will be the same as for the microcontroller: setting up a simple circuit, using a multimeter and some code written for testing each of the pins can be tested in the case there is some issue that needs to be checked with the SBC where the pins are deemed suspect. Power testing is not an incredibly pressing need as it is expected that the draw of the SBC will be quite significant regardless, so sticking with manufacturer's specifications will be fine unless there is some fault discovered that needs troubleshooting. For the operability with other devices this portion of testing will be covered in the sections on transmitter testing.

8.1.3 Transmitter: Radio Control

Testing the connections between the module and the microcontroller are and will only be done in the case there are issues in any of the other tests between the two. To test the set up the two communication modules will both need to be connected, as the operation of both is necessary to verify their operation. For the tests the devices connected to the modules will have code uploaded to them that will set the parameters for the operation of the modules, establishing what channels are used and how many bits are read for each transmission between the two. If the setup is successful, it can be determined that the modules are properly setup for use with the devices they're connected to. Once the devices are setup the modules will need to have messages communicated between the two to test whether the two modules are able to properly communicate with each other. Once it can be confirmed that they can indeed communicate with each other, the tests will need to be run to determine if said communications are able to be used by the devices themselves. To test this a simple LED circuit will be connected to each of the devices and both devices will send a message to the other that should tell the other device to activate their LED. If both LEDs are activated, the test successfully shows that both devices are properly set up for use with their transmission modules.

8.1.4 Transmitter: Video

For the video transmitters the devices will be tested to determine the ease of use in configuring the correct channels to use for the transmitter and transceiver, latency in the video at the demonstration range, and the image quality of the video at the demonstration range. Given this project is to design something that will be operating in a large empty field these tests may have benefits from also being done at some more significant range if there is time permitting in our schedule. This would allow us to better understand what additional considerations are needed for this scale, whether it be beefier antennas for longer range or investments in better transmitters in a final product to better achieve the range that we are expecting this project can be expanded to work at.

For the testing of the video transmitter, we will need to take the camera (if not available for testing a USB webcam or other such camera with the same I/O may be used as a temporary substitute), the SBC, a display interface of the same resolution as the camera, any adaptors needed for the proper connections, and the transmitter and receiver modules. The first configuration tested will have the camera directly connected to the SBC which will also be connected to the display interface and will be used as a control to contrast to the second configuration where configuration for testing will be connecting the camera to the video transmitter and the receiver module to the SBC, which will also be connected to the display. The process to setup the channels to be used between the transceiver and the receiver will be evaluated for ease and speed. The process is unlikely to change between the two configurations to be evaluated for so instead it will be tested in both configurations mostly to determine average speeds in setting up the channel connections between the transceiver and receiver. Once the setup is completed each configuration will be tested for latency between the camera input and the display output and evaluating the resolution of the output shown on the display. Latency can be tested by determining how long it takes for the covering of the camera lens to register on the display output. The resolution test is going to be initially a qualitative test to determine if the second configuration seems feasible for analysis of the camera input or if there will need to be a means to have the SBC directly connected to the camera to collect the camera data and a separate means for the camera to be adjusted prior to tracking. If more analysis on the resolution test is needed then a simple tracking program will be utilized in both configurations to determine how the identification and tracking of an object varies between the two configurations to better determine if this solution is effective.

8.2 Software Testing

Software testing is a necessary part of the project as it verifies the operability of the software components and makes sure that there's nothing amiss come demonstration. With software testing the testing occurs throughout the design and prototyping process to make sure that each function written is functional both before and after it is uploaded to the hardware and that the code written and uploaded is compatible with the code written and uploaded for the other parts of the project.

8.2.1 Unit Testing

The initial software testing stage will be testing the applications developed in a simulated environment to find all the logic errors and bugs in code that exist internally by testing through all of the individual parts of code that are to handle specific functions. This stage takes advantage of the various debugging features available in the main development environments used to best sort out any baseline issues that arise in development that may be detrimental to the project if not caught early. This initial stage does have its difficulties in trying to evaluate communications between devices, which requires some stand-in inputs for the purposes of testing to verify how the devices will act independently based on what the expected outputs of the other device are.

8.2.2 Integration Testing

In the integration testing stage testing will be to determine how the code written and simulated in the initial unit testing stage fares when actually uploaded and used in the actual hardware that will be used in the demonstration. It is in this stage where the utilization of devices like oscilloscopes and multimeters are necessary verify the integrity of the connections between devices if issues regarding connection arise and utilizing LEDs for troubleshooting to verify that communication between devices is occurring even if the action that is being requested from the device is not occurring. Much of the debugging that in the simulation phase in software testing is simply done through the testing environment has to be deliberately implemented in this phase of testing. This stage is meant to determine how all the parts of code developed up this point are able to merge together and become whole, integrated applications for each of the devices developed for. Once the integration testing is completed and all of the software is able to work together, system testing will take place to determine how the whole of the project is able to work together.

8.2.3 SBC

The SBC will have two software components that need to be tested throughout the development process, including but not limited to:

- Object tracking through OpenCV
- Wireless communications to other devices

Not only do each of these components need to be tested individually, but they also need to be tested for where they interact with the other components in the project.

8.2.4 Open Tracking

To ensure that the computer can accurately identify and track the laser beam's profile, the algorithm used by the computer must undergo training and testing to guarantee the identification of the beam and tracking is accurate. The computer will undergo training through exposure to the object it is meant to identify, initially just as static photo images of what the expected beam profile is be based on various factors. The images used for testing will have the limitations expected for what the program would likely end up seeing when in use (resolution, color, etc.). When the computer can adequately identify the beam profile those static images used for the identification training will then be used to test the tracking features of the computer and guarantee that the computer does not lose the beam for any extensive period that would lead to issues in data collection.

Once both prior parts of the training and testing are completed the computer will be stress tested to determine how much variation the computer can handle in identifying and tracking. The stress testing will entail testing how well the computer can analyze an image given some amount of degradation to the image and how well the computer can correctly track a beam given other objects being in view (i.e., bugs landing on the reflection surface). The aim will be to have the computer be able to decern between the actual beam profile and any other miscellaneous objects that may be enter the camera's view that will be unavoidable to keep away from the testing area.

Once the computer has reached the expected levels of accuracy the computer will continue to be tested on what it is able to track as to make sure there is no strange last-minute deviation that has not been accounted for prior to demonstration.

8.2.5 Microcontrollers

For the microcontroller the main software test that needs to be done is on how to handle incoming commands from the controller device and use them to operate the 3 motors used. The tests will also need to handle how much adjustment needs to be made by the motor depending on the input of the control device. For the motor control testing the software will be tested to calibrate how the input translates into actual motor movement. This will be done by connecting the microcontroller to the motors used through the driver boards for the motors and to whatever means are used for through the controller device's interface to adjust the particular motors being adjusted. Based on what is deemed to be necessary to allow for best control over the motors, whether it be increasing the sensitivity to make the adjustments quicker or lower the sensitivity to make the adjustments more refined, the code used on the microcontroller is altered to make the needed adjustments and is tested once again to verify if the changes are to the liking of the users. This can also be used to test how the microcontroller is able to handle incoming commands from the control device and allow for determinations of what needs to be done to improve whatever variable needs to be improved, such as latency between the commands of the control device and the actions being done by the microcontroller.

9. Part List

Parts list	Part name	Manufacturer	Part number	Cost
Biconvex Lens A	N-BK7 Bi-Convex Lens, Ø1", f = 75.0 mm, Uncoated	ThorLabs	LB1901	$24.50
Biconcave Lens B	N-BK7 Bi-Convex Lens, Ø1", f = 175.0 mm, Uncoated	ThorLabs	LB2297	$35.16
Biconvex Lens C	N-SF11 Bi-Concave Lens, Ø25.4 mm, f = -25.0 mm, Uncoated	ThorLabs	LB1294	$22.92
Camera	ZWO ASI 385 Color CMOS Telescope Camera	OptCorp	SKU : ZWO-ASI385MC	$299(sale – normally $349)
Laser Source	532 nm 50 mW green laser diode	Amazon (Lilly Electronics)	532MD-50-1348-CAB	$20.00
Full Spectrum Light	Full Spectrum 800 Lumen Lightbulb	NorbSMILE	A19 LED	$19.99
Short Pass Filter	D = 12.50 mm Cut off 550 nm Transmission: 400 – 535 nm > 85% @ 532 OD = 2 Angle of Incidence: 0	Edmunds Optics	#47-813	$92.50
Fan 1	Fan Tubeaxial	AdaFruit Industries LLC	3368	$3.50
Fan 2	Fan Tubeaxial	AdaFruit Industries LLC	3368	$3.50

Parts list	Part name	Manufacturer	Part number	Cost
Long Pass Filter	D = 12.50 mm Cut on 500 nm Transmission: 520 – 2000 nm > 85% @ 532 OD = 2 Angle of Incidence: 0	Edmunds Optics	#49-026	$64.75
PIN Photodiode	3mm Si PIN Photodiode 300-1200 nm	Civil Laser		$6.00*(10) = $60.00
Plano Convex Lens		ThorLabs		$
MCU	Arduino Nano Every	Arduino AG		$28.20/3 = $9.40
SBC	Raspberry Pi 4 Model B 8 GB	Raspberry Pi Trading LTD		~~$95~~($0, preowned
RF Transmitter/Receiver	nRF24L01+	Nordic Semiconductor ASA		$4
Stepper Motor 1	Nemas 17, 63.74 Oz.in	StepperOnline	17HS15-1504S1	$8.67
Stepper Motor 2	Nemas 17, 63.74 Oz.in	StepperOnline	17HS15-1504S1	$8.67
Stepper Motor 3	Nemas 17, 18.4 Oz.in	StepperOnline	17HS10-0704S	$8.56
Stepper Motor 4	Nemas 17, 18.4 Oz.in	StepperOnline	17HS10-0704S	$8.56
Battery	LifePO4	Eco-Worthy	Sku: L13060202004-1	$60.32

Table 17: Parts List

10. Expected Results

By the end of this project, it is expected to have a fully functioning device that is capable of remotely locating a laser beam off a diffused surface and be able to track and record characteristics about the beam profile. Data transmission will be efficient and remote.

References

"Ambient Light Sensor: Types, Circuit and Applications." *ElProCus*, 29 July 2019, https://www.elprocus.com/ambient-light-sensor-working-and-applications/.

(Andor, 2018, 2019; Brunner, 2017; *CMOS Cameras*, 2021; Instuments; Kingslake, 1989; Plumridge, 2018, 2019, 2020; Riyo Youngworth, 2012; Sasian, 2019)

Andor. (2018). *How to Define the Quantum Efficiency of CCD Cameras*. Oxford Instruments.
Retrieved 10/28 from https://andor.oxinst.com/learning/view/article/ccd-spectral-response-(qe)

Andor. (2019). *Understanding Read Noise in sCMOS Cameras*. Oxford insturments. Retrieved 10/27 from https://andor.oxinst.com/learning/view/article/understanding-read-noise-in-scmos-cameras

Arduino AG. (n.d.). *Arduino Nano Every - Pack 3*. Arduino Nano Every. Retrieved November 5, 2021, from https://store-usa.arduino.cc/products/arduino-nano-every-pack?variant=40377141854415

A., Saleh Bahaa E. *Introduction to Subsurface Imaging*. Cambridge University Press, 2011.

Battery University. "BU-201: How Does the Lead Acid Battery Work?" Battery University, 27 Oct. 2021, https://batteryuniversity.com/article/bu-201-how-does-the-lead-acid-battery-work.

Brunner, D. (2017, 10/28). Frame Rate: A Beginner's Guide. https://www.techsmith.com/blog/frame-rate-beginners-guide/

Bluetooth SIG, Inc. (n.d.). *Learn About Bluetooth: Bluetooth Technology Overview*.
Retrieved October 20, 2021, from https://www.bluetooth.com/learn-about-bluetooth/tech-overview/

Cass, S. (2021, July 28). *Quickly embed AI into your projects with Nvidia's Jetson Nano*. IEEE Spectrum. Retrieved November 19, 2021, from https://spectrum.ieee.org/quickly-embed-ai-into-your-projects-with-nvidias-jetson-nano#toggle-gdpr.

CMOS Cameras. (2021). OPT. Retrieved 9/25 from
Instuments, P. *Full Well Capacity*. teledyne imaging group. Retrieved 10/29 from
Karim Nice, T. V. W. G. G. (2020). *How Digital Cameras Work*. Retrieved 11/3 from https://electronics.howstuffworks.com/cameras-photography/digital/question362.htm

Demeritt, Clint. "12V Battery Types: Which One Is for You?" Battle Born Batteries, 18 May 2021, https://battlebornbatteries.com/12v-battery-types/.
Electromaker. (n.d.). *Nvidia Jetson Nano Development Kit-B01*. Nvidia Jetson Nano Development Kit-b01. Retrieved November 19, 2021, from https://www.electromaker.io/shop/product/nvidia-jetson-nano-development-kit-b01.

Hecht, Eugene. *Optics*. Pearson Education, Inc., 2016.

HuddleCamHD. (2021, September 27). *About*. Retrieved November 5, 2021, from https://huddlecamhd.com/webcam/.

isaac879. (2020, September 5). *Pan-Tilt-Mount*. Retrieved November 5, 2021, from https://github.com/isaac879/Pan-Tilt-Mount.

Juneau, John-Michael, "The Simulation, Design, and Fabrication of Optical Filters" (2017). Graduate Theses - Physics and Optical Engineering. 21. https://scholar.rose-hulman.edu/optics_grad_theses/21

Kingslake, R. (1989). *A history of the photographic lens*. Academic press.
Plumridge, J. (2018). *Backfocus in Astrophotography*. Atik cameras. Retrieved 10/29 from https://www.atik-cameras.com/news/backfocus-astrophotography-cameras/

Kumar, V. (2020, December 2). How to detect objects in real-time using opencv and python. Medium. Retrieved November 19, 2021, from https://towardsdatascience.com/how-to-detect-objects-in-real-time-using-opencv-and-python-c1ba0c2c69c0.

Last Minute Engineers. (2020, December 18). *In-depth: How NRF24L01 wireless module works & interface with Arduino*. Last Minute Engineers. Retrieved November 5, 2021, from https://lastminuteengineers.com/nrf24l01-arduino-wireless-communication/.

Microchip Technologies Inc. (2019). 48-pin Data Sheet – megaAVR® 0-series.

“Nonpolarizing Transmissive Filters.” *Enhanced Optical Filter Design*, pp. 135–146., https://doi.org/10.1117/3.869055.ch12.

Nordic Semiconductor ASA. (2008, March). nRF24L01+ Single Chip 2.4GHz Transceiver
Preliminary Product Specification v1.0.

NVIDIA Corporation. (2021, April 14). *Jetson Nano Developer Kit*. NVIDIA Developer. Retrieved November 19, 2021, from https://developer.nvidia.com/embedded/jetson-nano-developer-kit.

OpenCV team. (2020, November 4). About. OpenCV. Retrieved November 19, 2021,
from https://opencv.org/about/.

“Optical Filters: Edmund Optics.” *Edmund Optics Worldwide*, https://www.edmundoptics.com/knowledge-center/application-notes/optics/optical-filters/.

“Optical Filter Spectral Features - CWL, FWHM, Transmission, and Blocking.” *Alluxa Optical Filters and Thin-Film Coatings*, 24 May 2021, https://www.alluxa.com/optical-filter-specs/spectral-features/.

“Optical Filter Spectral Features - CWL, FWHM, Transmission, and Blocking.” *Alluxa Optical Filters and Thin-Film Coatings*, 24 May 2021, https://www.alluxa.com/optical-filter-specs/spectral-features/.

“Optical Filters: Edmund Optics.” *Edmund Optics Worldwide*, https://www.edmundoptics.com/c/optical-filters/610/.

Plumridge, J. (2019). *What is dynamic and tonal range?* Lifewire. Retrieved 10/27 from https://www.lifewire.com/what-is-dynamic-range-493728

Plumridge, J. (2020). *Why You Should Care About Your Camera's ADC*. Lifewire. Retrieved 10/29 from https://www.lifewire.com/the-adc-of-a-digital-camera-493714

Raspberry Pi Trading LTD. (n.d.). *Raspberry pi documentation*. RP2040. Retrieved November 5, 2021, from https://www.raspberrypi.com/documentation/microcontrollers/rp2040.html#welcome-to-rp2040

Raspberry Pi Trading Ltd. (2020). RP2040 Datasheet.

Raspberry Pi Trading Ltd. (2019, June). Raspberry Pi 4 Model B Datasheet.

Raspberry Pi. (n.d.). *Raspberry pi 4 model B*. Raspberry Pi. Retrieved November 5, 2021, from https://www.raspberrypi.com/products/raspberry-pi-4-model-b/.

Riyo Youngworth, E. B. (2012). Fundamental considerations for zoom lens design (tutorial). SPIE optical engineering and applications, san diego, califorina.

Sasian, J. (2019). Zoom lenses. In *Introduction to lens design* (pp. 196-206). cambridge university press.

ssheshadri. (2019, December 17). Jetson Nano Developer Kit User Guide. NVIDIA Corporation.

Texasinstruments, director. YouTube, Texas Instruments, 10 Dec. 2018, https://www.youtube.com/watch?v=Gk4Hib99wkc. Accessed 5 Nov. 2021.

Torvalds, Linus (2005, April 7). "Re: Kernel SCM saga." linux-kernel. Retrieved November 19, 2021.

U.S. Department of Commerce National Telecommunications and Information Administration Office of Spectrum Management. (2016, January). United States Frequency Allocation Chart.